

CLASSIFICATION CANCELLED

CONFIDENTIAL

RM No. 516L12

1104
Republic
F-12/2



PERMANENT FILE COPY

RESEARCH MEMORANDUM

for the

Air Materiel Command, Army Air Forces

LONGITUDINAL STABILITY AND STALLING CHARACTERISTICS OF
A 1/8.33-SCALE MODEL OF THE REPUBLIC XF-12 AIRPLANE

By

Edward Pepper and Gerald V. Foster

Langley Memorial Aeronautical Laboratory
Langley Field, Va.

CLASSIFICATION CANCELLED

Activity H. L. Dryden Date 10-7-52
Dir., Aeron. Research
NACA

OCS

This document contains classified information affecting the national defense of the United States within the meaning of the Espionage Act, USC 50131 and 32. Its transmission or the communication of its contents in any manner to an unauthorized person is prohibited by law. Information so classified may be imparted only to persons in the military and naval services of the United States, to the Government and its agencies, to the press, and to United States citizens of known loyalty and discretion who of necessity must be informed thereof.

NACA change #
1254

CONTAINS PROPRIETARY INFORMATION

NATIONAL ADVISORY COMMITTEE FOR AERONAUTICS

FILE COPY

WASHINGTON
JAN 17 1947

To be returned to
the files of the National
Advisory Committee

for Aeronautics
Washington, D. C.

CLASSIFICATION CANCELLED

CONFIDENTIAL



CLASSIFICATION CANCELLED

NATIONAL ADVISORY COMMITTEE FOR AERONAUTICS

RESEARCH MEMORANDUM

for the

Air Materiel Command, Army Air Forces

LONGITUDINAL STABILITY AND STALLING CHARACTERISTICS OF
A 1/8.33-SCALE MODEL OF THE REPUBLIC XF-12 AIRPLANE

By Edward Pepper and Gerald V. Foster

SUMMARY

The XF-12 airplane is a high performance, photo-reconnaissance aircraft designed by the Republic Aviation Corporation for the Army Air Forces. A series of tests of a 1/8.33-scale powered model was conducted in the Langley 19-foot pressure tunnel to obtain information relative to the aerodynamic design of the airplane. This report presents the results of tests to determine the static longitudinal stability and stalling characteristics of the model.

From this investigation it was indicated that the airplane will possess a positive static margin for all probable flight conditions. The stalling characteristics are considered satisfactory in that the stall initiates near the root section and progresses toward the tips. Early root section stalling occurs, with the flaps retracted and may cause undesirable tail buffeting and erratic elevator control in the normal flight range. From considerations of sinking speed landing flap deflections of 40° may be preferable to 55° or 65°.

INTRODUCTION

The XF-12 airplane was designed by the Republic Aviation Corporation to provide a long-range, high-altitude, high-speed, photo-reconnaissance aircraft for the Army Air Forces. The airplane is conventional in design with a normal gross weight of 103,000 pounds, a wing span of 129.17 feet and a wing area of 1640 square feet. The airplane is equipped with four supercharged Pratt & Whitney R-4360 engines, capable of delivering 3000 horsepower at take-off.

CONFIDENTIAL
CLASSIFICATION CANCELLED

During the early design stages of the XF-12 airplane, a preliminary analysis of the longitudinal stability characteristics was made by NACA (reference 1). Subsequent investigations by NACA were made to determine the aerodynamic characteristics of several of the component parts of the XF-12 airplane, the results of which are reported in references 2 to 9.

To furnish additional information pertinent to the aerodynamic characteristics of the XF-12 design, the Air Materiel Command, Army Air Forces, has requested that an investigation be conducted in the Langley 19-foot pressure tunnel of a 1/8.33-scale complete model of the XF-12 airplane. This paper presents the results of that part of the investigation made to determine the static longitudinal stability and stalling characteristics for various power conditions and flap deflections.

COEFFICIENTS AND SYMBOLS

The positive directions of the forces, moments, and angular displacements of the airplane and control surfaces are shown in figure 1. The coefficients and symbols used are as follows:

C_L	lift coefficient (L/qS)
C_X	longitudinal-force coefficient (X/qS)
C_m	pitching-moment coefficient (M/qSc)
T_c	effective thrust coefficient ($T/2qD^2$)
Q_c	torque coefficient ($Q/2qD^3$)
L	lift ($-Z$)
X	force along longitudinal axis
Z	force along vertical axis
M	pitching-moment about center of gravity
T	effective thrust of one propeller
Q	torque of one propeller

- q free-stream dynamic pressure ($\frac{1}{2}\rho V^2$)
 \bar{c} mean aerodynamic chord (M.A.C.) of wing
 $(2/S \int_0^{b/2} c^2 dy = 1.61 \text{ ft for the model})$
 c airfoil section chord
 b wing span (15.51 ft for the model)
 S wing area (23.6 sq ft for the model)
 D propeller diameter (1.941 ft for the model)
 ρ mass density of air
 V free-stream velocity
 V_e velocity at duct inlet
 V_i indicated velocity
 R Reynolds number ($\rho V S / \mu$)
 M Mach number (V/a)
 a sonic velocity
 μ coefficient of viscosity
 α angle of attack of wing root chord line
 i_t stabilizer incidence relative to wing root chord line,
 positive with trailing edge down
 δ_e elevator deflection with respect to stabilizer chord
 line, positive with trailing edge down; subscript
 "trim" denotes elevator deflection when $C_m = 0$
 δ_f flap deflection with respect to adjacent wing section
 chord line
 β propeller blade angle at 0.75 tip radius

$\partial C_m / \partial i_t$ variation of pitching-moment coefficient with stabilizer incidence

$\partial C_m / \partial \delta_e$ variation of pitching-moment coefficient with elevator deflection

Symbols for the several power conditions are presented in table I.

MODEL AND TESTS

Model

The 1/8.33-scale complete model of the XF-12 airplane is shown in figure 2 set up in the test section of the Langley 19-foot pressure tunnel. Principal dimensions and general design features are presented in figure 3 and table II. The model is of steel-reinforced wood construction. The surfaces were sprayed with lacquer and kept smooth by filling irregularities with glazing putty and finishing with fine abrasive paper. The electric, water, and pressure-tube leads were conducted to the model through the rear support strut fairing.

Wing.— The wing embodies the Republic Aircraft Corporation airfoil sections designated as R-4, 40-318-1 at the root and R-4, 40-413-.6 at the tip. The pressure distributions over these airfoil sections are approximately the same as those of NACA 65-series sections with similar camber and thickness. (See reference 5.) The ordinates of these sections are presented in table III. The maximum thickness of the root and tip sections are 18 and 13 percent, respectively, at 40 percent chord. The wing tips have a geometric washout angle of 4° formed by a uniform twist from 52.5 percent of the semispan as shown in figure 3. A straight line perpendicular to the axis of symmetry connects all the 50-percent chord locations.

The wing is equipped with double-slotted, partial-span flaps that extend spanwise from the fuselage to approximately 61.5 percent of the semispan. The model flaps may be deflected 20° , 40° , 55° , and 65° from the retracted position as shown in figure 5 and are fixed in position by suitable steel brackets.

Dive-recovery flaps used during the tests were installed on the lower surface of the wing as shown in figure 6 at 15 percent of the wing chord between the fuselage and the outboard nacelles. Details of the dive-recovery flap installation are given in figure 7.

Tail surfaces.— The horizontal tail is attached above the fuselage to the vertical tail. The model elevators differ from the full-scale tail design in that internally sealed balances are not provided. (See fig. 8.) Felt wiper seals are installed to prevent air-flow through the stabilizer-elevator gap. No elevator trim tabs are provided. The elevator was set manually through a range from 15° to -25° and was fixed in the desired position by hinge clamps. The stabilizer incidence is adjustable through a range from 3° to -6.5° to the wing root chord line. The rudder was locked in the neutral position for this investigation.

The complete empennage (horizontal and vertical tail and after portion of the fuselage) is removable and was replaced by a fuselage tail cone for the test runs with the tail removed. (See fig. 9.)

Wing ducts and nacelles.— The model has duct inlets situated at the leading edge of the wing between the inboard and outboard nacelles. It was found, from studies of the original Republic designed ducts in the Langley propeller-research tunnel, that internal flows of this duct limited the critical speeds of the airplane to unsatisfactorily low values. Consequently a new set of duct lips, designated NACA wing duct inlet number 5, were developed (reference 9) to allow larger values of airplane critical speed. Both duct inlets were tested on the model. A comparison of the physical characteristics of the two sets of duct lips is given in figure 10.

The internal air flows were regulated by means of adjustable doors at the exit ports, located on the underside of the nacelles as noted in figure 6. Measurements of the quantity rate of flow through the ducts were obtained with the aid of total- and static-pressure tubes located in the exit ports and connected to a multiple-tube manometer.

Each of the four model nacelles was provided with adjustable cowl exit openings to allow regulation of the internal flow through the cowl. The model nacelle afterbodies are faired to moderately streamlined shapes. The full-scale nacelle installations differ from this in that the afterbodies are cut off blunt to allow an opening for the turbo-supercharger exhaust (to augment the propeller thrust).

Propellers and motors.— The four-blade, right-hand, adjustable-pitch, tractor model propellers are geometrically similar to the airplane propellers. The propeller hubs are externally contoured to simulate the spinners. Dummy spinners were available for tests with propellers removed.

Each of the four propellers was driven by a water-cooled induction motor that was housed within the nacelle and was capable of continuously developing 20 foot-pounds of torque at rotational speeds up to approximately 6000 rpm. A variable frequency alternator supplied the current and speed control for the four motors.

Fuselage and protuberances.— The fuselage has a fineness ratio of 9.03:1 and is circular in cross section about a straight line extending from the nose to the tail. The maximum diameter of the fuselage occurs at the 50 percent chord line of the wing root chord or about 38.6 percent of the fuselage length from the nose. The fuselage is equipped with models of an astrodome and a radar dome.

When the flaps were deflected the tricycle landing gear and wheel-well doors were extended to simulate the full-scale airplane configuration. The wheel wells in the fuselage and under surface of the wing were not reproduced on the model.

Test Conditions and Methods

The investigation was made with the density of the air in the tunnel maintained at approximately 0.00535 slug per cubic foot. Most of the tests were conducted at a dynamic pressure of approximately 27.5 pounds per square foot which gave a Reynolds number of about 2,400,000 and a Mach number of approximately 0.09. A few test runs were conducted with propellers removed at a dynamic pressure of approximately 55 pounds per square foot, which roughly corresponds to a Reynolds number of 3,400,000 and a Mach number of 0.13.

Stabilizer and elevator tests.— Most of the tests were made by varying the angle of attack from low to high values for each of the selected stabilizer and elevator settings. The stabilizer characteristics were obtained for i_t equal to 3° , -2° , and -6.5° with δ_e equal to 0° . For the elevator tests the stabilizer incidence was set at -2° and values of δ_e were chosen to cover a satisfactory range of flight conditions.

Power conditions.— The full-scale power conditions simulated during the test are listed in table I. The model propellers were operated so that T_C varied with C_L for the several power conditions as shown in figure 11. The power condition for a gross weight of 77,500 pounds was selected to cover the condition with very light loading and may also be used to some extent to estimate the airplane characteristics with power ratings above 3000 horsepower

per engine. The values given in figure 10 are based on estimates of the full-scale propeller characteristics with the thrust line incidence equal to 0° . The variation of T_C with C_L for the 100-percent rated-power condition (not shown) and $(M.P.)_2$ are approximately the same. No attempt was made to simulate the relatively small amount of thrust due to the reaction of the full-scale turbosupercharger exhaust. Calibrations of the model propeller were made with the thrust line incidence at 0° to determine the variation of T_C with Q_C . A blade angle setting of 21.5° was selected to obtain a reasonable approximation of Q_C as shown in figure 12. An analysis indicated that variations from these curves would have small effect on the longitudinal stability results and therefore did not warrant other blade angle settings during the test.

Test runs of the model with power on were made by varying the thrust coefficient with the angle of attack at a constant value of dynamic pressure to simulate constant power conditions. For the military power conditions, the maximum values of lift coefficient that could be attained during the tests were limited by the amount of torque available from the model motors.

Duct and nacelle air-flow conditions.— While most of the investigation of the 1/8.33-scale complete model of the Republic XF-12 airplane was conducted with the NACA wing duct inlet number 5, some preliminary tests were made to determine the effect of the Republic designed wing duct inlets on the stall progression and maximum lift coefficient. As it was infeasible to simulate full-scale air flow for all flight conditions, values of duct entrance velocity ratio were selected that would closely represent the full-scale conditions most generally approached in flight. An attempt was made to simulate these conditions by adjustment of the exit port doors. The values of V_e/V obtained during the test are as follows:

δ_f (deg)	α (deg)	V_e/V			
		Oil cooler		Intercooler and charge air	
		Desired	Obtained	Desired	Obtained
0	2.2	0.40	0.39	0.20	0.21
65	11.2	.55	.39 ^a	.62	.61

^aMaximum opening of exit port.

The exit port opening used for the tests with the original Republic duct inlets were duplicated for the subsequent test runs with NACA wing duct inlet number 5. The following values of V_e/V resulted:

δ_f (deg)	α (deg)	V_e/V	
		Oil cooler	Intercooler and charge air
0	2.3	0.63	0.27
65	11.6	.41	.86

The changes in entrance velocity ratio were roughly proportional to the inlet area change of the two duct configurations so that values of flow coefficient for the two ducts were approximately the same. When the flaps were deflected 20° , 40° , and 55° , the exit-port settings were the same as for the condition with the flaps deflected 65° .

No measurements were made of the quantity rate of air flow through the nacelles. However, high values were sustained by utilizing the maximum openings at the cowl exits in all tests except where noted.

Test runs with tufts attached to the model were made with maximum opening of cowl exit and with cowl entrances sealed as shown in figure 13. These tests indicated that the internal air flows obtained during the investigation should not adversely influence the longitudinal stability results to any appreciable extent.

Tuft studies.— The flow characteristics over the upper surface of the wing, nacelles, and fuselage were determined by the observation of wool tufts. The tufts were fastened to the wing upper surface with thin strips of cellulose tape at approximately 30, 50, 70, and 90 percent of the wing chord and spaced about 5 inches spanwise. The attitude of the model was changed during the test runs from low to high values of angle of attack. At every angle of attack that the flow pattern changed appreciably, as indicated by the tuft behavior, sketches were made and motion picture film records were obtained.

DATA COMPUTATIONS AND CORRECTIONS

The data are referred to the stability axes, which are a system of axes having their origin at the center of gravity in which the Z-axis is in the plane of symmetry and perpendicular to the

relative wind, the X-axis is in the plane of symmetry and perpendicular to the Z-axis and the Y-axis is perpendicular to the plane of symmetry. (See fig. 1.) The pitching moments are computed about the normal center of gravity located on the fuselage center line at 27.43 percent of the mean aerodynamic chord.

Tares caused by model support-strut interference effects were determined from tests of the model with propellers removed. These tares have been applied to the lift, longitudinal-force, and pitching-moment values. Jet-boundary interference corrections have been applied to the longitudinal-force, pitching-moment, and angle-of-attack values. The longitudinal-force and angle-of-attack values have also been corrected for stream angle mis-alignment.

Test accuracy.— In general, the test accuracy is believed to be as follows:

C_L	± 0.005
C_X	± 0.0003
C_m	± 0.004
α , degrees	± 0.05
δ_e , degrees	± 0.10
i_t , degrees	± 0.10

RESULTS AND DISCUSSION

The aerodynamic forces and moments measured during the investigation and analysis of the data are presented in non-dimensional coefficient form in figures 14 to 36. All the data are for the model with the NACA wing duct inlet number 5 unless otherwise noted.

STATIC LONGITUDINAL STABILITY

Stabilizer characteristics.— The effects of stabilizer incidence on several aerodynamic characteristics are presented in figures 14 to 17. The results were obtained for several power and flap conditions. Test data of comparable model configurations with the tail removed are also included in these figures. The results indicate that no serious loss of tail effectiveness due

to tail stalling will occur. Increases of power caused increases in the values of $\partial C_m / \partial i_t$. The most pronounced changes occur for flaps retracted with values ranging from -0.042 for $T_c = 0$ to -0.072 for (M.P.)₁ at C_L equal 1.40 . For all the flaps deflected conditions tested values of $\partial C_m / \partial i_t$ were within the preceding limits. Values of $\partial C_m / \partial i_t$ decrease slightly with angle of attack for $T_c = 0$ or propellers removed conditions. It should be noted that sharp breaks in the pitching-moment curves are experienced when the flaps are retracted and the power is moderately high. A possible cause of the breaks may be a decrease in the downwash at the tail resulting from early stalling of the wing-root sections. The wing stalling characteristics are discussed in detail in a subsequent section of this paper.

Elevator characteristics.— Test results are presented in figures 18 to 22 to show the effects of the elevator deflection on several aerodynamic characteristics of the model. The results are for several flap and power conditions. Trends in the variation of $\partial C_m / \partial \delta_e$ are similar to those noted for $\partial C_m / \partial i_t$ as expected. The most pronounced changes occur for the flaps retracted condition with values ranging from -0.029 for $T_c = 0$, $C_L = 1.20$ to -0.046 for (M.P.)₁, $C_L = 1.6$. Breaks occur in the pitching-moment curves similar to those experienced with the stabilizer tests as expected. These breaks occur at lift coefficients below the stall and indicate the possibility of encountering erratic elevator control in the high altitude climb condition.

Analysis.— Inasmuch as elevator hinge moments were not measured during the tests, an analysis has been made to estimate only the elevator-fixed static longitudinal stability characteristics of the XF-12 airplane using the results presented in figures 18 to 22. The relation of the center-of-gravity location with the elevator deflection necessary for trim throughout the speed range was estimated for the airplane and is presented in figure 23 for the several flap and power conditions. Also shown on these curves are the corresponding elevator-fixed neutral points determined from figures 14 to 18 by methods explained in reference 10. It is assumed in the derivation of these curves that the elevator effectiveness will not be affected by control-tab deflection and that the effect of the drag component of the airplane on the pitching-moment may be neglected. It is believed that these assumptions are reasonable on the premise that for the range of elevator settings required for trim the control-tab deflection will probably be small so that the variation of tail lift with elevator deflection will not be appreciably affected. Moreover, for all but the low values of V_1 the effect of the drag component of the airplane is negligible and therefore will not

seriously affect the results in the normal speed range. It is believed that the foregoing assumptions are consistent with the accuracy of the test measurements.

In determining V_1 a design gross weight of 77,500 pounds was included in the conventional lift equation for level flight to give $V_1 = 135.896 (C_L)^{-1/2}$, miles per hour for (M.P.)₁ and 103,000 pounds to give $V_1 = 156.642 (C_L)^{-1/2}$, miles per hour for the remaining power conditions. Although these equations are correct for only one speed (level flight), the error involved, is less than 4 percent and corrections are therefore neglected.

It is convenient to use figure 23 to find the elevator deflection necessary for trim for any normal speed and normal center-of-gravity location (25 to 30 percent M.A.C.). It is indicated from these results that sufficient elevator deflection for trim will be available for any flight condition encountered.

For convenience in determining the effects of power on the longitudinal stability, the neutral point results are summarized in figure 24. It may be seen from this figure that, in general, power has a destabilizing effect. The results of the neutral points analysis indicates that a positive static margin will exist for all flight conditions with the gross weight equal to 103,000 pounds when the center of gravity is located at 30 percent mean aerodynamic chord (most rearward location). For flight conditions with (M.P.)₁ the airplane will have a tendency toward instability at speeds below 130 miles per hour.

LIFT AND STALL CHARACTERISTICS

NACA wing duct inlet number 5.— The effects of flap deflection and increase of Reynolds number on the lift characteristics for the model with the propellers removed are shown in figure 25. Also included are the longitudinal-force and pitching-moment characteristics. An increase of Reynolds number caused an increase in maximum lift and the angle of attack at which maximum lift occurs. At the higher Reynolds numbers the maximum untrimmed lift coefficient with flaps retracted is 1.41; with flaps deflected 55° it is 1.98; and with flaps deflected 65° it is 2.05.

A rough analysis of the landing flight conditions was made for the airplane with flap deflections of 40°, 55°, and 65° at 110-percent stalling speed as indicated:

δ_f (deg)	Power	Sinking speed (ft/sec)	110-percent stalling speed (mph)	α (deg)
40	$T_c = 0$	24	121	9.2
	0.50(R.P.)	4	103	11.2
55	$T_c = 0$	26	116	8.2
	0.50(R.P.)	7	100	10.1
65	$T_c = 0$	29	118	7.1
	0.50(R.P.)	10	97	10.1

From the preceding values it may be seen that flap deflections of 40° are more favorable from considerations of sinking speed. There is little choice between 55° and 65° for lowest landing speeds. It seems likely that power will be necessary for landing as the sinking speeds for $T_c = 0$ are considered high. It should be noted that the ground angle for landing can not exceed 9.5° .

An indication of the effects of power on the lift and pitching-moment characteristics may be readily obtained from figure 26 for all the flight conditions tested. It is apparent that increase of power caused marked increases in the value of lift coefficient for all but the low angles of attack and caused decreases in the stable variation of pitching-moment coefficient with lift coefficient.

Lift values measured during the stall studies are shown in figure 27. When the tufts were attached to the wing surface the lift decreased by a slight amount below maximum lift as expected. The effects of the tufts on the stall are believed to be negligible.

The stall progressions for the model with flaps retracted are indicated in figure 28 for $T_c = 0$ and 0.75 (R.P.). The stall initiated along the trailing edge and gradually spread forward toward the leading edge of the wing as the angle of attack was increased. The stall appeared to be evenly distributed along the wing span so that the tip sections were not stalling out prematurely. The right wing tended to stall more rapidly, especially at the higher power. This phenomenon is associated with the increased angle of attack at the inboard sections of the right wing induced by propeller rotation. This effect indicates that the airplane will probably roll to the right in a stall. Root stalling is desirable at high angles of attack as a means for warning the

pilot through tail buffeting of approaching stall. Early root stalling, however, may be undesirable because of tail buffeting and erratic elevator control in the normal flight range.

Figure 29 contains the results of the stall studies of the model with flaps deflected 65° . Stall progression patterns similar to those with the flaps retracted are indicated except that less severe root stalling occurred. Increase of power tended to diminish the stall at the center sections (behind the wing duct inlet) but apparently affected the wing spanwise load distribution so that at high angles of attack the tip stall was more pronounced.

Stall studies were made with the propellers removed at a Reynolds number of about 3,400,000 as shown in figure 30. The stall was symmetrically situated over the wing span. The studies indicate that less tip stalling and more stalling over the center sections occurred than for the case of the model with propellers at a Reynolds number of about 2,400,000. These occurrences are not attributed to the change in test Reynolds number but rather demonstrate the influence of propeller operation on the stall. It is believed on the basis of the stall studies that the slipstream from the propellers, in addition to causing asymmetrical stalls also tends to clean up the stall between the nacelles by decreasing the boundary-layer thickness over the wing and hence delaying separation.

With the nacelle cowl entrance sealed the stall results in figure 31 show little change from those with maximum internal air flow. (See fig. 30.)

Original wing duct inlet.— The results of preliminary studies of the aerodynamic characteristics of the model equipped with the original Republic designed wing duct inlet are presented in figure 32. A comparison with the lift and pitching-moment characteristics of the NACA wing duct inlet number 5 (fig. 26) indicates that the model with the original duct lips has slightly lower values of maximum lift coefficient. The differences in the pitching-moment characteristics for the two wing duct inlet arrangements are small.

The stall progressions for the model with the original wing ducts are presented in figures 33 and 34. Little difference is noted between the stalling characteristics of the model equipped with the NACA wing duct inlet number 5 and of the model with the original duct inlet.

EFFECT OF DIVE-RECOVERY FLAPS AND LANDING GEAR

Dive-recovery flaps.— The effect of dive-recovery flaps on the aerodynamic characteristics of the model with and without the tail is presented in figure 35. For these tests at comparatively low Mach numbers, the results are consistent with results of tests of other dive-recovery flaps. (See reference 11.) For the condition with the dive-recovery flaps removed, it is believed that model deterioration occurred during the time that elapsed between the runs with the tail on and the tail removed. This would explain to a great extent the apparent discrepancy in the longitudinal-force data where the tail-on condition shows less negative values than the tail-removed condition.

Landing gear.— It is evident from figure 36 that for the condition with propellers removed, extension of the landing gear will not appreciably affect the variation of lift and pitching-moment coefficient with angle of attack; but the longitudinal trim speed will be affected and the lift coefficient values will be decreased by a constant amount. The landing gear also caused a constant increment increase in longitudinal-force coefficient throughout the lift range.

CONCLUSIONS

On the basis of tests of a 1/8.33-scale complete powered model of the Republic XF-12 airplane, the following conclusions are indicated:

1. The airplane will possess a positive static margin for the most rearward center-of-gravity location at 30 percent mean aerodynamic chord except at low speeds at sea level with military power and a low gross weight of 77,500 pounds.
2. Sufficient elevator will be available to trim for all conditions.
3. The stalling characteristics are considered satisfactory for all flight conditions although flap deflection tends to produce less root stalling. However, with flaps retracted early root section stalling occurs and may cause undesirable tail buffeting and erratic elevator control in the normal flight range.

4. Landing flap deflections of 40° may be preferable to 55° or 65° from considerations of sinking speed.

5. The NACA wing duct inlet number 5 will allow slightly larger values of maximum lift coefficient than the Republic designed wing duct inlets.

Langley Memorial Aeronautical Laboratory
National Advisory Committee for Aeronautics
Langley Field, Va.

Edward Pepper

Edward Pepper
Aeronautical Engineer

Gerald V. Foster

Gerald V. Foster
Aeronautical Engineer

Clinton H. Dearborn

Approved:

Clinton H. Dearborn
Chief of Full-Scale Research Division

CJB

REFERENCES

- ✓ 1. White, M. D.: Detail Calculations of the Estimated Shift in Stick-Fixed Neutral Point Due to the Windmilling Propeller and to the Fuselage of the Republic XF-12 Airplane. NACA MR No. L4J16, Army Air Forces, 1944.
- ✓ 2. Denaci, H. G.: Wind-Tunnel Tests of a 1/5-Scale Semispan Model of the Republic XF-12 Horizontal Tail Surface. NACA MR No. L5D12, Army Air Forces, 1945.
- ✓ 3. MacLachlan, Robert: Wind-Tunnel Tests of a 1/6-Scale Model of Republic XF-12 Vertical Tail with Stub Fuselage and Stub Horizontal Tail. NACA MR No. L5E21, Army Air Forces, 1945.
- ✓ 4. MacLachlan, Robert, and Miller, Sadie M.: Wind-Tunnel Tests of a 1/6-Scale Model of Republic XF-12 Vertical Tail Incorporating a De-Icing Air Duct. NACA MR No. L5G18a, Army Air Forces, 1945.
- ✓ 5. Klein, Milton M.: Aerodynamic Characteristics of Four Republic Airfoil Sections from Tests in Langley Two-Dimensional Low-Turbulence Tunnels. NACA MR No. L5I19, Army Air Forces, 1945.
- ✓ 6. Cahill, Jones F.: Aerodynamic Data for a Wing Section of the Republic XF-12 Airplane Equipped with a Double Slotted Flap. NACA MR No. L6A08a, Army Air Forces, 1946.
- 1115.5
Republic
F-12/2 ✓ 7. Graham, Robert R., Martina, Albert P., and Salmi, Reino J.: Effects of Wing Flaps and Wing Duct Inlet on the Lift and Stalling Characteristics of a 1/4-Scale Partial-Span Model of the Republic XF-12 Airplane in the Langley 19-Foot Pressure Tunnel. NACA RM No. L6J22, Army Air Forces, 1946.
- 1136.3
Republic
F-12/1 ✓ 8. Graham, Robert R., Martina, Albert P., and Salmi, Reino J.: Characteristics of a Sealed Internally Balanced Aileron from Tests of a 1/4-Scale Partial-Span Model of the Republic XF-12 Airplane in the Langley 19-Foot Pressure Tunnel. NACA RM No. L6I18, Army Air Forces, 1946.
- 1115.5
568 ✓ 9. Bartlett, Walter A., Jr., and Goral, Edwin B.: Wind-Tunnel Investigation of Wing Inlets for a Four-Engine Airplane. NACA RM No. L6L11, 1946.

- ✓ 10. Schuldenfrei, Marvin: Some Notes on the Determination of the Stick-Fixed Neutral Point from Wind-Tunnel Data.
NACA RB No. 3I20, 1943.
- ✓ 11. Hood, Manley J., and Allen, H. Julian: The Problem of Longitudinal Stability and Control at High Speeds.
NACA CB No. 3K18, 1943.

TABLE I
FULL-SCALE POWER CONDITIONS

[Simulated in tests of the 1/8.33-scale model of the XF-12 airplane]

Power condition	Symbol	Brake horsepower (per engine)	Cooling-fan horsepower (per fan)	Airplane gross weight (lb)	Altitude (ft)	Engine speed (rpm)	Gear ratio	Propeller speed (rpm)
Military power	(M.P.) ₁	3000	54	77,500	0 (Sea level)	2700	0.425	1148
Military power	(M.P.) ₂	3000	54	103,000	0 (Sea level)	2700	.425	1148
75-percent rated power	0.75 (R.P.)	1875	20	103,000	0 (Sea level)	1500	.425	638
50-percent rated power	0.50 (R.P.)	1250	14	103,000	0 (Sea level)	1500	.425	638
T _C = 0	T _C = 0	Low	Low	All	All	Low	.425	Low

NATIONAL ADVISORY
COMMITTEE FOR AERONAUTICS

TABLE II

DESIGN CHARACTERISTICS OF THE REPUBLIC XF-12 AIRPLANE
AND A 1/8.33-SCALE XF-12 MODEL

Item	Full scale	1/8.33 scale
Wing:		
Root chord (theoretical)		
Section (Republic)	R-4,40-318-1	R-4,40-318-1
Chord	17.79 ft	25.63 in.
Angle of incidence	2°	2°
Tip chord (theoretical)		
Section	R-4,40-413-.6	R-4,40-413-.6
Chord	7.70 ft	11.09 in.
Angle of incidence	-2°	-2°
Area (projected)	1639.62 sq ft	23.62 sq ft
Span (projected)	129.17 ft	15.51 ft
Aspect ratio	10.18	10.18
Mean aerodynamic chord	13.43 ft	19.34 in.
Sweepback (at 50 percent chord)	0°	0°
Taper ratio	2.31	2.31
Dihedral (from wing-root chord plane)	6°	6°
Aileron (one surface)		
Area (projected)	42.38 sq ft	87.88 sq in.
Span (projected)	23.08 ft	33.24 in.
Root chord	2.08 ft	3.00 in.
Tip chord	1.59 ft	2.29 in.
Deflection	-22.5° to 17.5°	-22.5° to 17.5°
Flaps:		
Area (total)	185.14 sq ft	2.68 sq ft
Span (one side)	34.53 ft	49.72 in.
Deflection	65° maximum	65° maximum
Horizontal tail:		
Root chord		
Section (NACA)	651-012	651-012
Chord	11.88 ft	17.11 in.
Tip chord (theoretical)		
Section (NACA)	651-012	651-012
Chord	5.94 ft	8.55 in.
Area (total projected)	388.88 sq ft	5.63 sq ft
Span	44.00 ft	63.36 in.
Aspect ratio	5.14	5.14
Taper ratio	2	2
Mean aerodynamic chord	9.27 ft	13.35 in.

TABLE II - Continued

DESIGN CHARACTERISTICS OF THE REPUBLIC XF-12 AIRPLANE
AND A 1/8.33-SCALE XF-12 MODEL - Continued

Item	Full scale	1/8.33 scale
Horizontal tail: Continued		
Dihedral (to chord plane)	6°	6°
Sweepback (at 68 percent horizontal tail chord)	0°	0°
Tail length (27.43 percent wing M.A.C. to 25 percent tail M.A.C.)	52.1 ft	75.02 in.
Elevator (one surface)		
Area (projected behind hinge line)	52.59 sq ft	7.58 sq in.
Span (projected)	18.65 ft	26.86 in.
Root chord	3.62 ft	5.21 in.
Tip chord	2.01 ft	2.89 in.
Deflection	-25° to 15°	-25° to 15°
Vertical tail (original)		
Area (fuselage not included)		
Vertical	213.56 sq ft	3.08 sq ft
Dorsal fin	49.82 sq ft	0.72 sq ft
Ventral fin	10.23 sq ft	0.15 sq ft
Root chord (theoretical)	13.33 ft	19.20 in.
Section (NACA)	65 ₁ -011	65 ₁ -011
Aspect ratio	2.06	2.06
Sweepback (at 65 percent vertical tail chord)	0°	0°
Mean aerodynamic chord	11.91 ft	17.14 in.
Span	21.67 ft	31.21 in.
Tail length (27.43 percent wing M.A.C. to 25 percent tail M.A.C.)	51.09 ft	74.67 in.
Rudder		
Area (behind hinge line)	54.87 sq ft	0.79 sq ft
Root chord	4.54 ft	6.54 in.
Tip chord	1.94 ft	2.79 in.
Span	15.00 ft	21.60 in.
Deflection	-20° to 20°	-20° to 20°

TABLE II - Continued

DESIGN CHARACTERISTICS OF THE REPUBLIC XF-12 AIRPLANE
AND A 1/8.33-SCALE XF-12 MODEL - Continued

Item	Full scale	1/8.33 scale
Vertical tail (revised)		
Area (fuselage not included)		
Vertical	213.56 sq ft	3.08 sq ft
Dorsal fin	49.82 sq ft	0.72 sq ft
Ventral fin	10.23 sq ft	0.15 sq ft
Root chord (theoretical)	13.33 ft	19.20 in.
Section (NACA)	651-011	651-011
Sweepback (at 68 percent vertical tail chord)	0°	0°
Mean aerodynamic chord	11.25 ft	16.2 in.
Span	24.9 ft	35.88 in.
Tail length (27.43 percent wing M.A.C. to 25 percent tail M.A.C.)	51.5 ft	74.22 in.
Rudder:		
Area (behind hinge line top rudder)	66.6 sq ft	0.96 sq ft
Root chord	4.54 ft	6.54 in.
Tip chord	1.94 ft	2.79 in.
Span (top rudder only)	18.03 ft	25.95 in.
Deflection	-20° to 20°	-20° to 20°
Fuselage:		
Length	92.54 ft	133.26 in.
Maximum diameter	10.25 ft	14.76 in.
Frontal area	82.52 sq ft	1.20 sq ft
Nacelles:		
Length		
Inboard	29.38 ft	42.31 in.
Outboard	27.82 ft	40.06 in.
Maximum width	5.21 ft	7.50 in.
Maximum height	5.22 ft	7.52 in.
Frontal area	21.33 sq ft	0.31 sq ft
Direction of thrust line	Parallel to fuselage center line	
Propellers:		
Number	4	4
Number of blades per propeller	4	4
Diameter	16 ft 2 in.	23.29 in.
Activity factor per blade	118.5	118.5
Type	Aeroproducts C-40-198-4	

TABLE II - Concluded

DESIGN CHARACTERISTICS OF THE REPUBLIC XF-12 AIRPLANE
AND A 1/8.33-SCALE XF-12 MODEL - Concluded

Item

FOR FULL-SCALE AIRPLANE

Weight normal	103,000 lb
Wing loading	62.8 lb/sq ft
Engines	
Number	4
Type	P & W R-4360-31
Rating per engine	
Military	3000 hp at 2700 rpm
Normal	2500 hp at 2550 rpm
Gear ratio	0.425
Superchargers	
Number	2 per engine
Type	G.E. BM-4 & BM-5 (one each per engine)
Power loading	7.33 hp/sq ft
Ground angle (from root chord)	
Static position	4° 45'
Maximum tail down position	9° 30'

NATIONAL ADVISORY
COMMITTEE FOR AERONAUTICS

TABLE III

WING ORDINATES
[Percent chord]

Station	Root section (theoretical) R-4,40-318-1		Tip section (theoretical) R-4,40-413-.6	
	Upper	Lower	Upper	Lower
0.50	1.759	1.119	1.408	0.709
.75	2.084	1.412	1.667	.888
1.25	2.609	1.885	2.095	1.175
2.50	3.595	2.700	3.768	1.646
5.00	4.967	3.768	4.120	2.231
7.50	5.993	4.520	5.019	2.609
10.00	6.813	5.103	5.771	2.869
15.00	8.089	5.972	6.930	3.238
20.00	9.023	6.569	7.818	3.459
25.00	9.707	6.986	8.467	3.606
30.00	10.183	7.248	8.938	3.654
35.00	10.482	7.379	9.247	3.654
40.00	10.609	7.396	9.399	3.606
45.00	10.569	7.281	9.399	3.053
50.00	10.365	7.052	9.242	3.346
55.00	9.991	6.698	8.922	3.140
60.00	9.447	6.220	8.429	2.896
65.00	8.742	5.625	7.736	2.653
70.00	7.882	4.920	6.886	2.398
75.00	6.869	4.129	5.879	2.101
80.00	5.733	3.286	4.791	1.765
85.00	4.494	2.419	3.638	1.402
90.00	3.141	1.534	2.436	1.002
95.00	1.663	.677	1.245	.563
100.00	.017	.017	.039	.039
Leading-edge radius height	0.234		0.234	
Leading-edge radius	2.025		1.057	

NATIONAL ADVISORY
COMMITTEE FOR AERONAUTICS

FIGURE LEGENDS

Figure 1.- System of axes and deflections. Positive values of forces and angles are as indicated by arrows.

Figure 2.- The $\frac{1}{8.33}$ -scale model of the XF-12 airplane in the test section of Langley 19-foot pressure tunnel.

(a) Front view; $\delta_f = 0^\circ$.

Figure 2.- Concluded.

(b) Rear view; $\delta_f = 55^\circ$.

Figure 3.- Three view drawing of a $\frac{1}{8.33}$ -scale model of the Republic XF-12 airplane.

Figure 4.- Wing rigging diagram of a $\frac{1}{8.33}$ -scale model of the Republic XF-12 airplane.

Figure 5.- Schematic diagram of flap of a $\frac{1}{8.33}$ -scale model of the Republic XF-12 airplane.

Figure 6.- Bottom of nacelles showing duct exits and dive recovery flap.

(a) Front view.

Figure 6.- Concluded.

(b) Rear view.

Figure 7.- Sketch of dive recovery flaps of a $\frac{1}{8.33}$ -scale model of the Republic XF-12 airplane.

Figure 8.- Plan view of horizontal tail of a $\frac{1}{8.33}$ -scale model of the Republic XF-12 airplane.

Figure 9.- The $\frac{1}{8.33}$ -scale model of the XF-12 airplane with the tail removed.

(a) Rear view.

Figure 9.- Concluded.

(b) Close-up.

Figure 10.- Sketch of the wing-duct lip of a $\frac{1}{8.33}$ -scale model of the Republic XF-12 airplane.

FIGURE LEGENDS - Continued

Figure 11.- Variation of thrust coefficient with lift coefficient for several power conditions at sea level.

Figure 12.- Variation of thrust coefficient with torque coefficient for sea level operation.

Figure 13.- Nacelle entrance sealed.

Figure 14.- Effect of stabilizer incidence on several aerodynamic characteristics. $\delta_f = 0^\circ$; $\delta_e = 0^\circ$; $R \approx 2,390,000$; $M \approx 0.09$.

(a) $(MP)_1$

Figure 14.- Continued.

(b) $(MP)_2$

Figure 14.- Continued.

(c) 0.75(R.P.)

Figure 14.- Continued.

(d) $T_c = 0$

Figure 14.- Concluded.

(e) Propellers removed.

Figure 15.- Effect of stabilizer incidence on several aerodynamic characteristics. $\delta_f = 20^\circ$; $\delta_e = 0$; $R \approx 2,380,000$; $M \approx 0.09$.

(a) $(MP)_1$

Figure 15.- Continued.

(b) $(MP)_2$

Figure 15.- Continued.

(c) 0.75(R.P.)

Figure 15.- Continued.

(d) 0.50(R.P.)

Figure 15.- Continued.

(e) $T_c = 0$

FIGURE LEGENDS - Continued

Figure 15.- Concluded.

(f) Propellers removed.

Figure 16.- Effect of stabilizer incidence on several aerodynamic characteristics. $\delta_f = 40^\circ$; $\delta_e = 0^\circ$; $R \approx 2,380,000$; $M \approx 0.09$.

(a) 0.50(R.P.)

Figure 16.- Continued.

(b) $T_c = 0$

Figure 16.- Concluded.

(c) Propellers removed.

Figure 17.- Effect of stabilizer incidence on several aerodynamic characteristics. $\delta_f = 65^\circ$; $\delta_e = 0^\circ$; $R \approx 2,370,000$; $M \approx 0.09$.

(a) 0.50(R.P.)

Figure 17.- Continued.

(b) $T_c = 0$

Figure 17.- Concluded.

(c) Propellers removed.

Figure 18.- Effect of elevator deflection on several aerodynamic characteristics. $\delta_f = 0^\circ$; $i_t = -2^\circ$; $R \approx 2,350,000$; $M \approx 0.09$.

(a) (MP)₁

Figure 18.- Continued.

(a) Concluded.

Figure 18.- Continued.

(b) (MP)₂

Figure 18.- Continued.

(b) Concluded.

FIGURE LEGENDS - Continued.

Figure 18.- Continued.

(c) 0.75(R.P.)

Figure 18.- Continued.

(c) Concluded.

Figure 18.- Continued.

(d) $T_c = 0$

Figure 18.- Concluded.

(d) Concluded.

Figure 19.- Effect of elevator deflection on several aerodynamic characteristics. $\delta_f = 20^\circ$; $i_t = -2^\circ$; $R \approx 2,340,000$; $M \approx 0.09$.

(a) $(MP)_1$

Figure 19.- Continued.

(a) Concluded.

Figure 19.- Continued.

(b) $(MP)_2$

Figure 19.- Continued.

(b) Concluded.

Figure 19.- Continued.

(c) 0.75(R.P.)

Figure 19.- Continued.

(c) Concluded.

Figure 19.- Continued.

(d) 0.50(R.P.)

Figure 19.- Continued.

(d) Concluded.

FIGURE LEGENDS - Continued

Figure 19.- Continued.

(e) $T_c = 0$

Figure 19.- Concluded.

(e) Concluded.

Figure 20.- Effect of elevator deflection on several aerodynamic characteristics. $\delta_f = 40^\circ$; $i_t = -2^\circ$; $R \approx 2,330,000$; $M \approx 0.09$.

(a) 0.50(R.P.)

Figure 20.- Continued.

(a) Concluded.

Figure 20.- Continued.

(b) $T_c = 0$

Figure 20.- Concluded.

(b) Concluded.

Figure 21.- Variation of C_m , α , and C_x with C_L . $\delta_f = 55^\circ$;
 $i_t = -2^\circ$; $R \approx 2,330,000$; $M \approx 0.09$.

(a) 0.50(R.P.)

Figure 21.- Continued.

(b) $T_c = 0$

Figure 21.- Concluded.

(c) Tail and propellers removed.

Figure 22.- Effect of elevator deflection on several aerodynamic characteristics. $\delta_f = 65^\circ$; $i_t = -2^\circ$; $R \approx 2,330,000$; $M \approx 0.09$.

(a) 0.50(R.P.)

Figure 22.- Continued.

(a) Concluded.

FIGURE LEGENDS - Continued

Figure 22.- Continued.

(b) $T_c = 0$

Figure 22.- Concluded.

(b) Concluded.

Figure 23.- Elevator-fixed static longitudinal stability characteristics for several flight conditions.

(a) $\delta_f = 0^\circ$

Figure 23.- Continued.

(a) Concluded; $\delta_f = 0^\circ$

Figure 23.- Continued.

(b) $\delta_f = 20^\circ$

Figure 23.- Continued.

(b) Concluded; $\delta_f = 20^\circ$

Figure 23.- Concluded.

(c) $\delta_f = 40^\circ$

(d) $\delta_f = 55^\circ$

(e) $\delta_f = 65^\circ$

Figure 24.- Variation of neutral point location with V_1 for several flight conditions.

Figure 25.- Effect of flap deflection and Reynolds number on several aerodynamic characteristics. Propellers removed; $i_t = -2^\circ$;
 $\delta_e = 0^\circ$.

Figure 26.- Effect of power on several aerodynamic characteristics.
 $i_t = -2^\circ$; $\delta_e = 0^\circ$; $R \approx 2,330,000$; $M \approx 0.09$.

(a) $\delta_f = 0^\circ$

Figure 26.- Continued.

(b) $\delta_f = 20^\circ$

Figure 26.- Continued.

(c) $\delta_f = 40^\circ$

FIGURE LEGENDS - Continued

Figure 26.- Continued.

(d) $\delta_f = 55^\circ$

Figure 26.- Concluded.

(e) $\delta_f = 65^\circ$

Figure 27.- Effect of tufts on lift coefficient for several flight conditions. $i_t = -2^\circ$; $\delta_e = 0^\circ$.

(a) $R \approx 2,390,000$; $M \approx 0.09$.

Figure 27.- Concluded.

(b) Propellers removed; $R \approx 3,380,000$; $M \approx 0.13$.

Figure 28.- Stall diagrams of the $\frac{1}{8.33}$ -scale model of the Republic XF-12 airplane; $\delta_f = 0^\circ$; $i_t = -2^\circ$; $\delta_e = 0^\circ$; $R \approx 2,430,000$; $M = 0.09$.

Figure 29.- Stall diagrams of the $\frac{1}{8.33}$ -scale model of the Republic XF-12 airplane; $\delta_f = 65^\circ$; $i_t = -2^\circ$; $\delta_e = 0^\circ$; $R \approx 2,350,000$; $M = 0.09$.

Figure 30.- Stall diagrams of the $\frac{1}{8.33}$ -scale model of the Republic XF-12 airplane; propellers removed; $i_t = -2^\circ$; $\delta_e = 0^\circ$; $R \approx 3,410,000$; $M = 0.13$

Figure 31.- Stall diagrams of the $\frac{1}{8.33}$ -scale model of the Republic XF-12 airplane; nacelle cowl-inlets sealed; propellers removed; $\delta_f = 0^\circ$; 2° ; $\delta_e = 0^\circ$; $R \approx 3,400,000$; $M = 0.13$.

Figure 32.- Effect of power on several aerodynamic characteristics. Original wing duct inlet; $i_t = -2^\circ$; $\delta_e = 0^\circ$.

(a) $\delta_f = 0^\circ$

Figure 32.- Continued.

(a) Concluded; $\delta_f = 0$

Figure 32.- Continued.

(b) $\delta_f = 65^\circ$

FIGURE LEGENDS - Concluded

Figure 32.- Concluded.

(b) Concluded; $\delta_f = 65^\circ$

Figure 33.- Stall diagrams of the $\frac{1}{8.33}$ -scale model of the XF-12 airplane.

Original Republic wing duct inlet; $\delta_f = 0^\circ$; $i_t = -2^\circ$; $\delta_e = 0$;
 $R \approx 2,380,000$; $M \approx 0.09$.

Figure 34.- Stall diagrams of the $\frac{1}{8.33}$ -scale model of the XF-12 airplane.

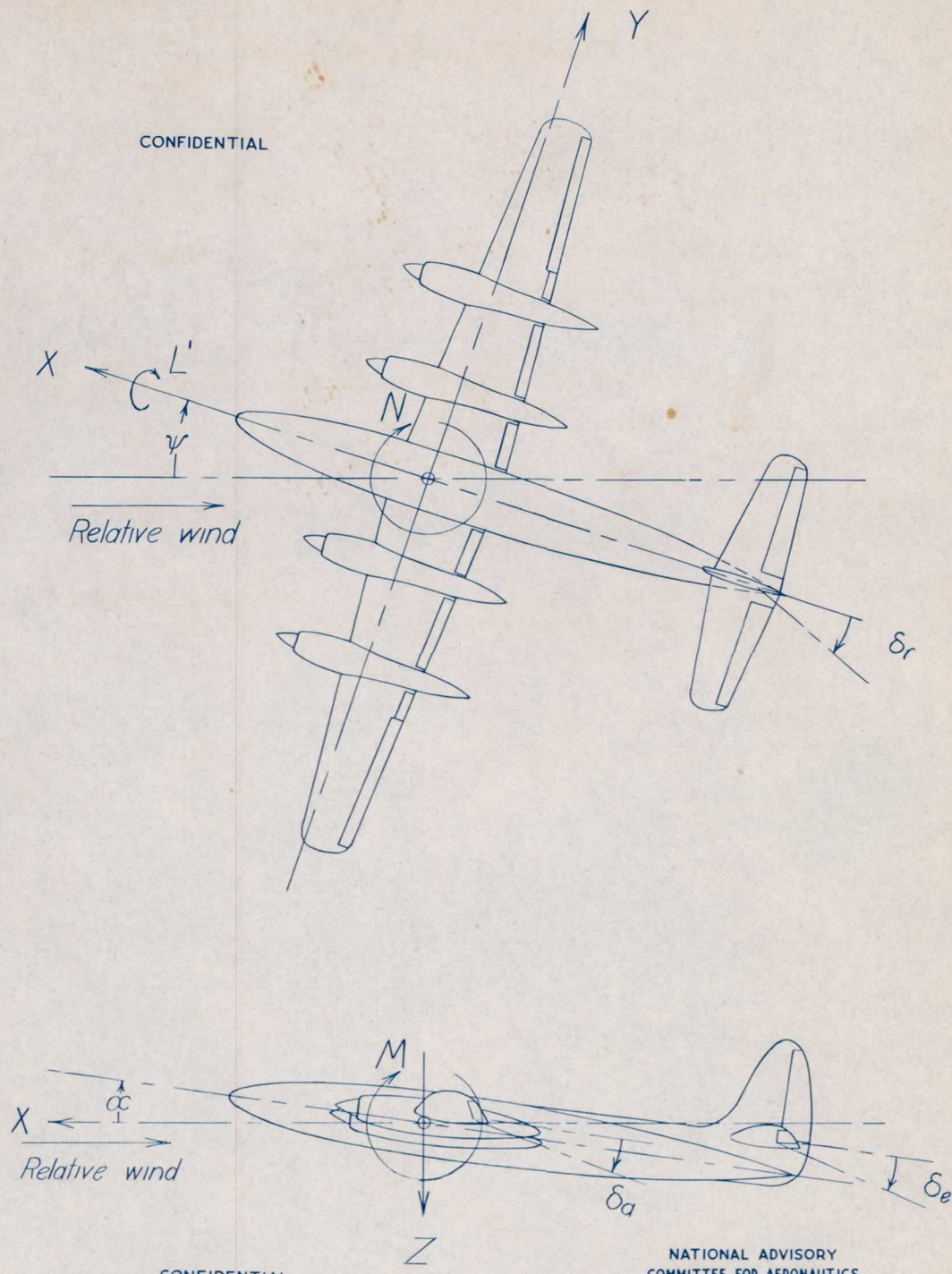
Original Republic wing duct inlet; $\delta_f = 65^\circ$; $i_t = -2^\circ$; $\delta_e = 0^\circ$;
 $R \approx 2,380,000$; $M \approx 0.09$.

Figure 35.- Effect of dive-recovery flaps on several aerodynamic characteristics. $T_c = 0$; $\delta_f = 0$; $R \approx 2,300,000$; $M \approx 0.09$.

Figure 36.- Effect of landing gear on several aerodynamic characteristics. Propellers removed; $\delta_f = 55^\circ$; $\delta_e = 0^\circ$; $i_t = -2^\circ$;
 $R \approx 3,180,000$; $M \approx 0.09$.



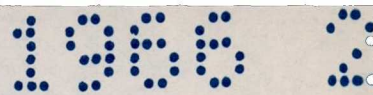
CONFIDENTIAL



CONFIDENTIAL

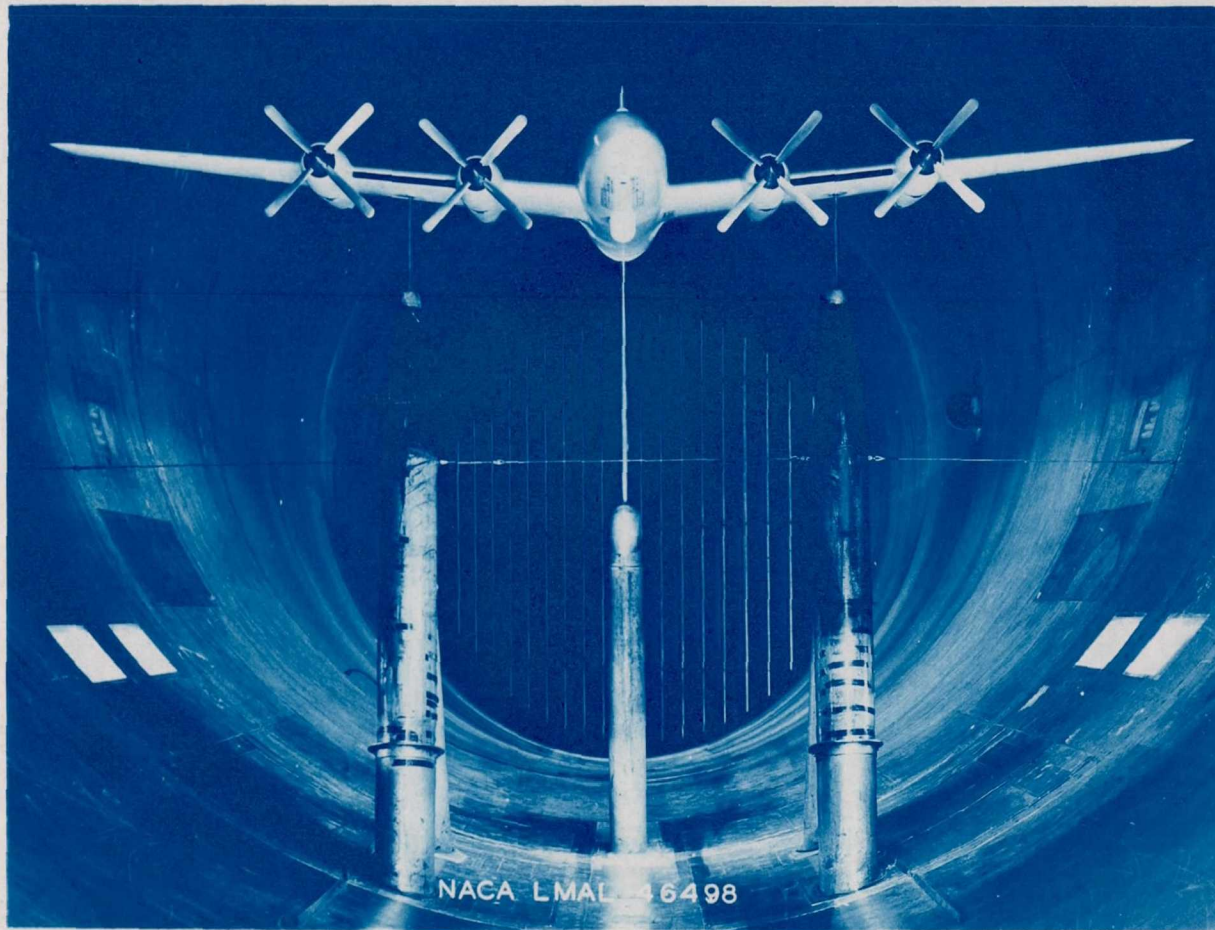
NATIONAL ADVISORY COMMITTEE FOR AERONAUTICS

Figure 1. - System of axes and deflections. Positive values of forces and angles are as indicated by arrows.



CONFIDENTIAL

NACA RM No. L6L12



(a) Front view; $\delta_f = 0^\circ$.

Figure 2.- The $\frac{1}{8.33}$ -scale model of the XF-12 airplane in the test section of Langley 19-foot pressure tunnel.

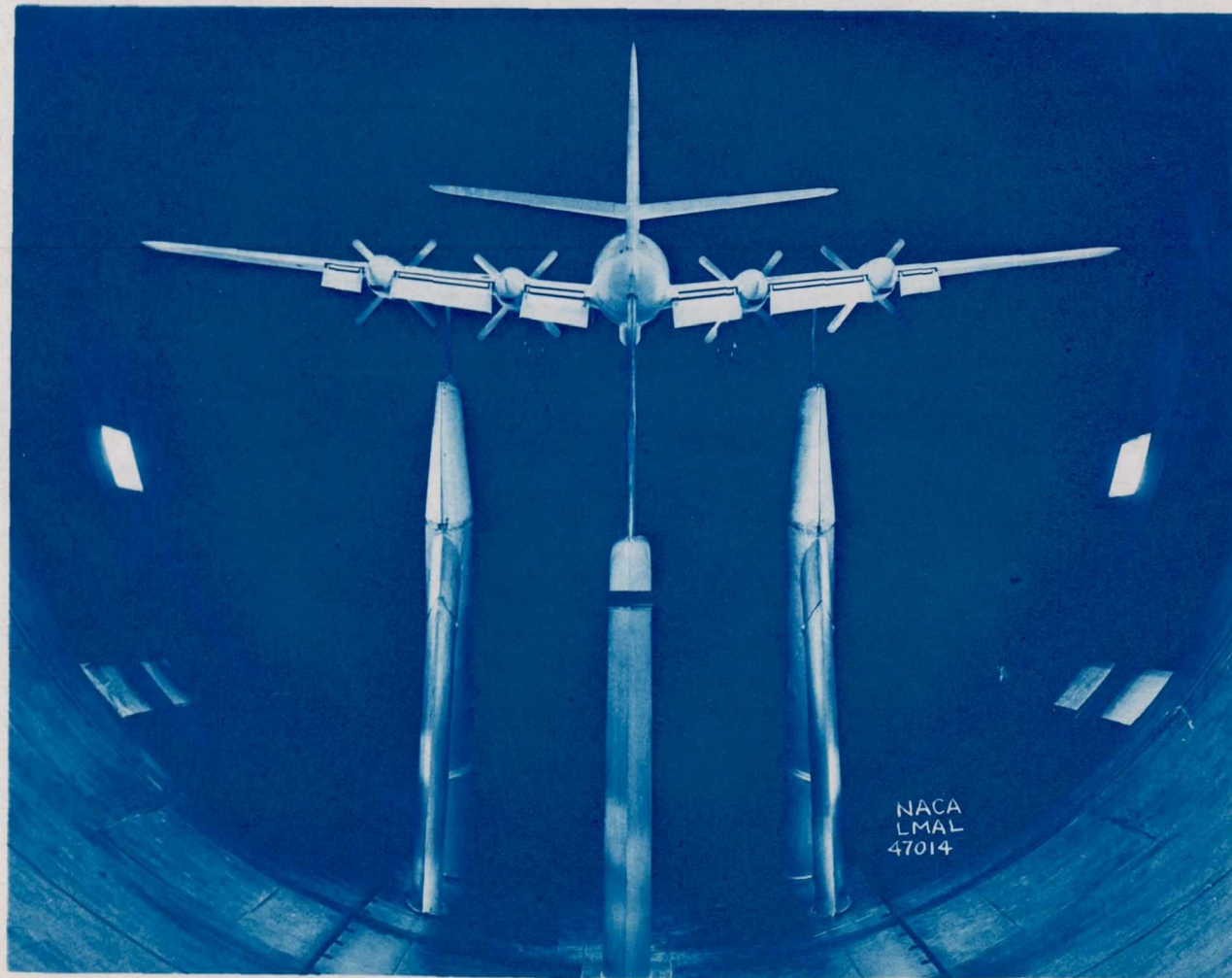
Fig. 2a

CONFIDENTIAL

NATIONAL ADVISORY COMMITTEE FOR AERONAUTICS
LANGLEY MEMORIAL AERONAUTICAL LABORATORY - LANGLEY FIELD, VA.

1958

CONFIDENTIAL

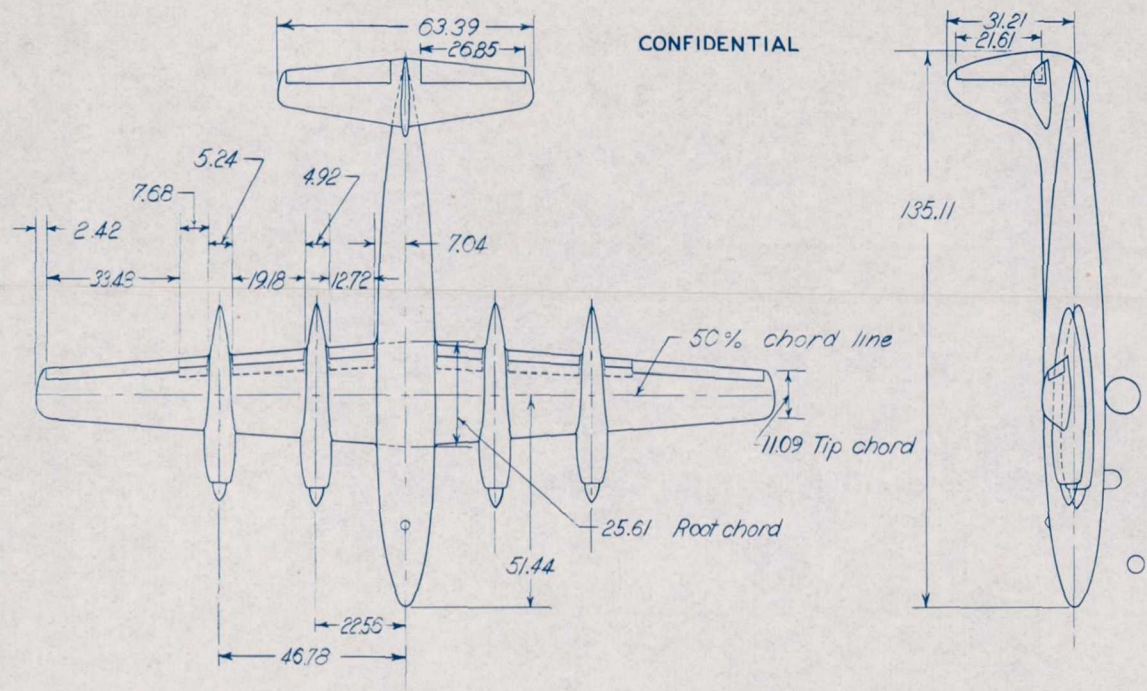


NACA RM No. L6L12

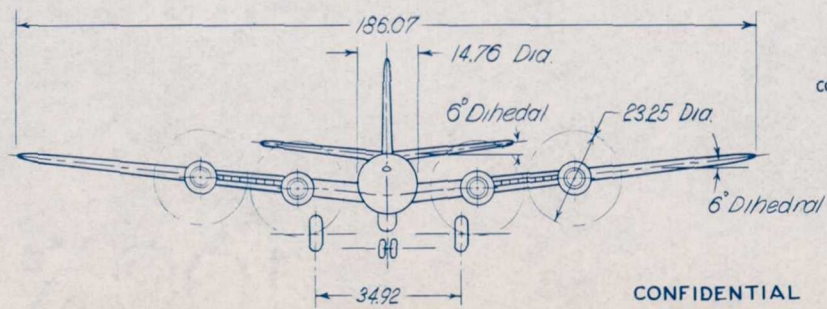
(b) Rear view; $\delta_f = 55$.

Figure 2.- Concluded.

Fig. 2b



CONFIDENTIAL



NATIONAL ADVISORY COMMITTEE FOR AERONAUTICS

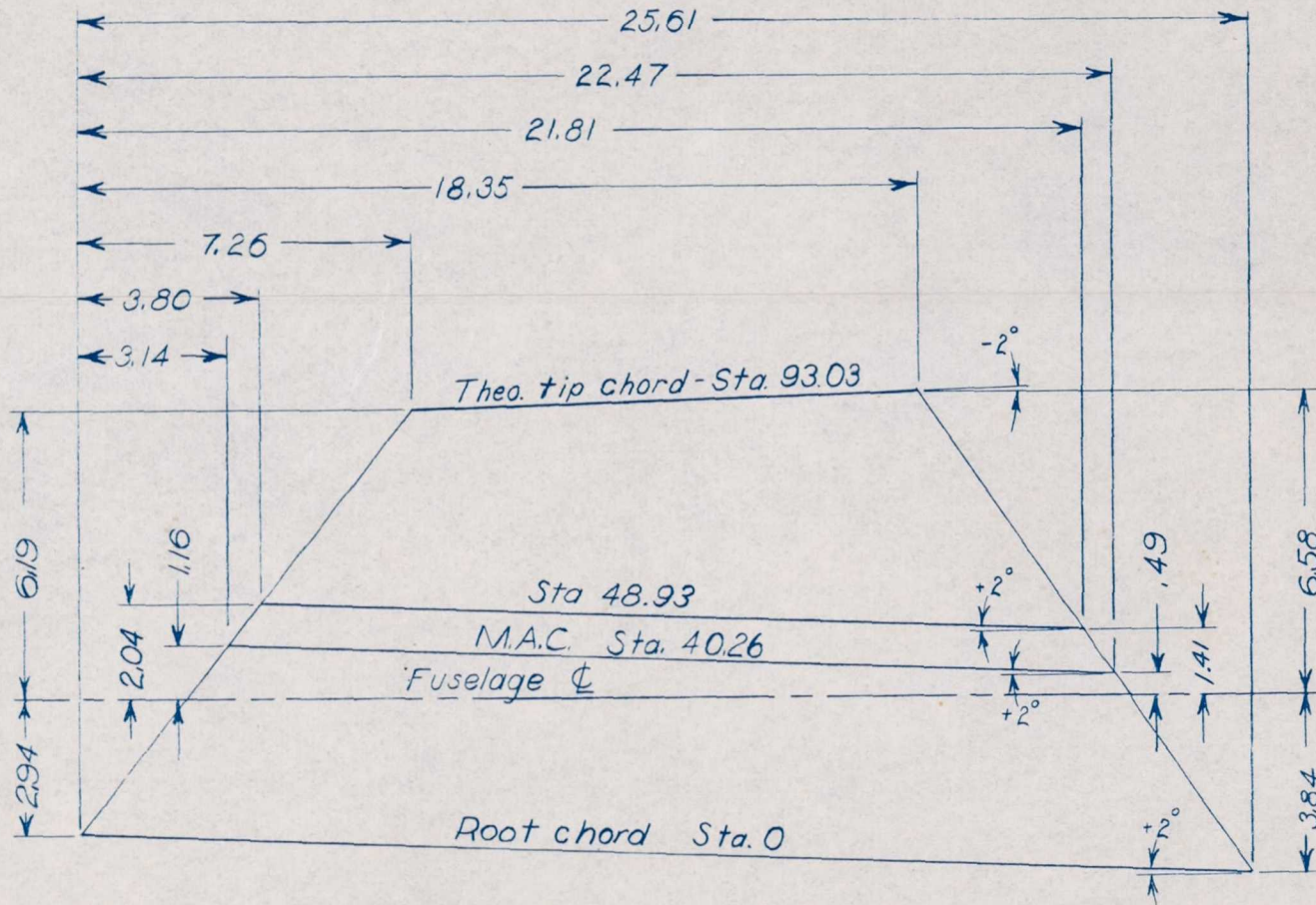
CONFIDENTIAL

Wing Root Airfoil	R-4,40-318-1
Wing Tip Airfoil	R-4,40-413-.6
Aspect Ratio	10.18
Taper Ratio	2.31 : 1
Wing Incidence	+2° to ϕ of fuselage
Wing Tip Twist (geometric)	-4°

Note: All dimensions are given in inches

Figure 3 .- Three view drawing of a 1/833 - scale model of the Republic XF-12 airplane.

CONFIDENTIAL

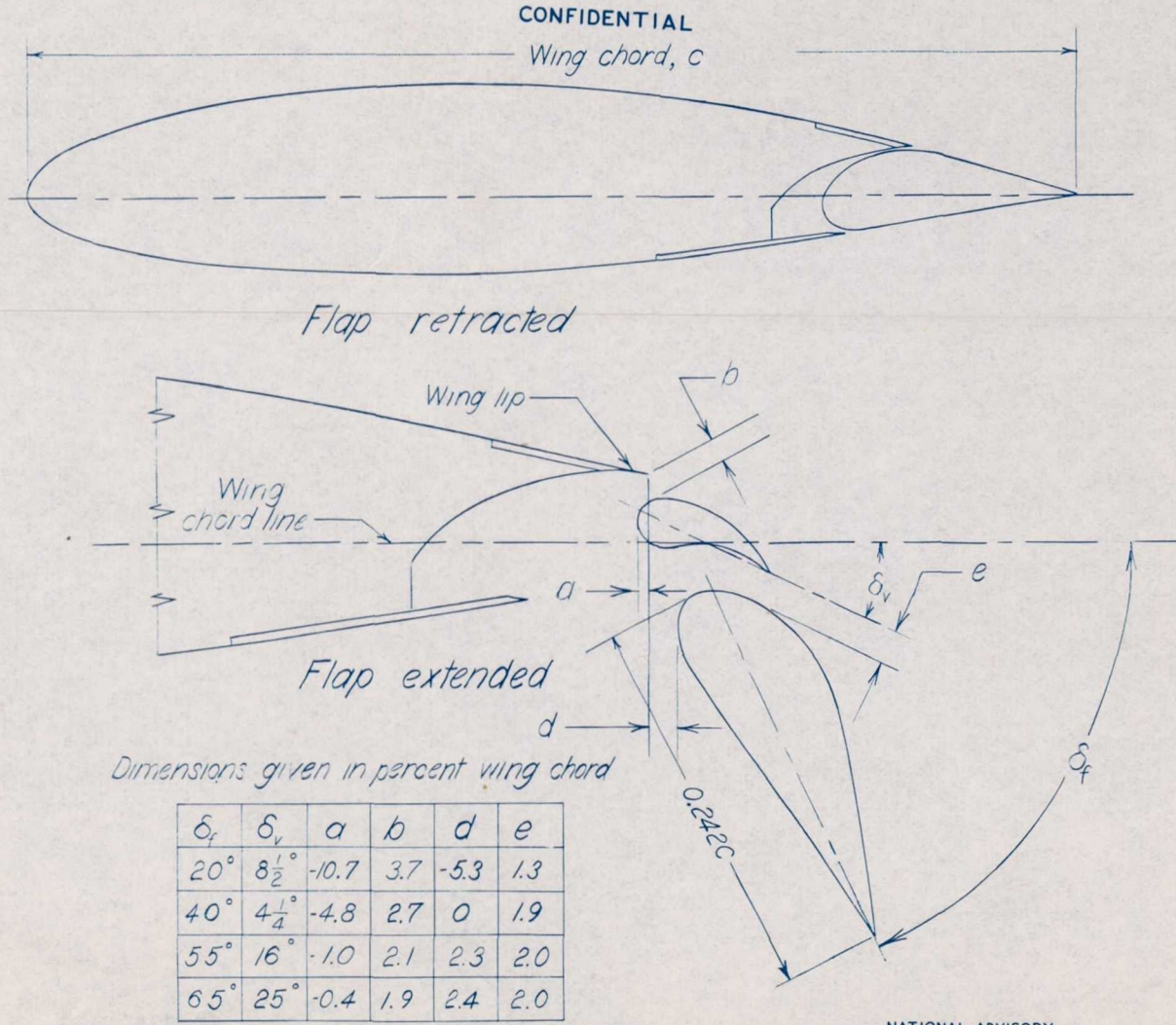


NOTE: All dimensions are given in inches.
Stations indicated are projected spanwise
distances from fuselage center line.

NATIONAL ADVISORY
COMMITTEE FOR AERONAUTICS

Figure 4. - Wing rigging diagram of a 1/8.33-scale model of the Republic XF-12 airplane

CONFIDENTIAL



Dimensions measured from wing lip toward wing leading edge are negative

NATIONAL ADVISORY COMMITTEE FOR AERONAUTICS

Figure 5 - Schematic diagram of flap of a $1/8.33$ -scale model of the Republic XF-12 airplane.

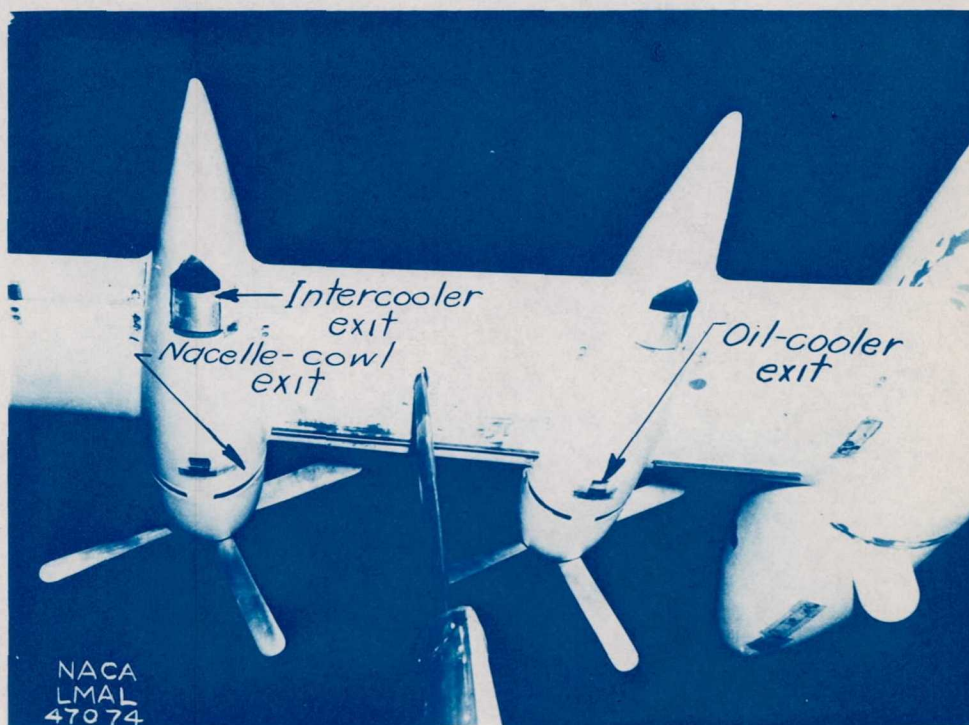


(a) Front view.

Figure 6.- Bottom of nacelles showing duct exits and dive recovery flap.

NATIONAL ADVISORY COMMITTEE FOR AERONAUTICS
LANGLEY MEMORIAL AERONAUTICAL LABORATORY - LANGLEY FIELD VA

CONFIDENTIAL



(b) Rear view.

Figure 6.- Concluded.

CONFIDENTIAL

NATIONAL ADVISORY COMMITTEE FOR AERONAUTICS
LANGLEY MEMORIAL AERONAUTICAL LABORATORY - LANGLEY FIELD, VA.

1966

NACA RM No. L6L12

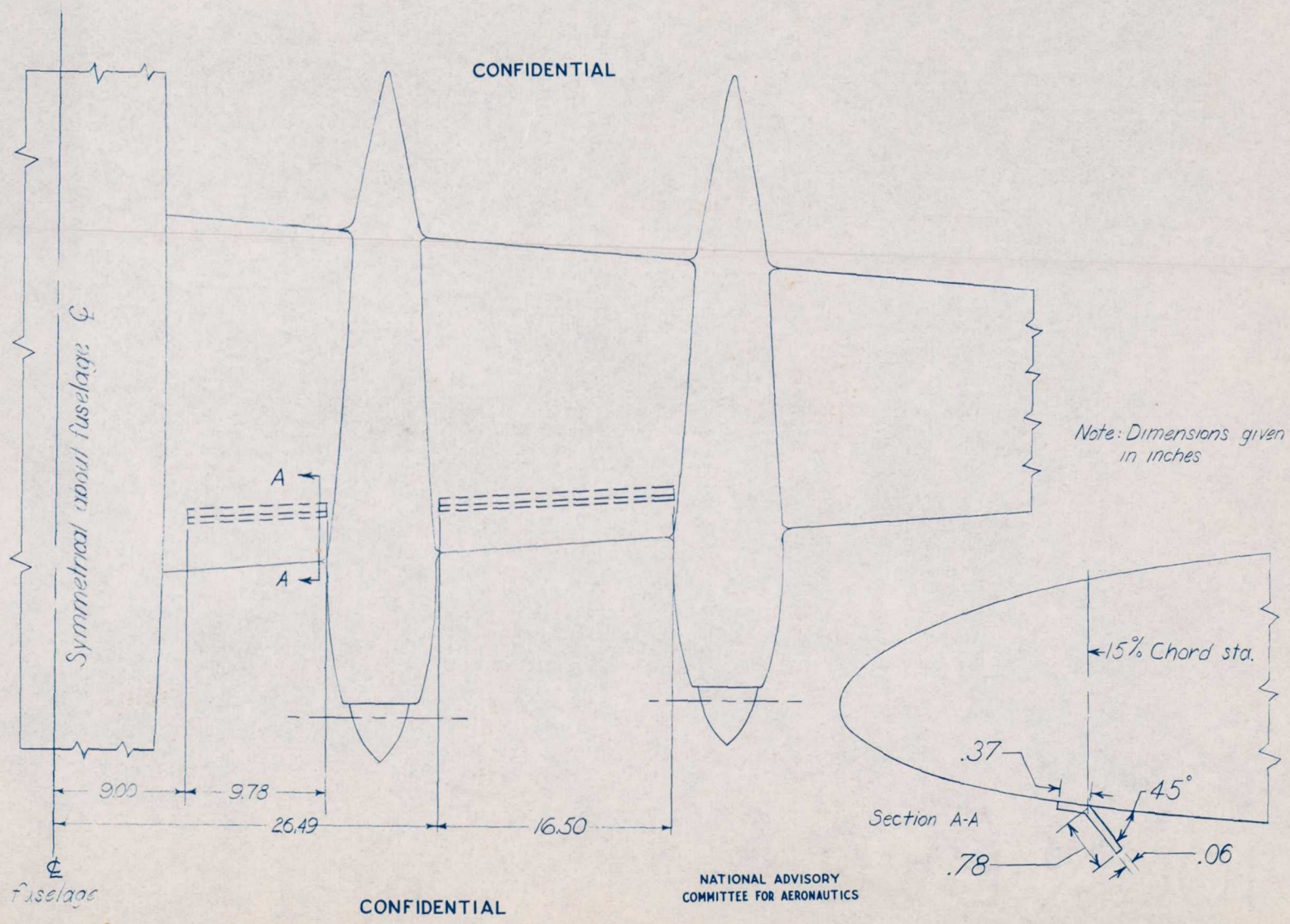


Figure 7.- Sketch of dive recovery flaps of a 1/8.33-scale model of the Republic XF-12 airplane.

Fig. 7

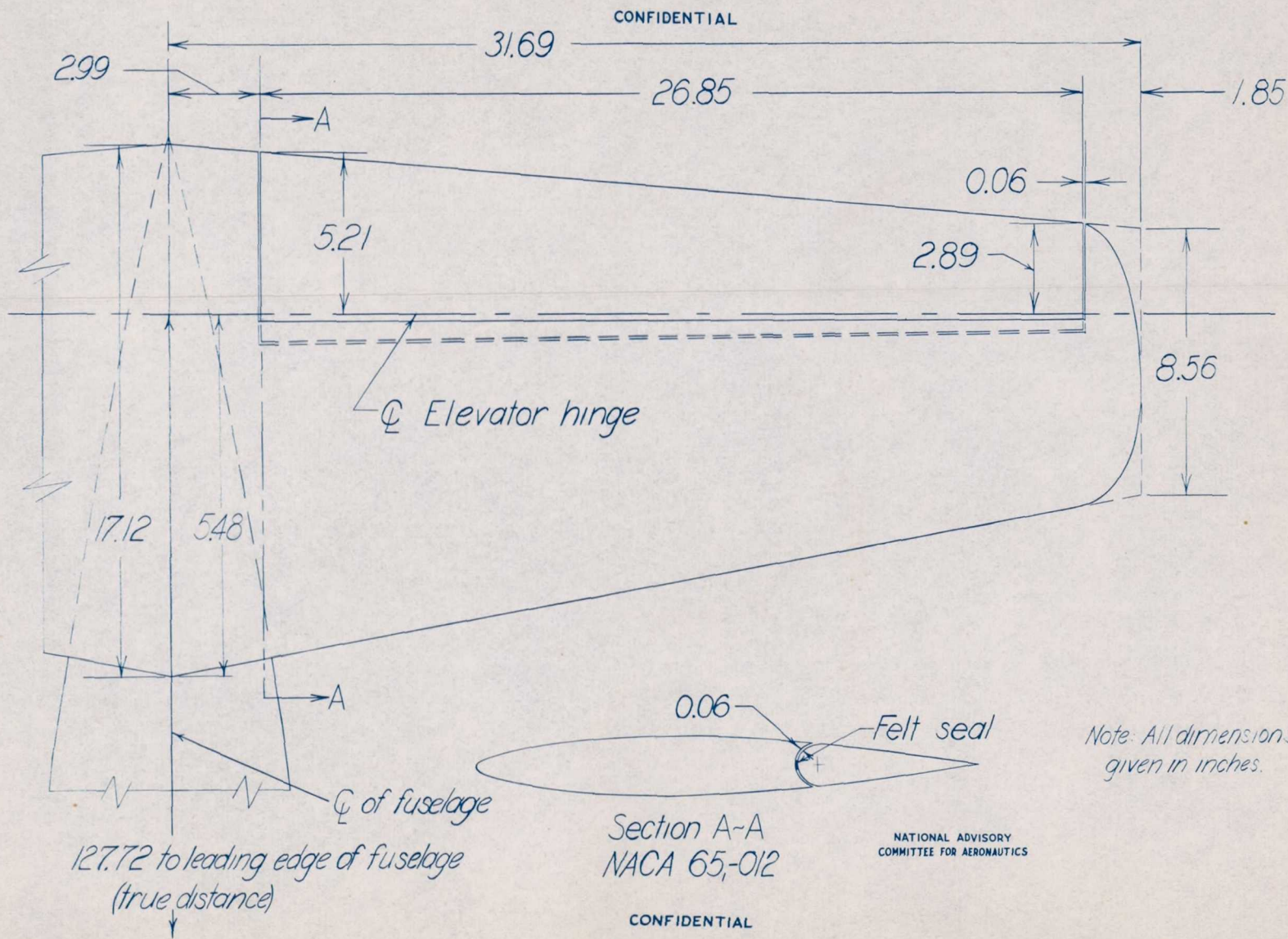


Figure 8.-Plan view of horizontal tail of a 1/8.33-scale model of the Republic XF-12 airplane.

CONFIDENTIAL

NACA RM No. L6L12



(a) Rear view.

Figure 9.- The $\frac{1}{8.33}$ -scale model of the XF-12 airplane with the tail removed.

Fig. 9a

CONFIDENTIAL



(b) Close-up.

Figure 9.- Concluded.

CONFIDENTIAL

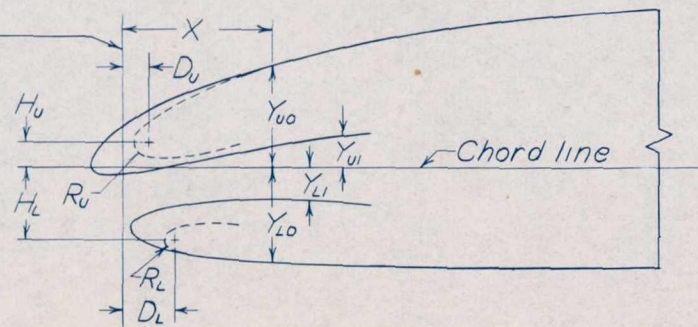
Republic duct lip					
X % chord	X inches	Y_{U0} inches	Y_{U1} inches	Y_{L0} inches	Y_{L1} inches
1.25	0.236	0.466			
2.50	0.473	0.644	0.102		
5.00	0.945	0.895	0.144	-1.083	-0.692
7.50	1.418	1.082	0.263	-1.132	-0.707
10.00	1.891	1.234		-1.163	
15.00	2.836	1.468		-1.195	
20.00	3.781	1.643		-1.211	
25.00	4.726	1.770		-1.222	
30.00	5.672	1.860		-1.223	
35.00	6.617	1.917		-1.218	

$R_U = 0.183$ in.	$R_L = 0.125$ in.
$H_U = 0.296$ in.	$H_L = -0.884$ in.
$D_U = 0.325$ in.	$D_L = 0.646$ in.

NACA duct lip #5					
X % chord	X inches	Y_{U0} inches	Y_{U1} inches	Y_{L0} inches	Y_{L1} inches
-2.00	-0.378	0	0		
-1.25	-0.236	0.278	-0.097		
0	0	0.480	-0.087		
0.48	0.091			-0.750	-0.750
1.25	0.236	0.629	-0.062	-0.898	-0.589
2.50	0.473	0.754	-0.020	-0.990	-0.511
5.00	0.945	0.958	0.074	-1.088	-0.431
7.50	1.418	1.105	0.165	-1.133	-0.394
10.00	1.891	1.241	0.254	-1.161	-0.385
15.00	2.836	1.468	0.388	-1.195	-0.432
20.00	3.781	1.648		-1.221	
25.00	4.726	1.769		-1.232	
30.00	5.672	1.853		-1.230	
35.00	6.617	1.917		-1.219	

NACA RM No. L6L12

Chordwise location of leading edge of basic section



----- Republic lip
 ————— NACA lip No. 5

Sta. 43.277
 Basic chord 18.905 in.

NATIONAL ADVISORY
 COMMITTEE FOR AERONAUTICS

CONFIDENTIAL

Figure 10.- Sketch of the wing-duct lip of a 1/8.33-scale model of the Republic XF-12 airplane.

Fig. 10

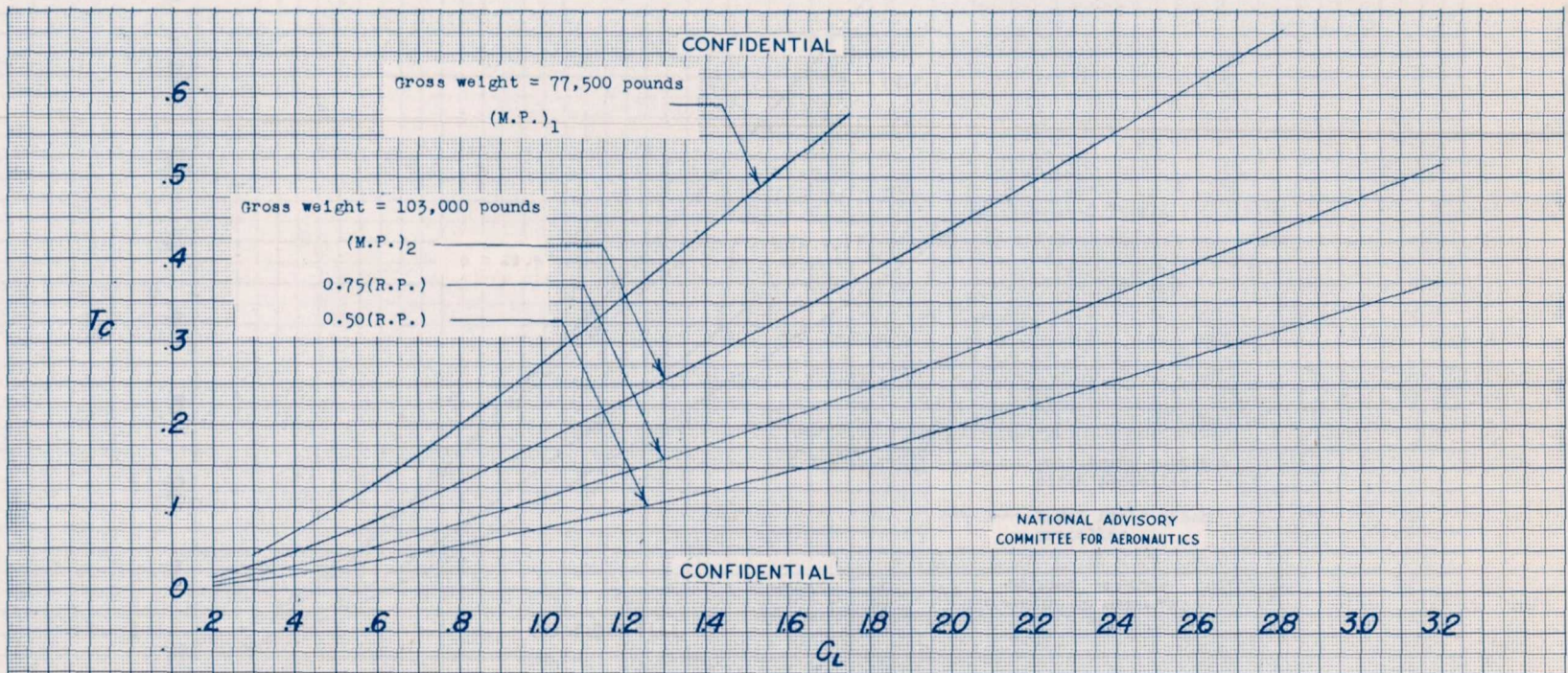


Figure 11.- Variation of thrust coefficient with lift coefficient for several power conditions at sea level.

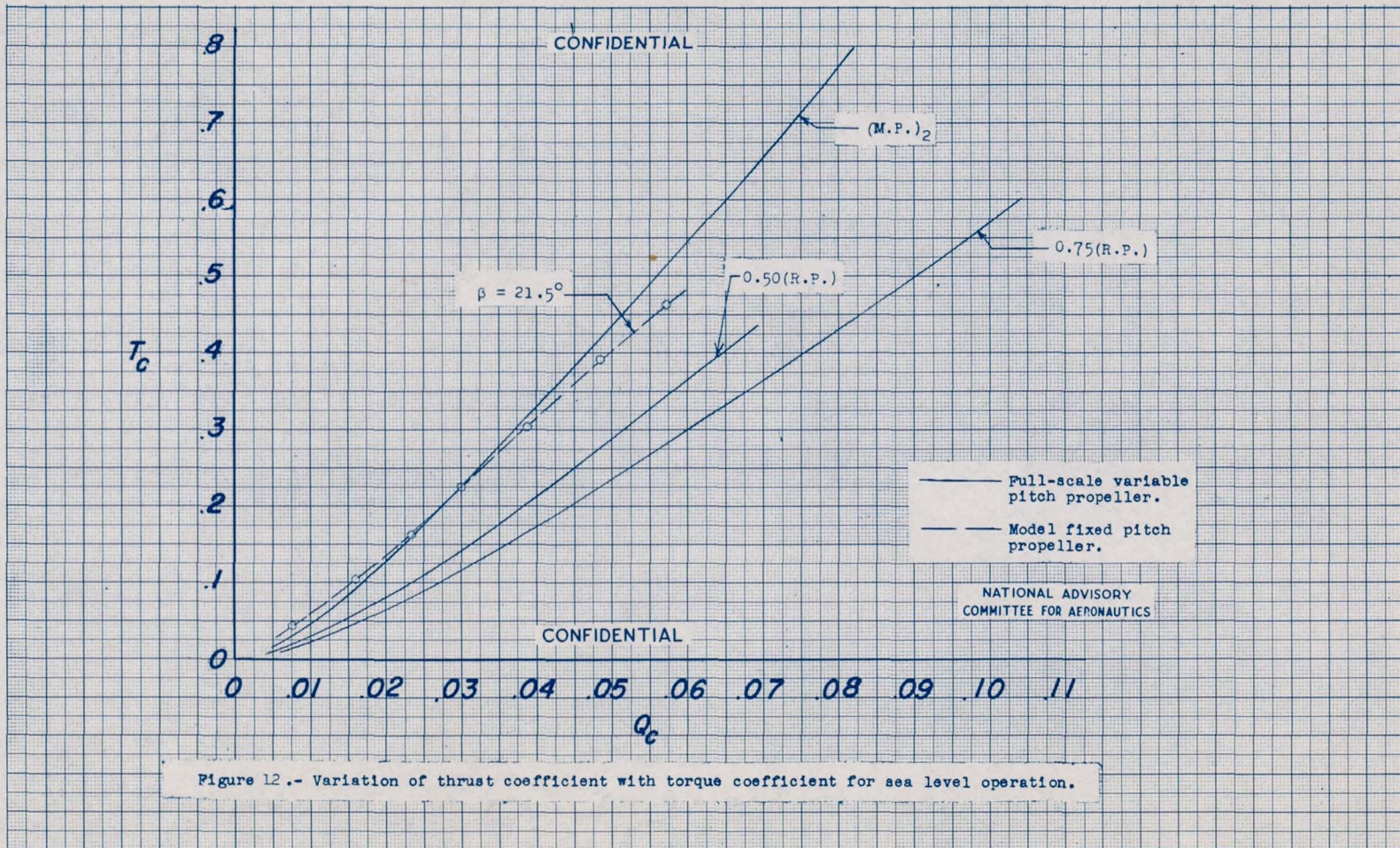


Figure 12.- Variation of thrust coefficient with torque coefficient for sea level operation.



Figure 13.- Nacelle entrance sealed.

NATIONAL ADVISORY COMMITTEE FOR AERONAUTICS
LANGLEY MEMORIAL AERONAUTICAL LABORATORY - LANGLEY FIELD, VA.

CONFIDENTIAL

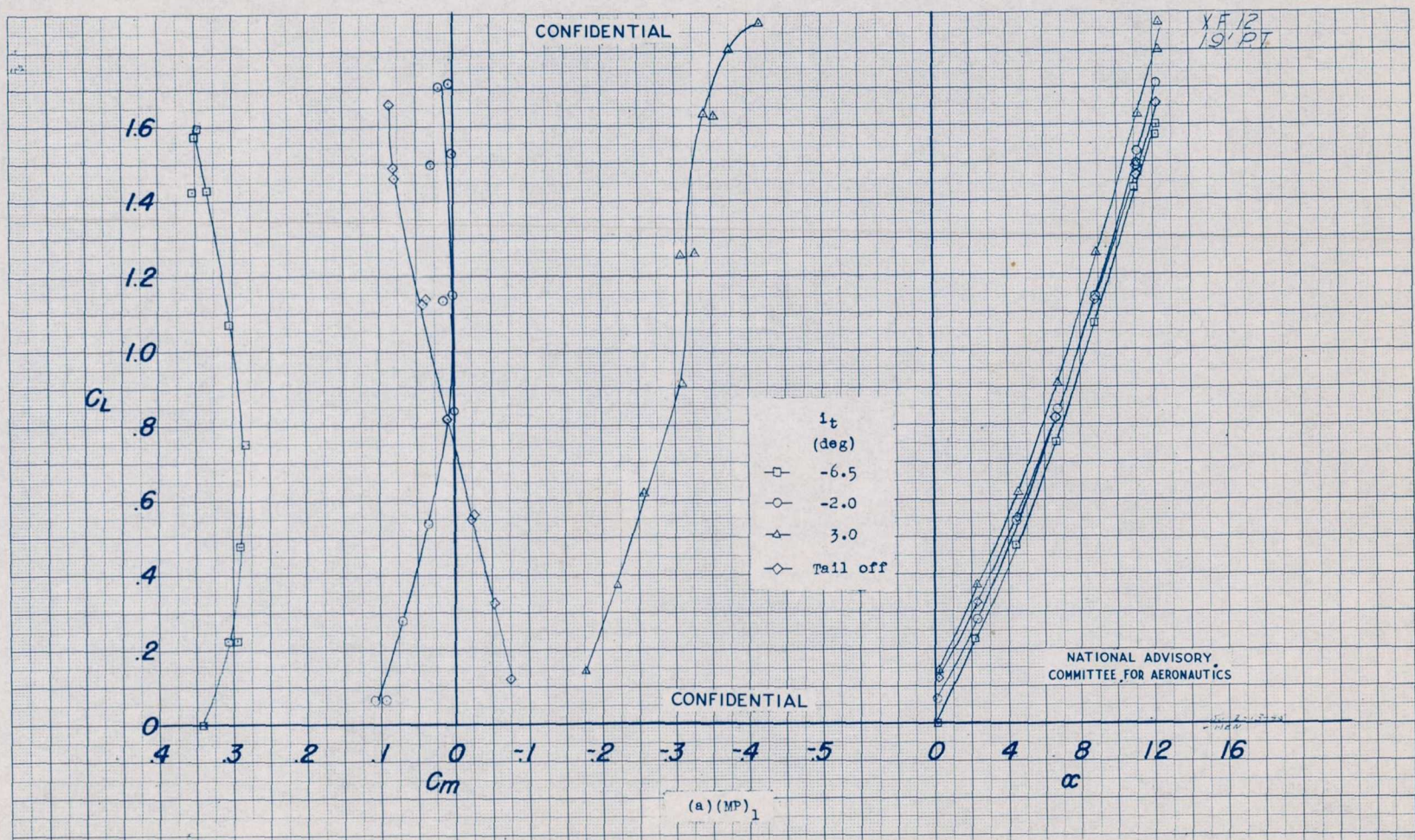


Figure 14.- Effect of stabilizer incidence on several aerodynamic characteristics. $\delta_f = 0^\circ$; $\delta_e = 0^\circ$; $R \approx 2,390,000$; $M \approx 0.09$.

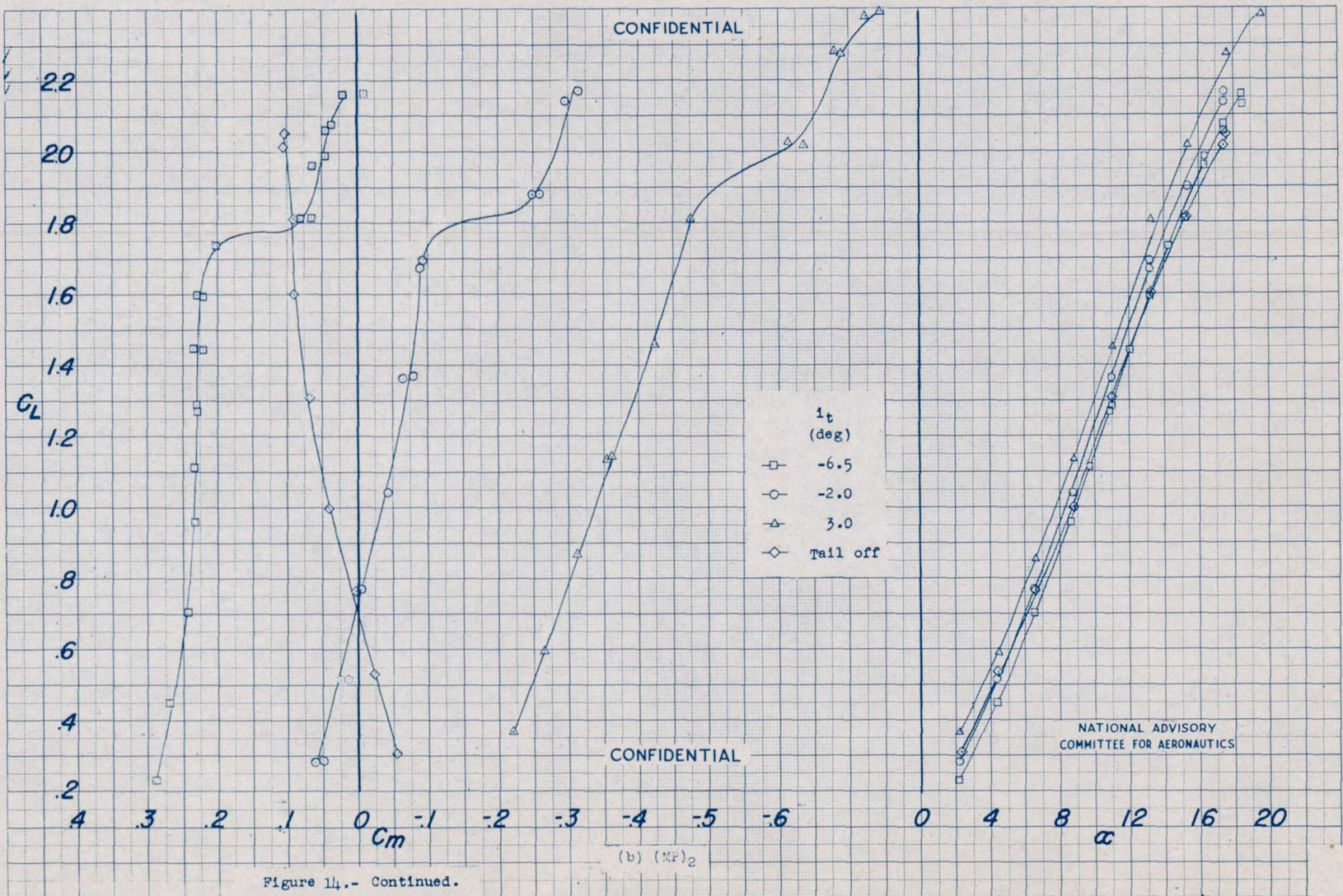


Figure 14.- Continued.

(b) (MF)₂

NATIONAL ADVISORY
COMMITTEE FOR AERONAUTICS

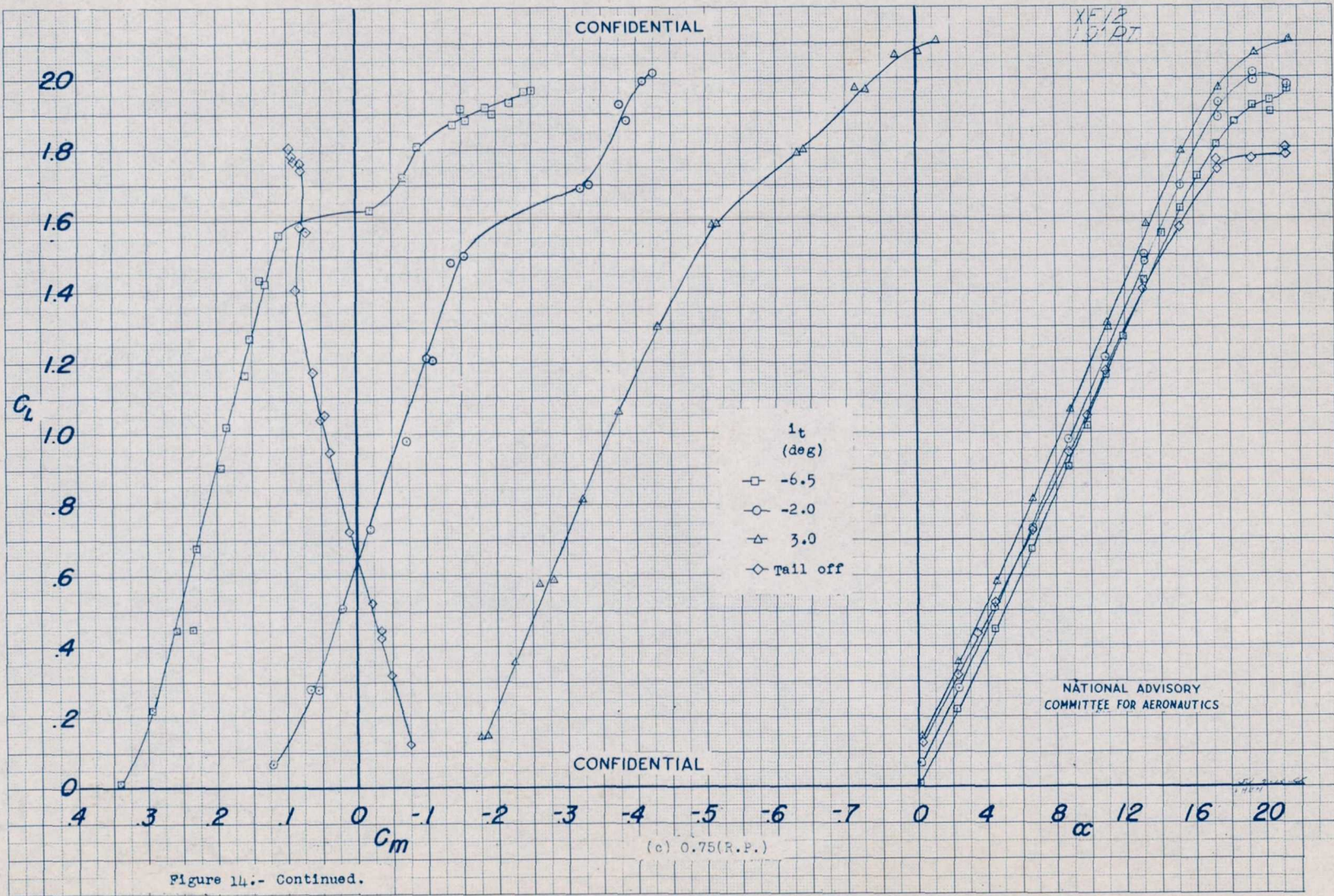


Figure 14c.- Continued.

XF12
19.5T

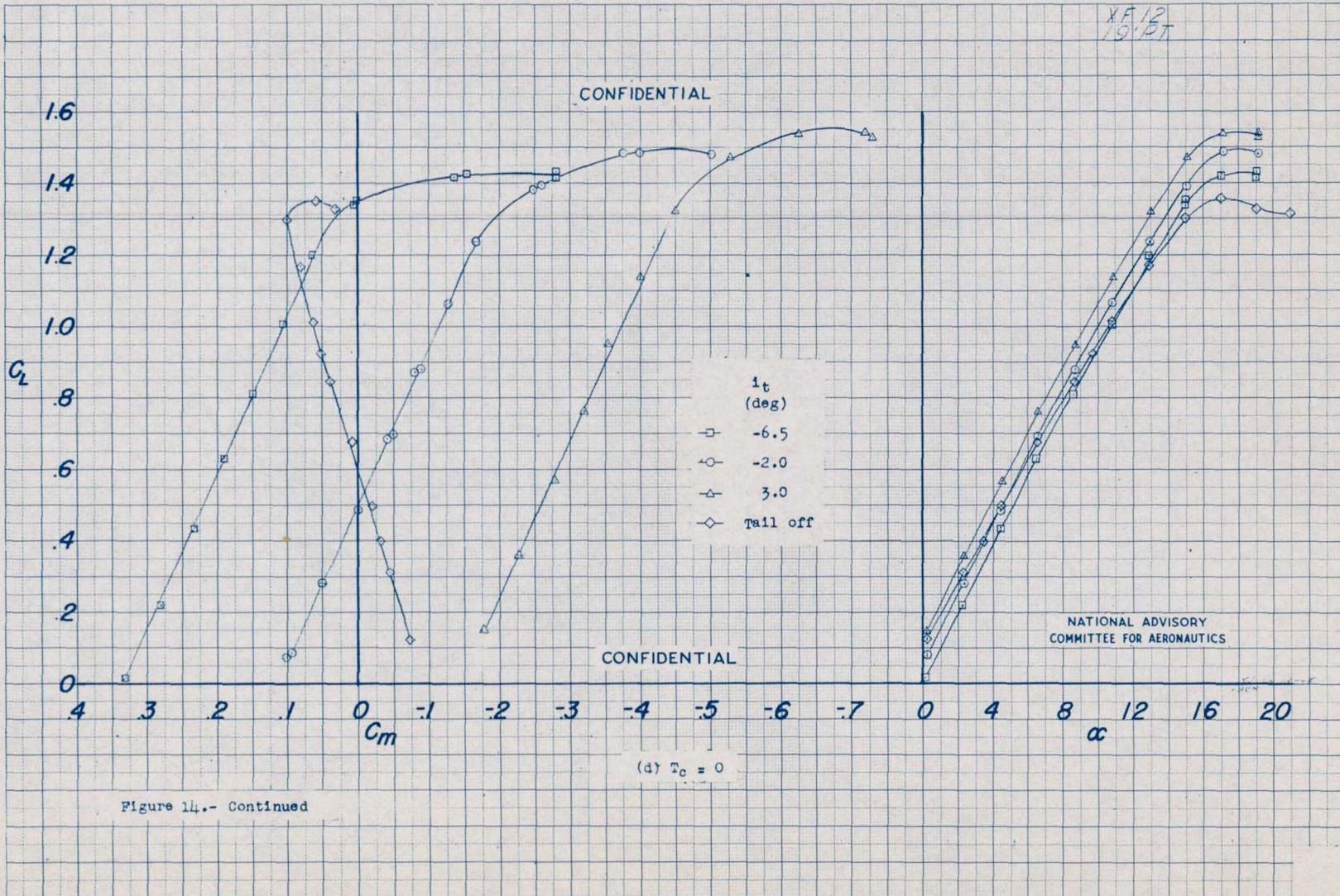
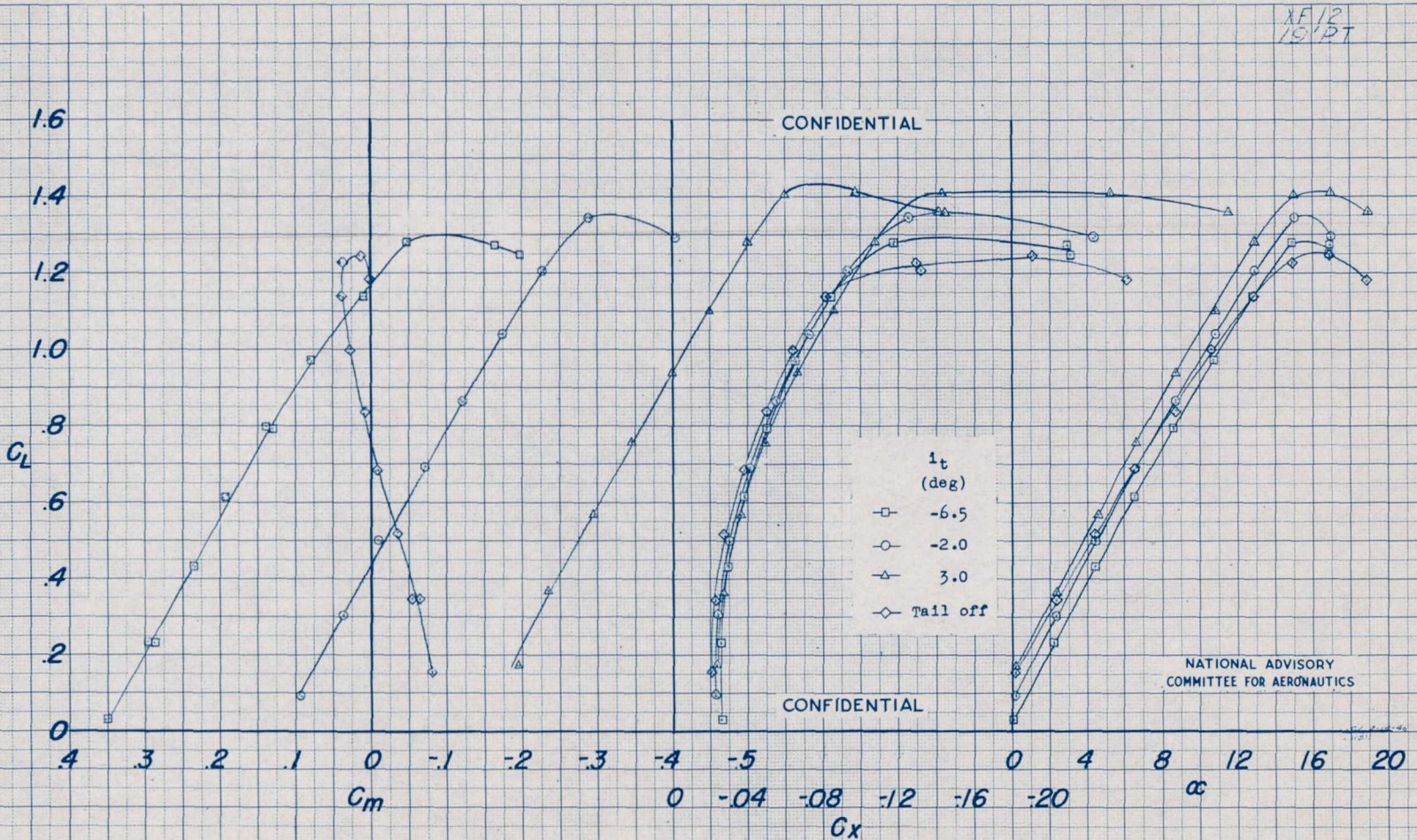


Figure 14.- Continued



XF12
19/27



(e) Propellers removed

Figure 14.- Concluded.

1955

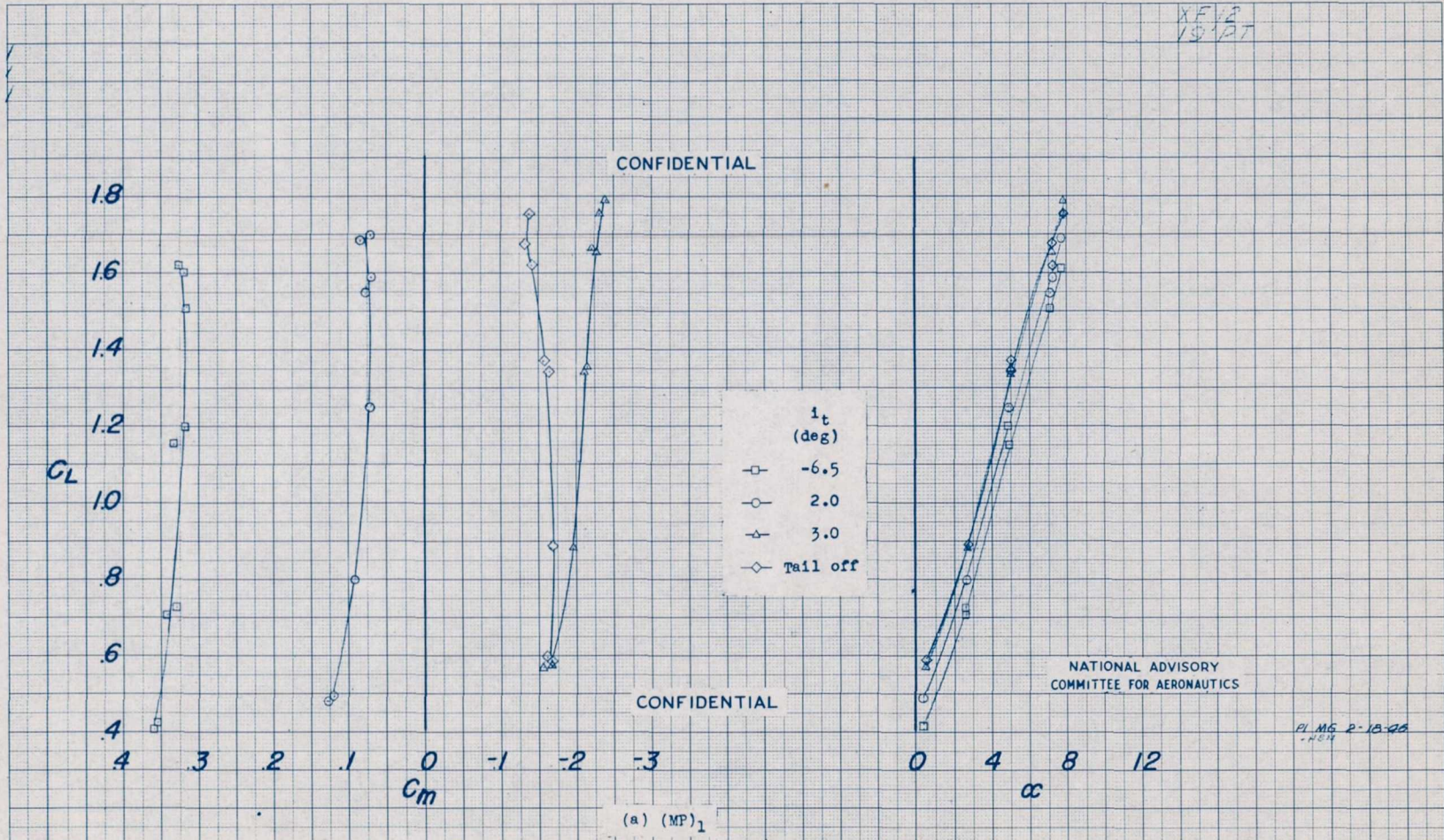


Figure 15.- Effect of stabilizer incidence on several aerodynamic characteristics. $\delta_r = 20^\circ$; $\delta_e = 0$; $R \approx 2,380,000$; $M \approx 0.09$.

1900

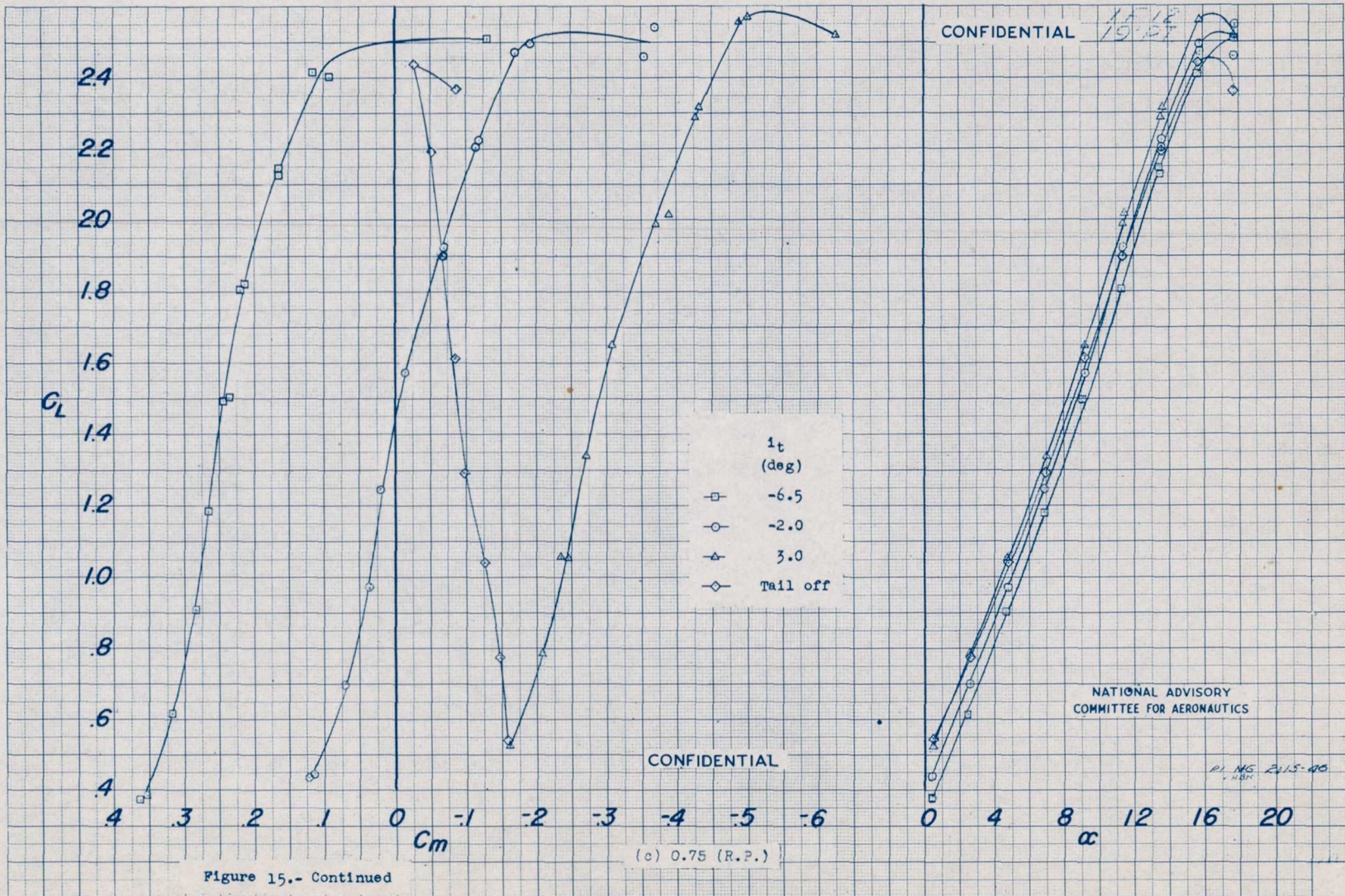


Figure 15.- Continued

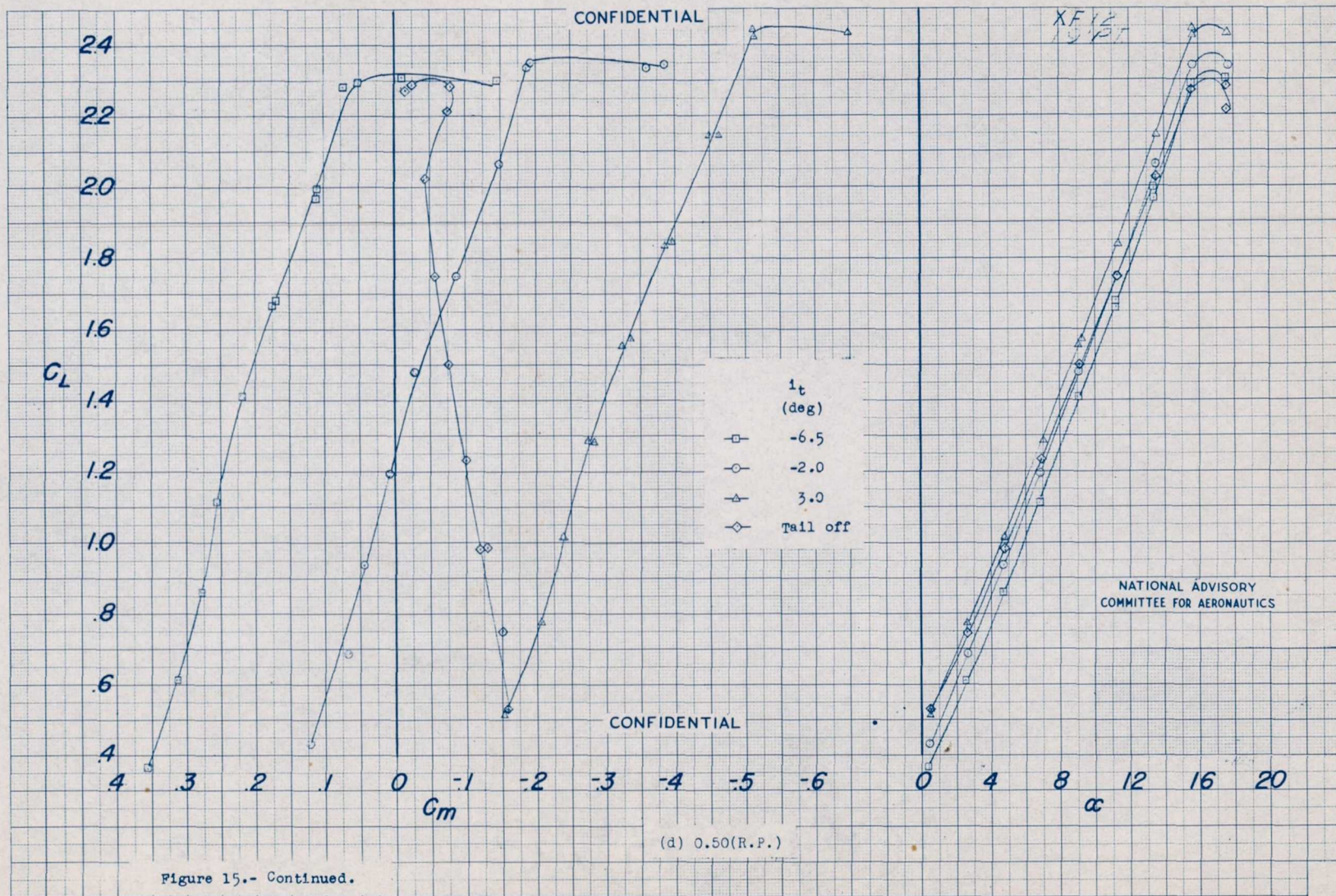


Figure 15.- Continued.

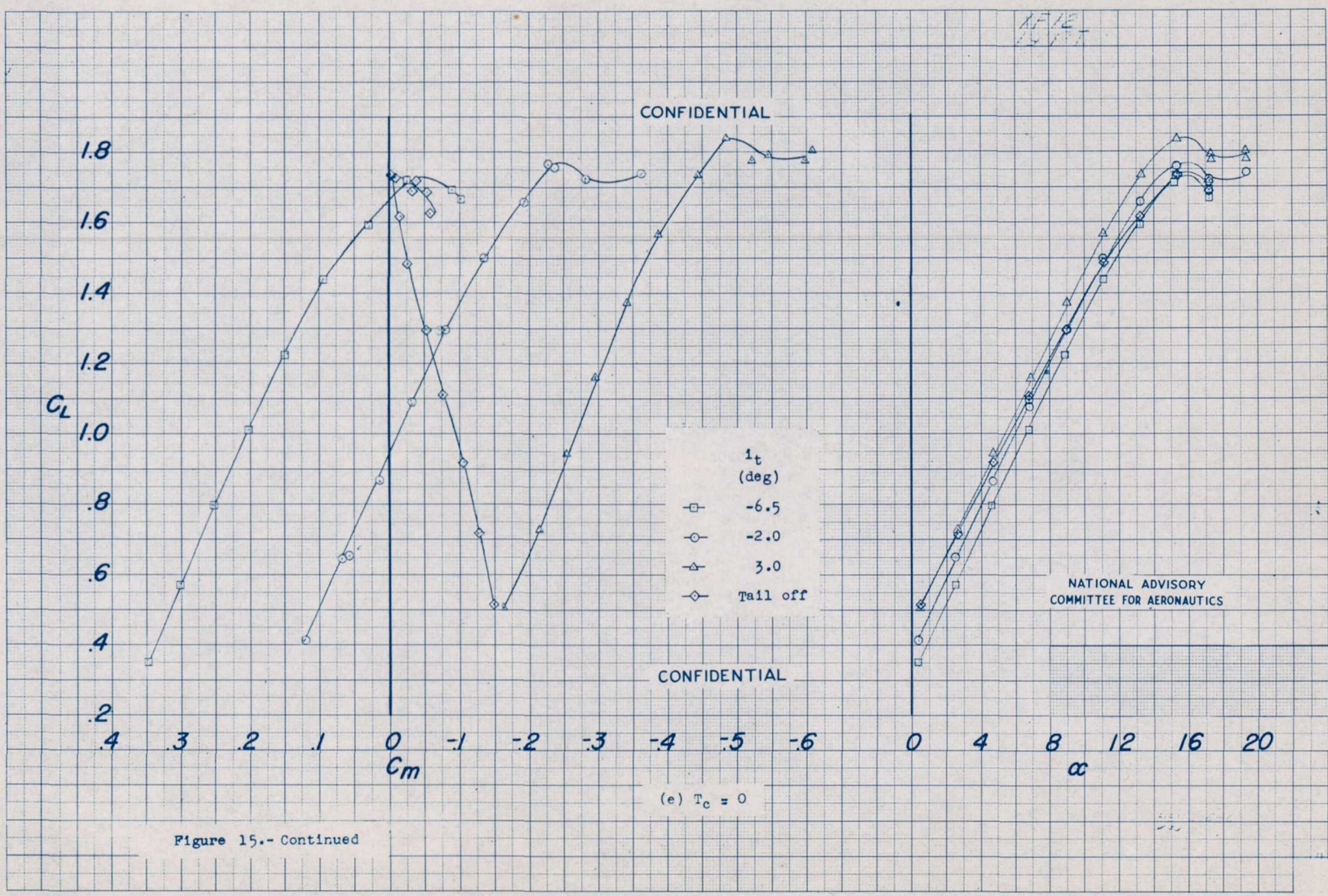


Figure 15.- Continued

Fig. 15e

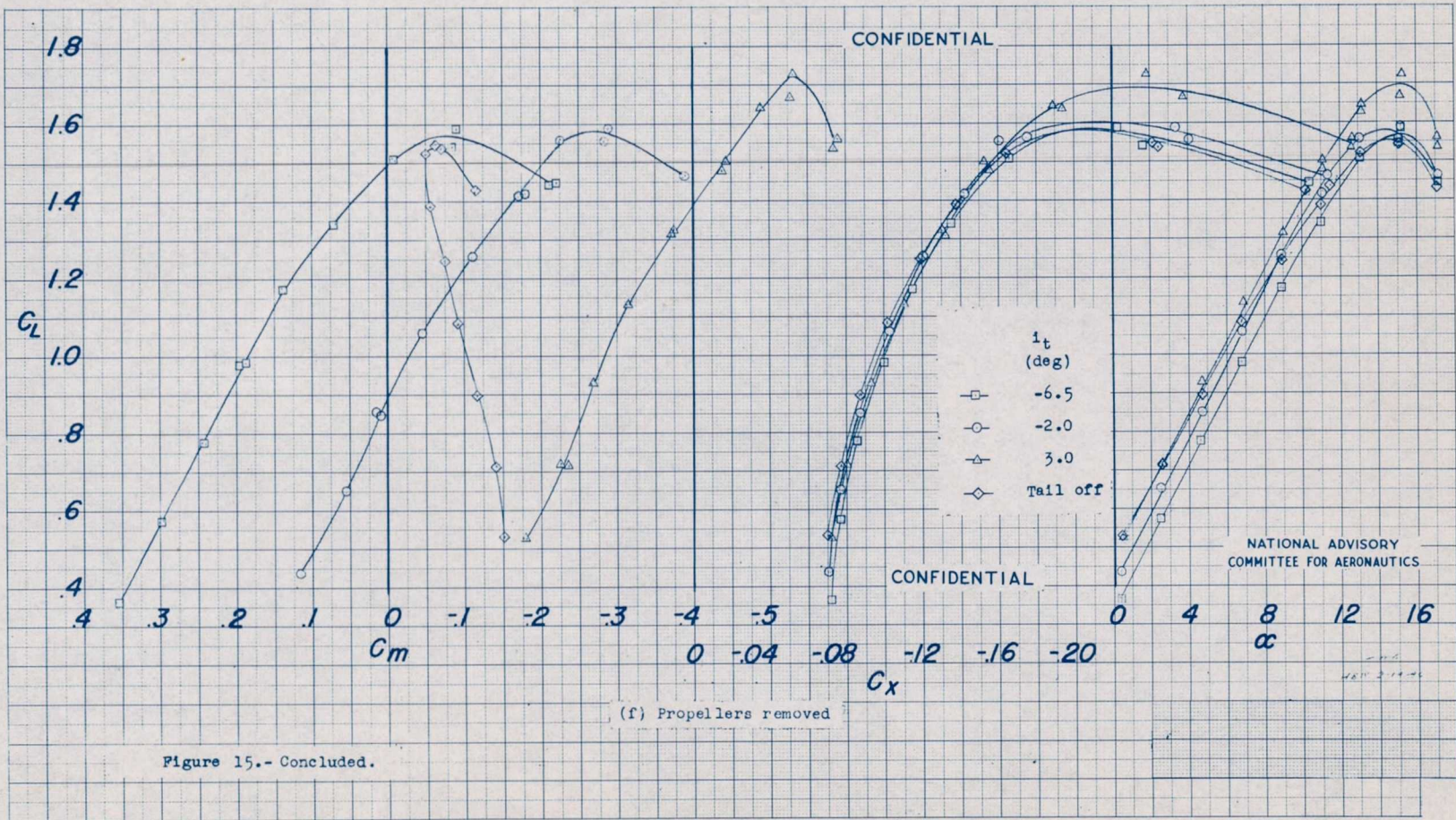


Figure 15.- Concluded.

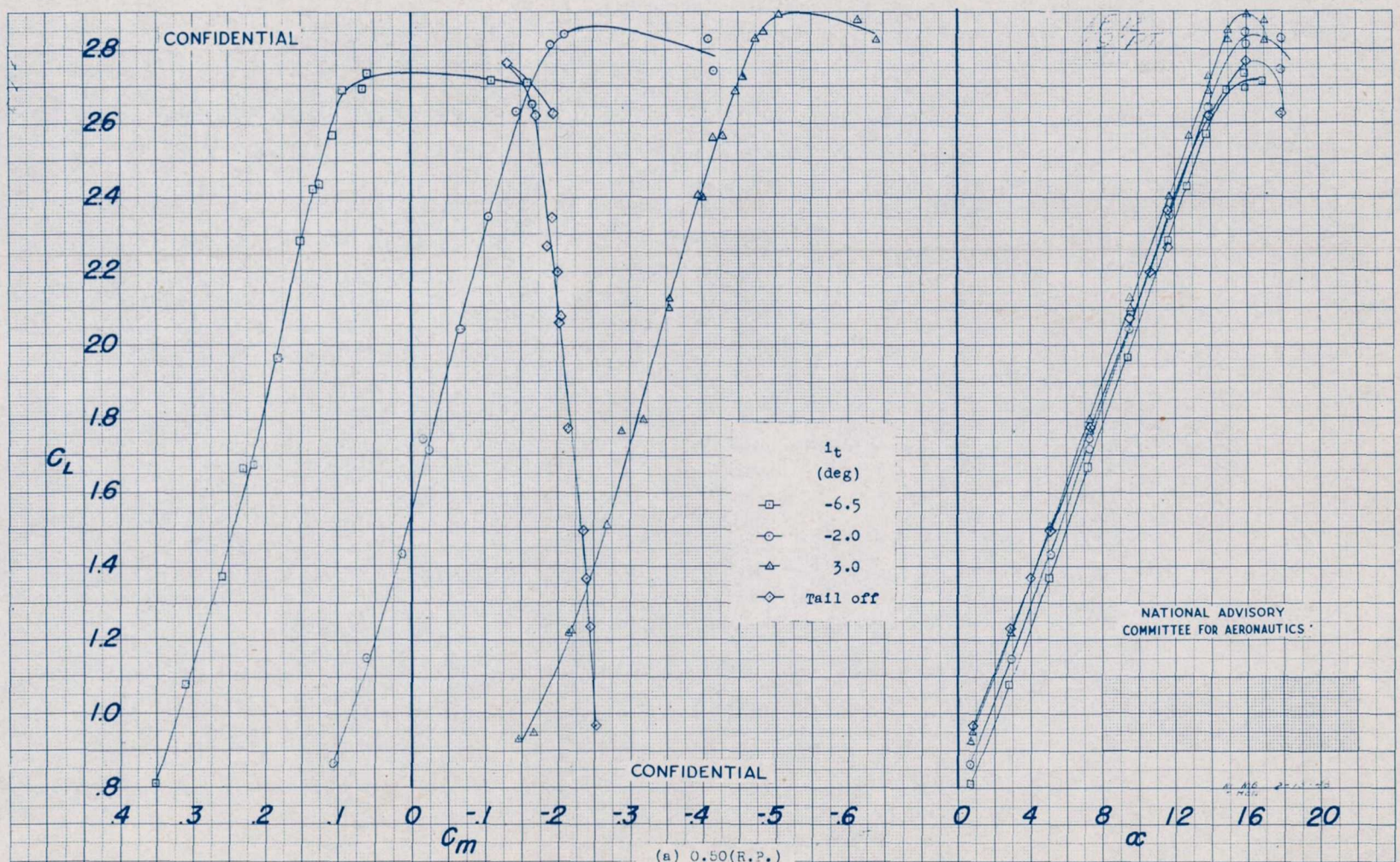


Figure 16.- Effect of stabilizer incidence on several aerodynamic characteristics. $\delta_r = 40^\circ$; $\delta_e = 0^\circ$; $R \approx 2,380,000$; $M \approx 0.09$.

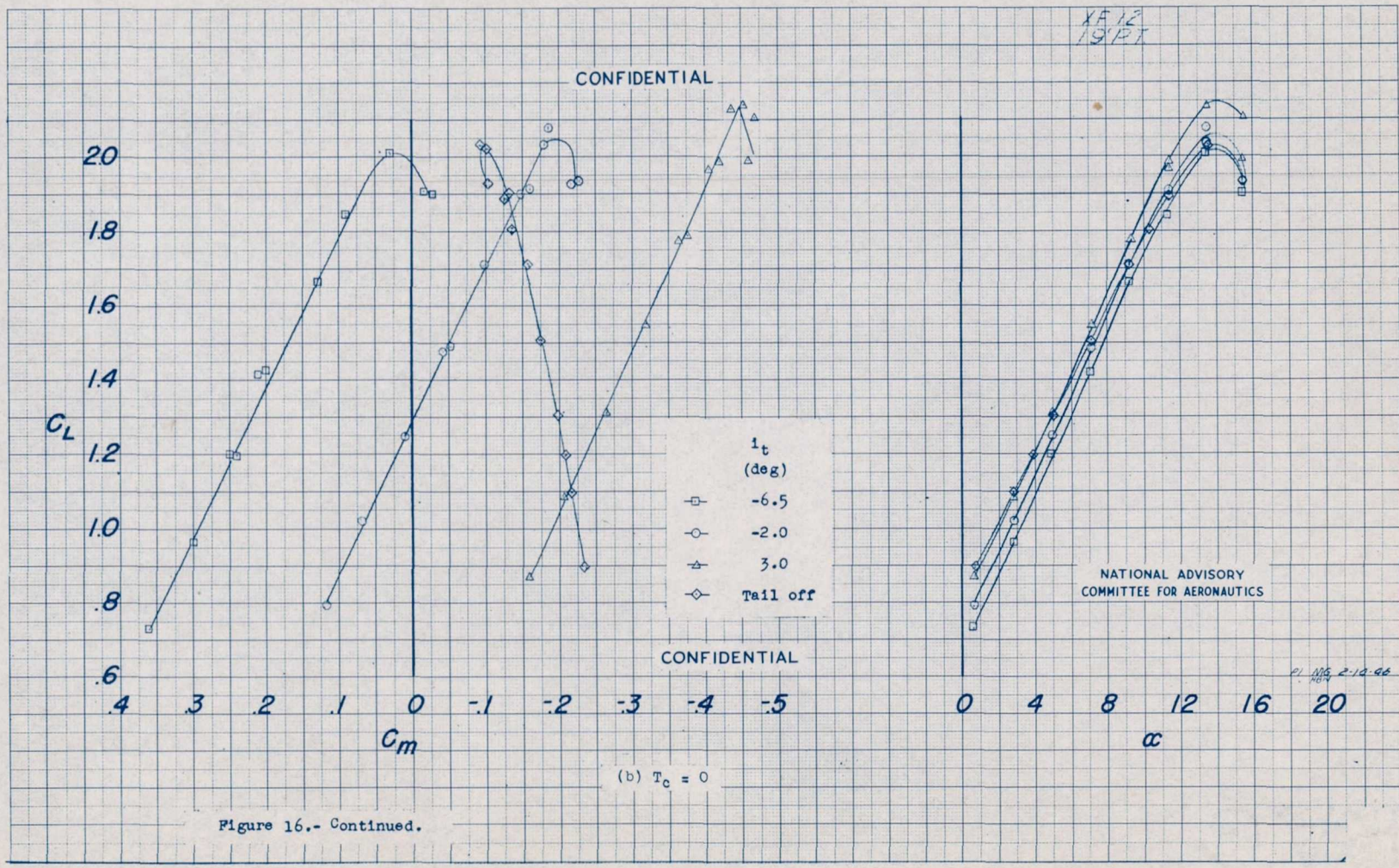
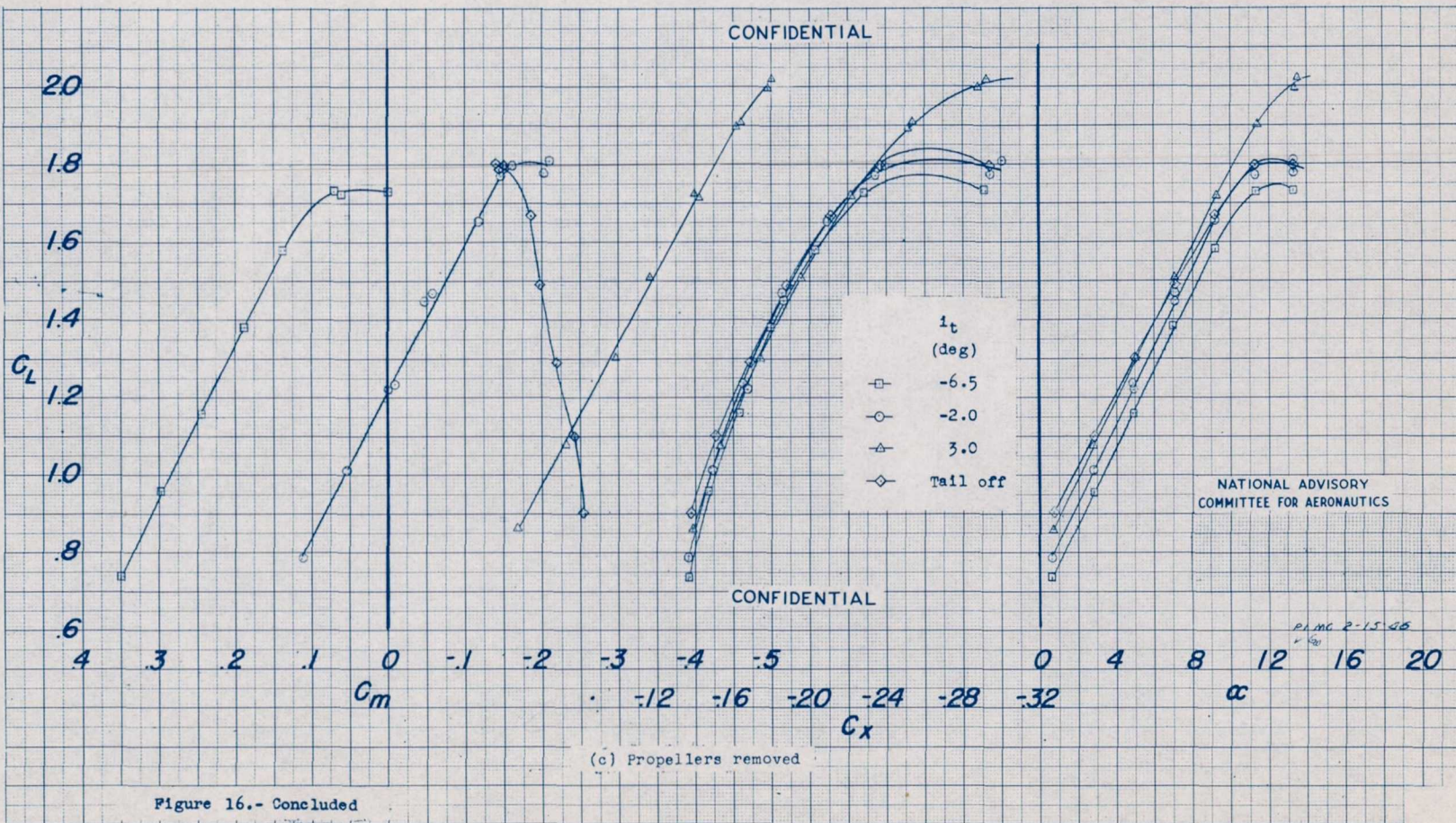


Figure 16.- Continued.



1968

NACA RM No. L6L12

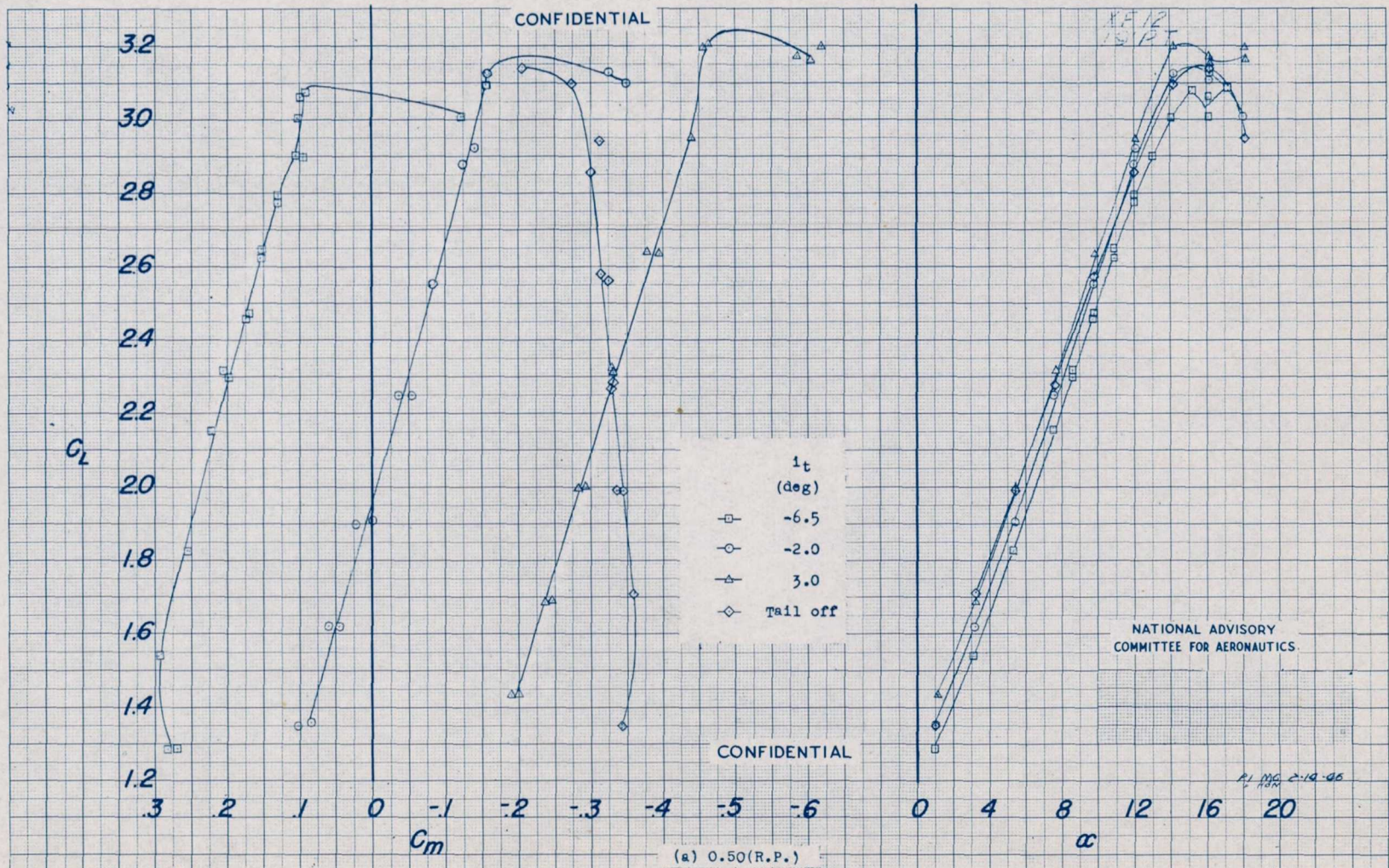


Figure 17.- Effect of stabilizer incidence on several aerodynamic characteristics. $\delta_r = 65^\circ$; $\delta_e = 0^\circ$; $R \approx 2,370,000$; $M \approx 0.09$.

Fig. 17a

1966

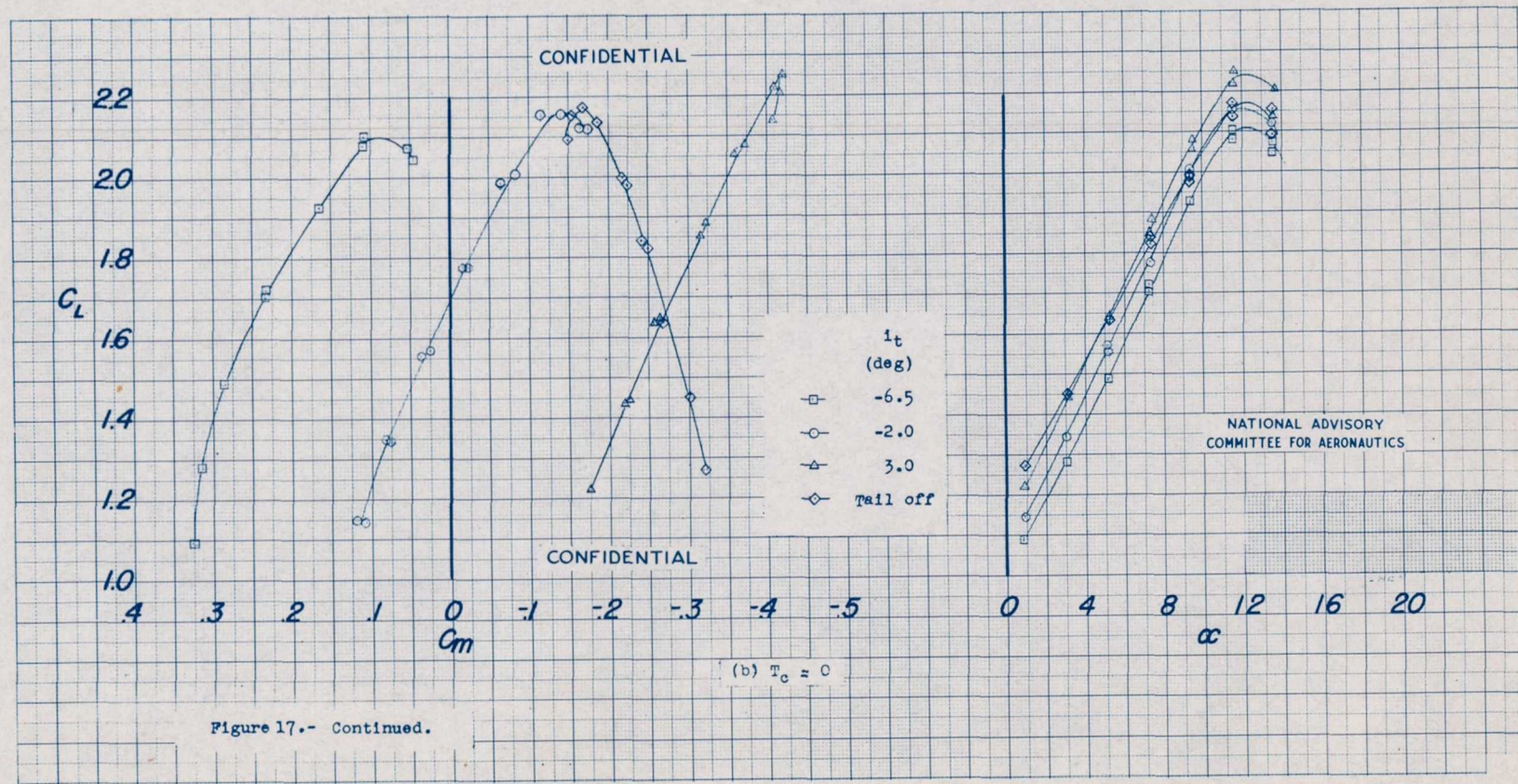


Figure 17.- Continued.

1955

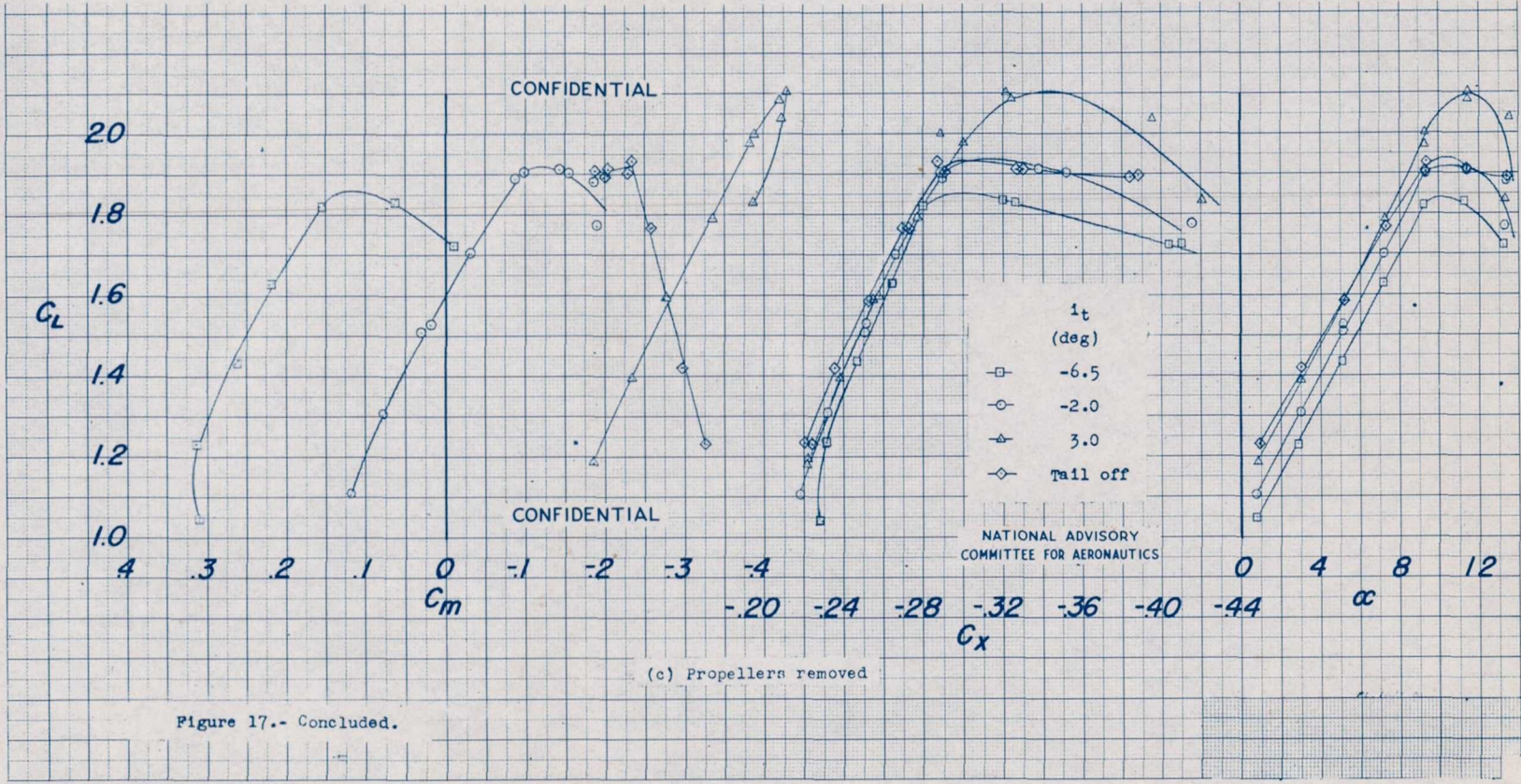


Figure 17.- Concluded.

(c) Propellers removed

1900

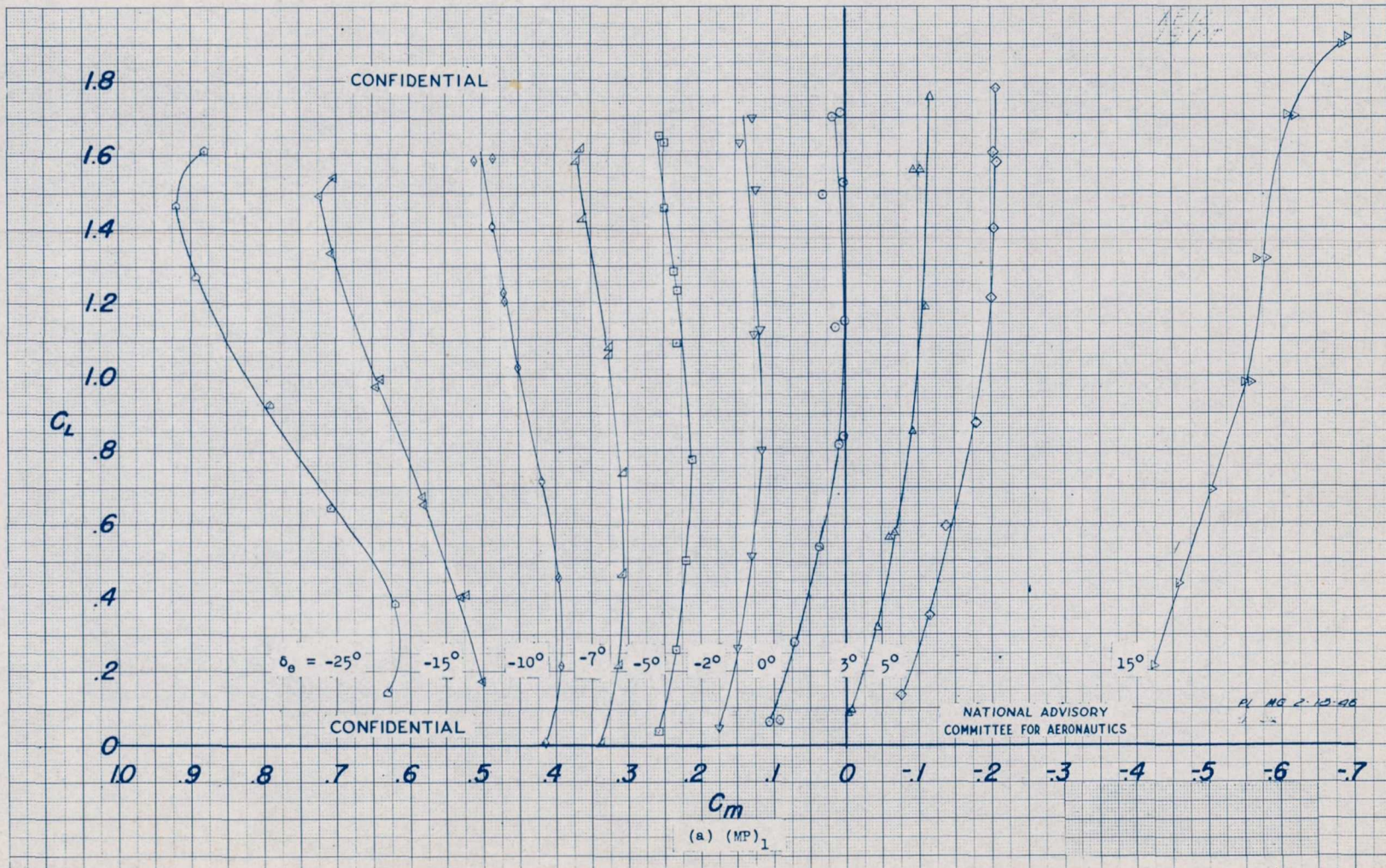


Figure 18.- Effect of elevator deflection on several aerodynamic characteristics. $\delta_f = 0^\circ$; $i_t = -2^\circ$; $R \approx 2,350,000$; $M \approx 0.09$.

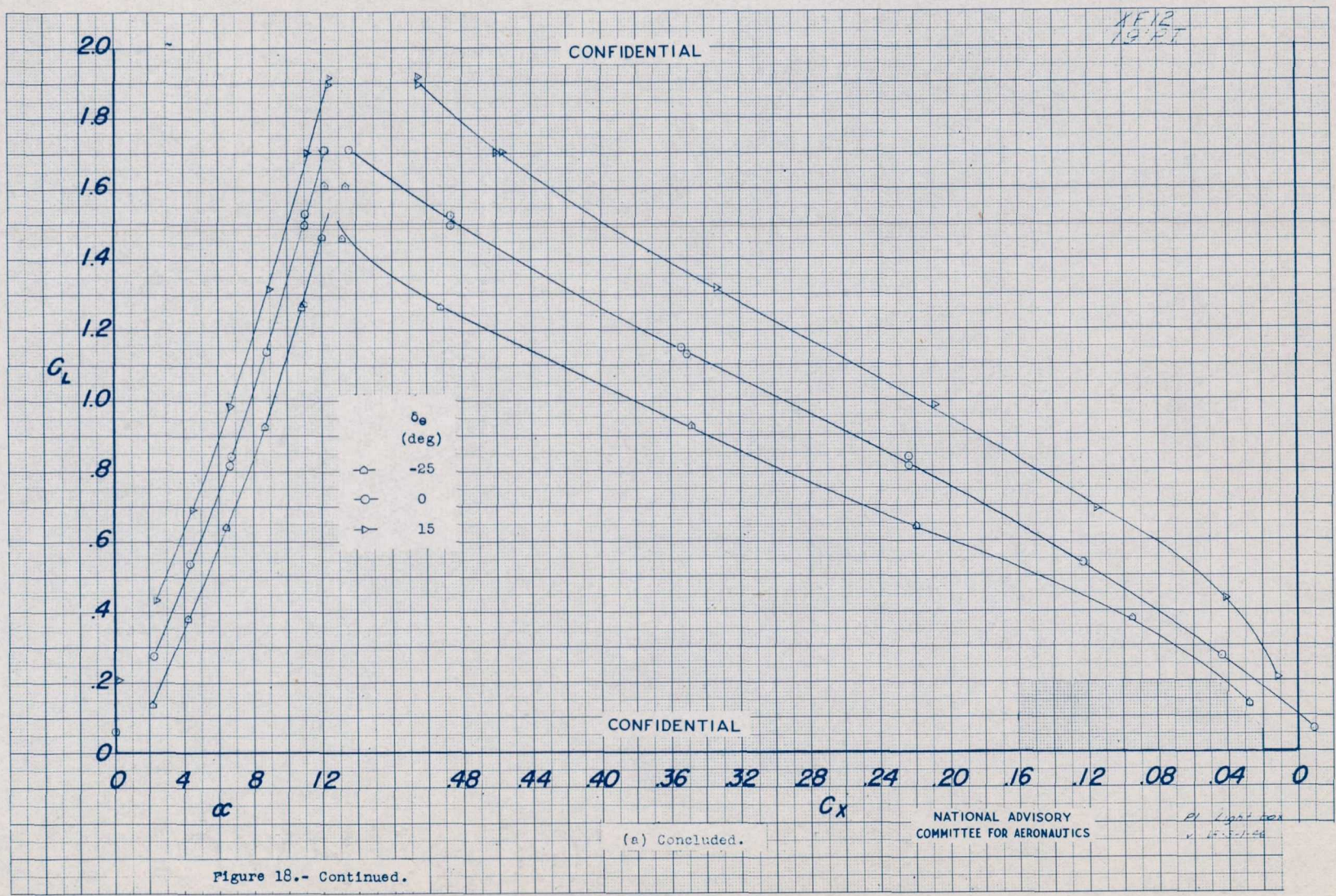


Figure 18.- Continued.

Fig. 18a conc.

1955

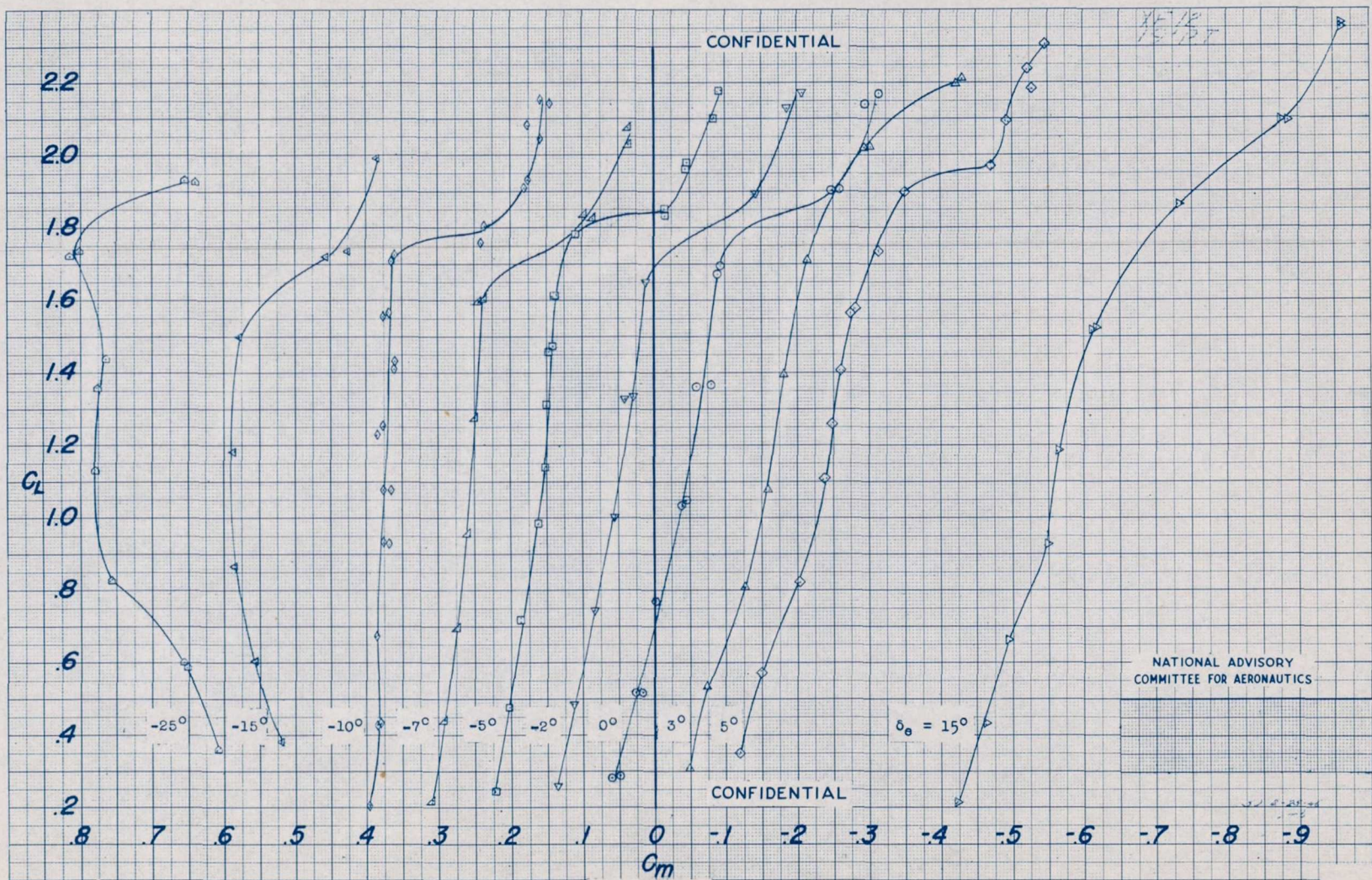


Figure 18.- Continued.

(b) (MF)₂

1956

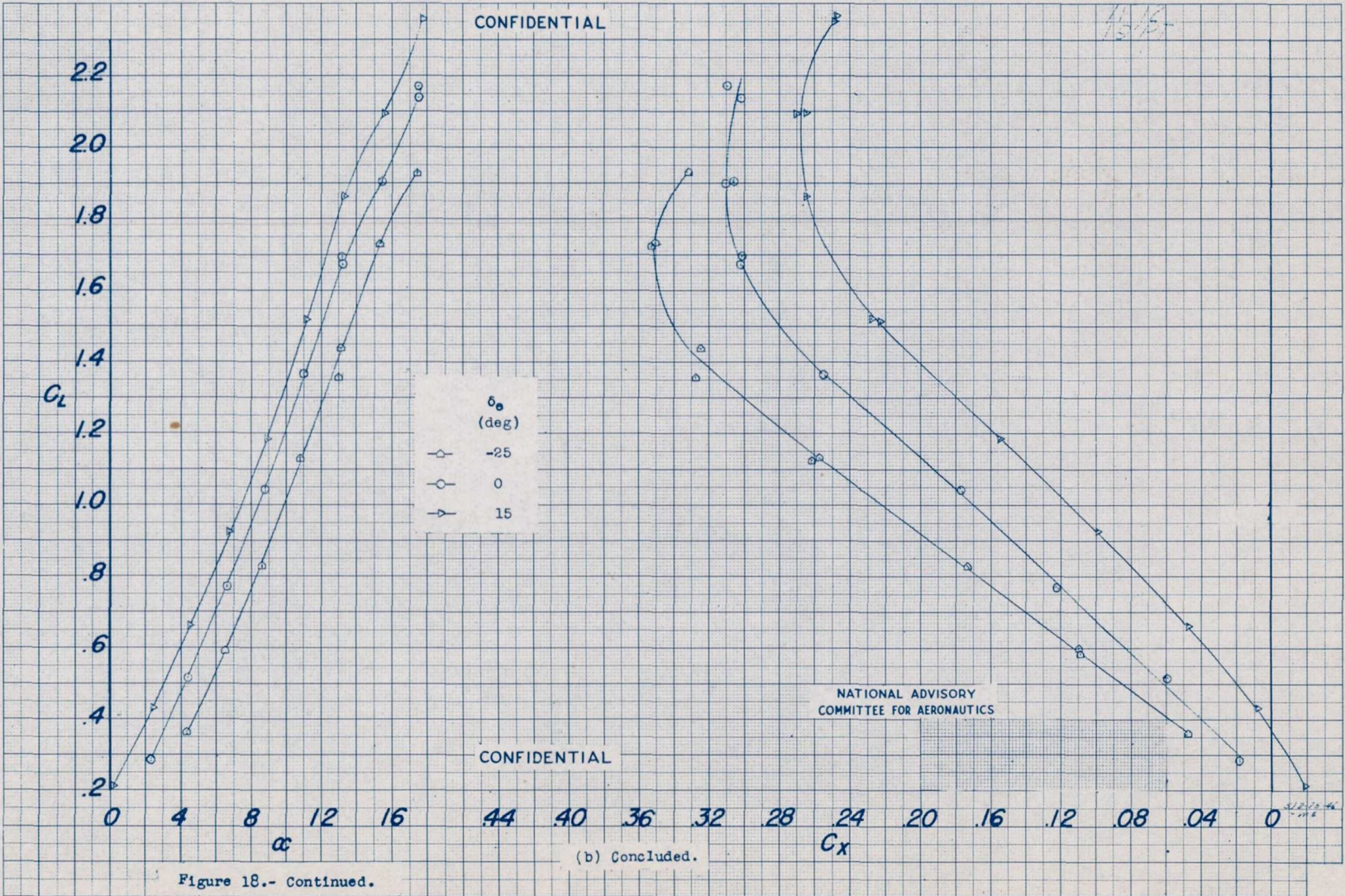


Figure 18.- Continued.

Fig. 18b conc.

1956

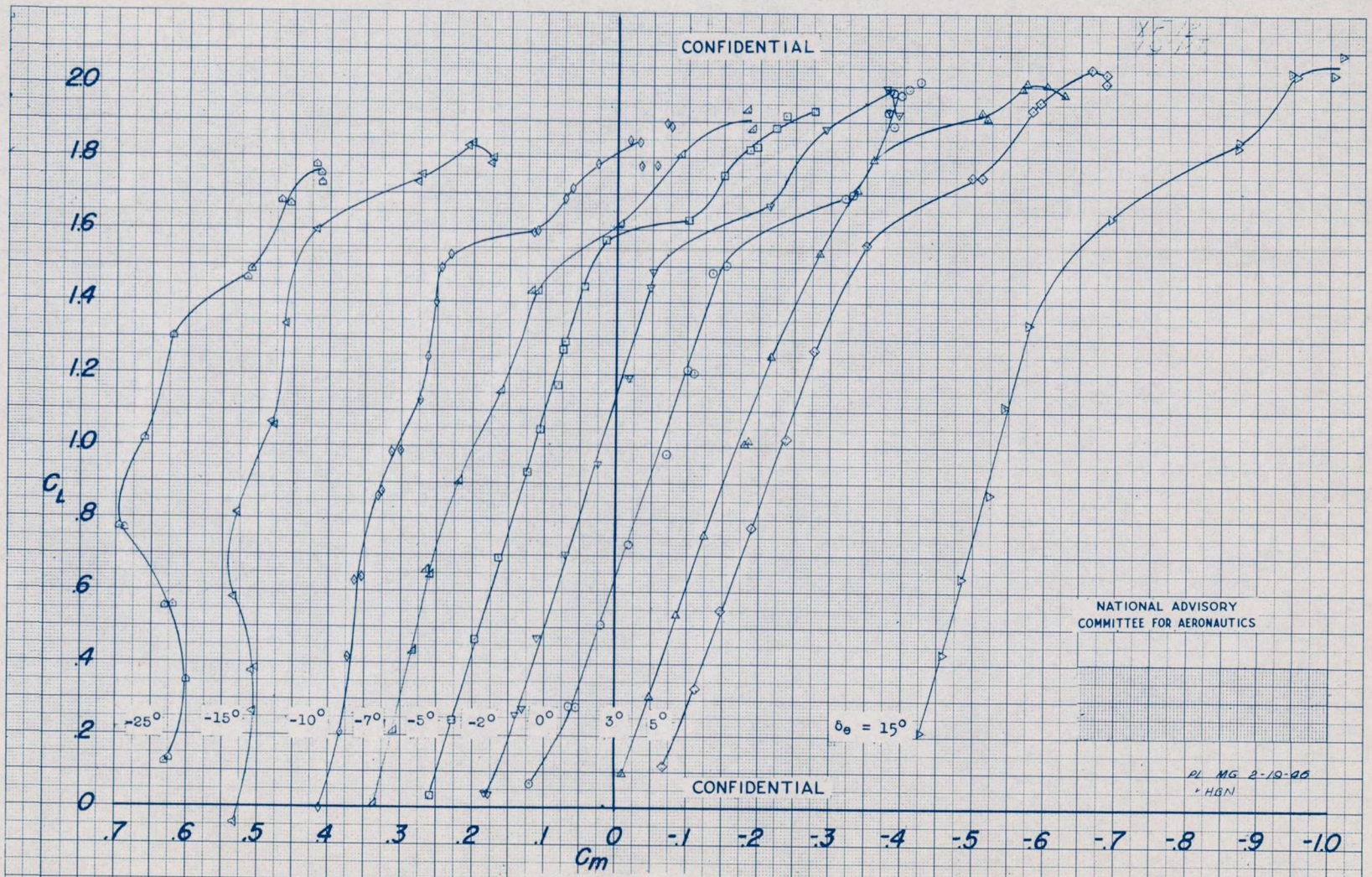


Figure 18.- Continued.

(c) 0.75(R.P.)

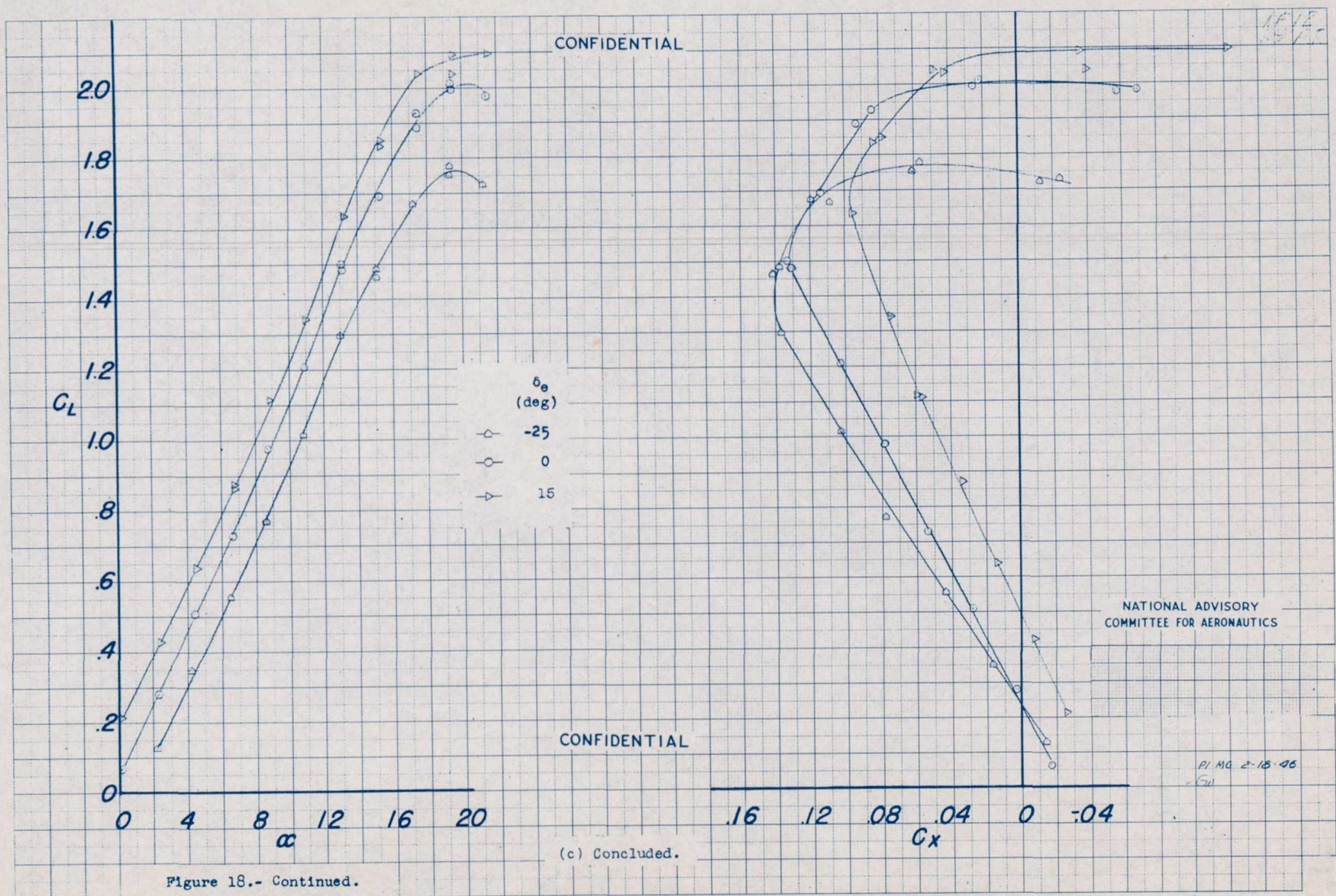
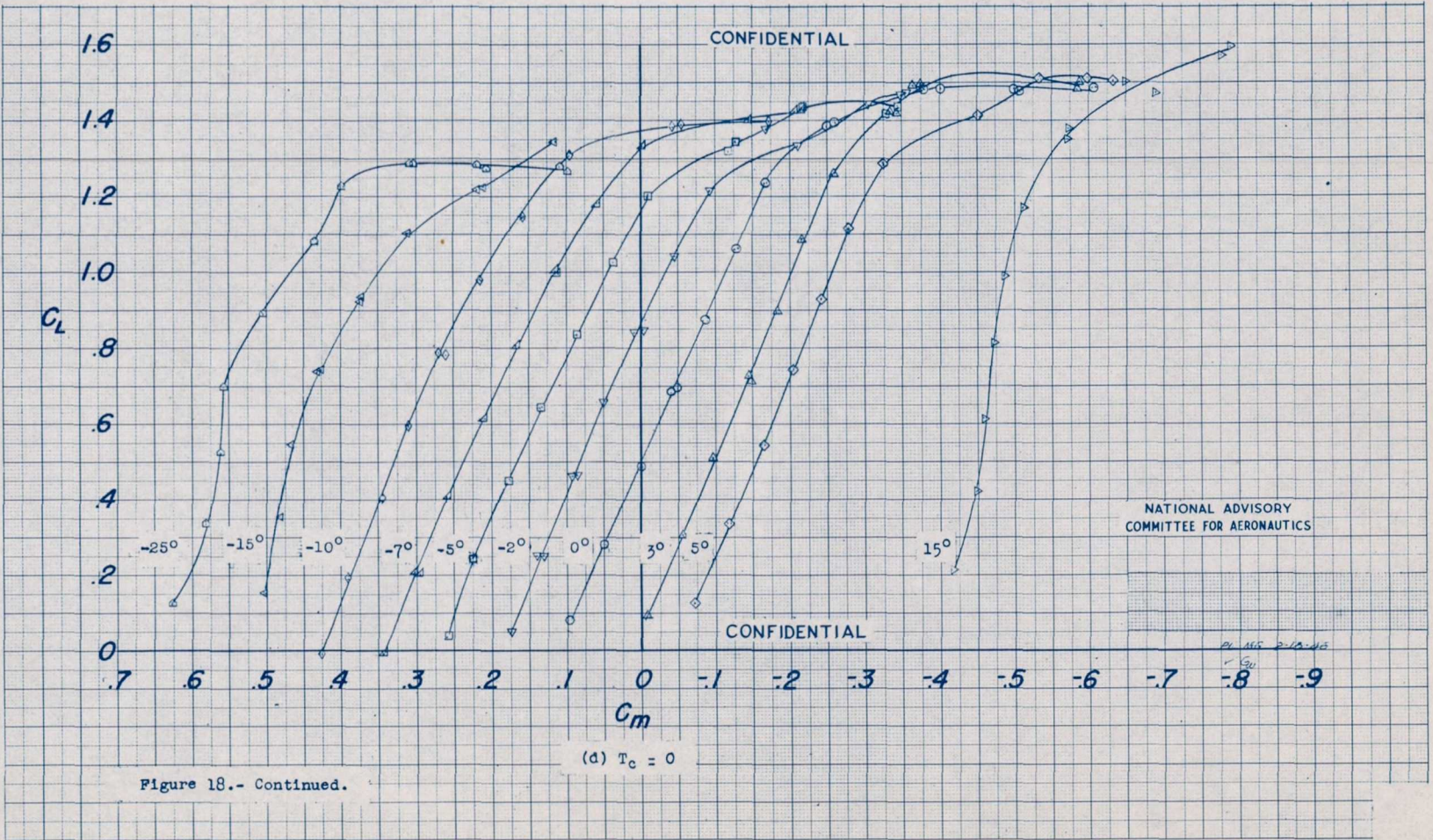


Figure 18.- Continued.

(c) Concluded.



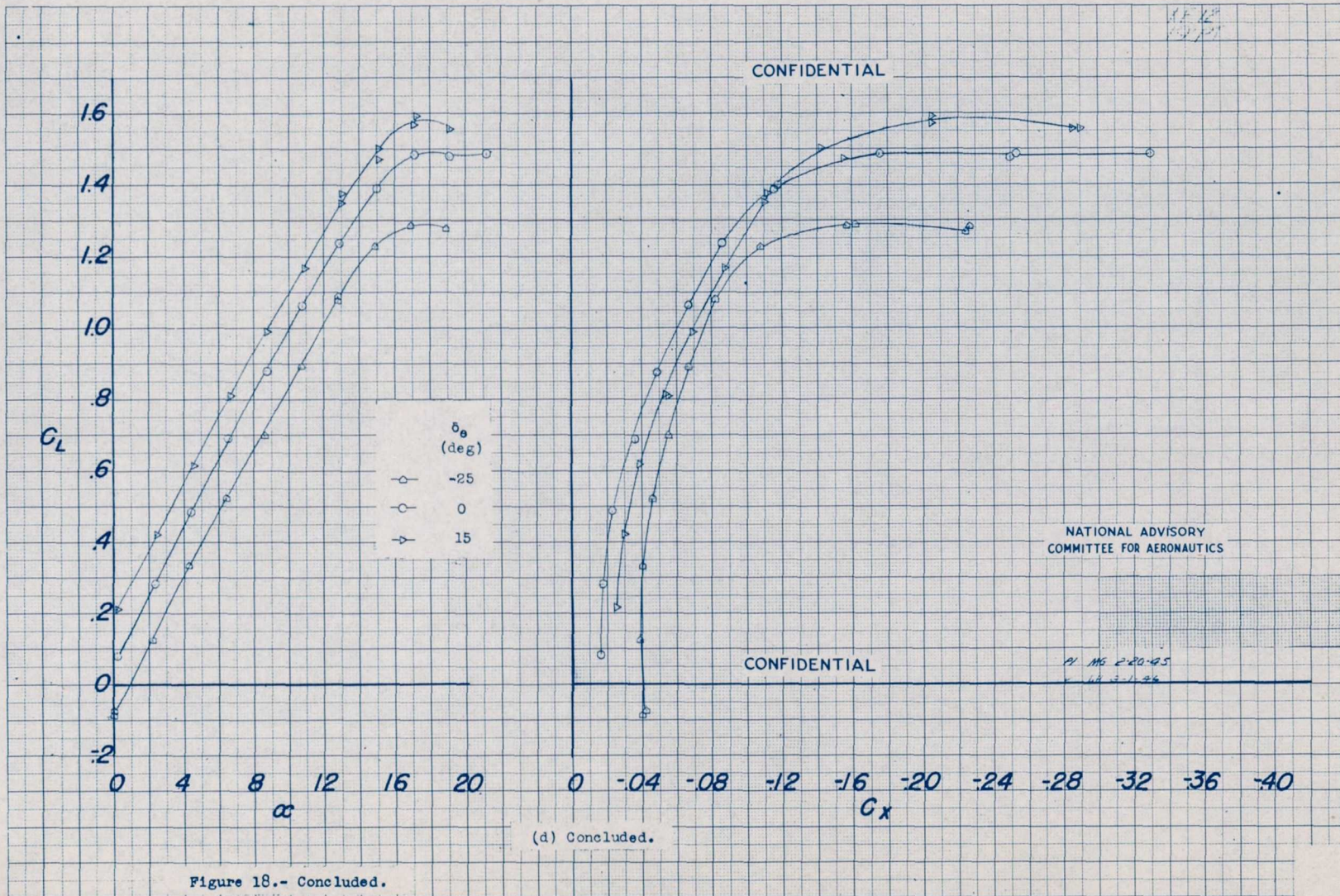
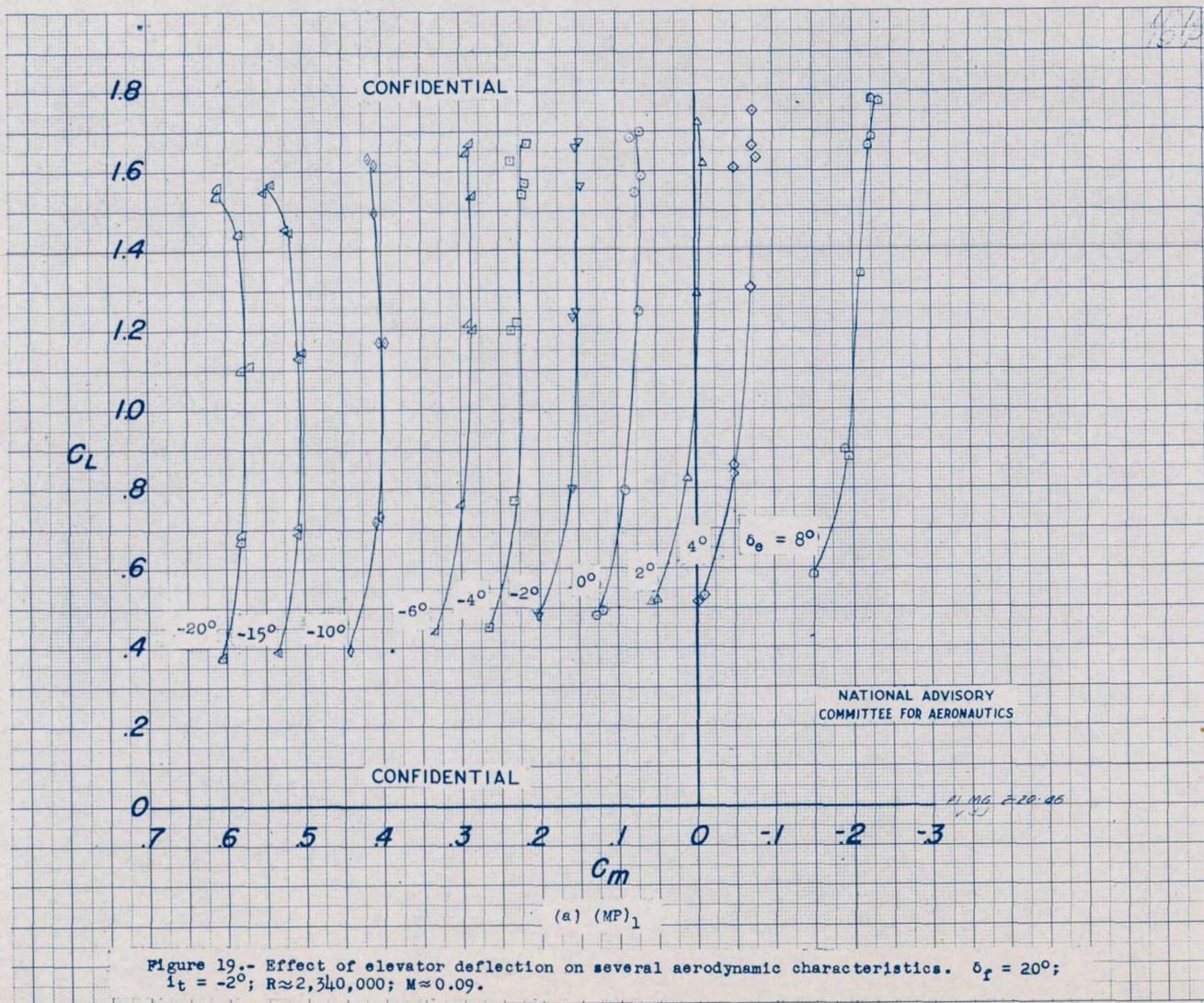


Figure 18.- Concluded.

Fig. 18d conc.



196619

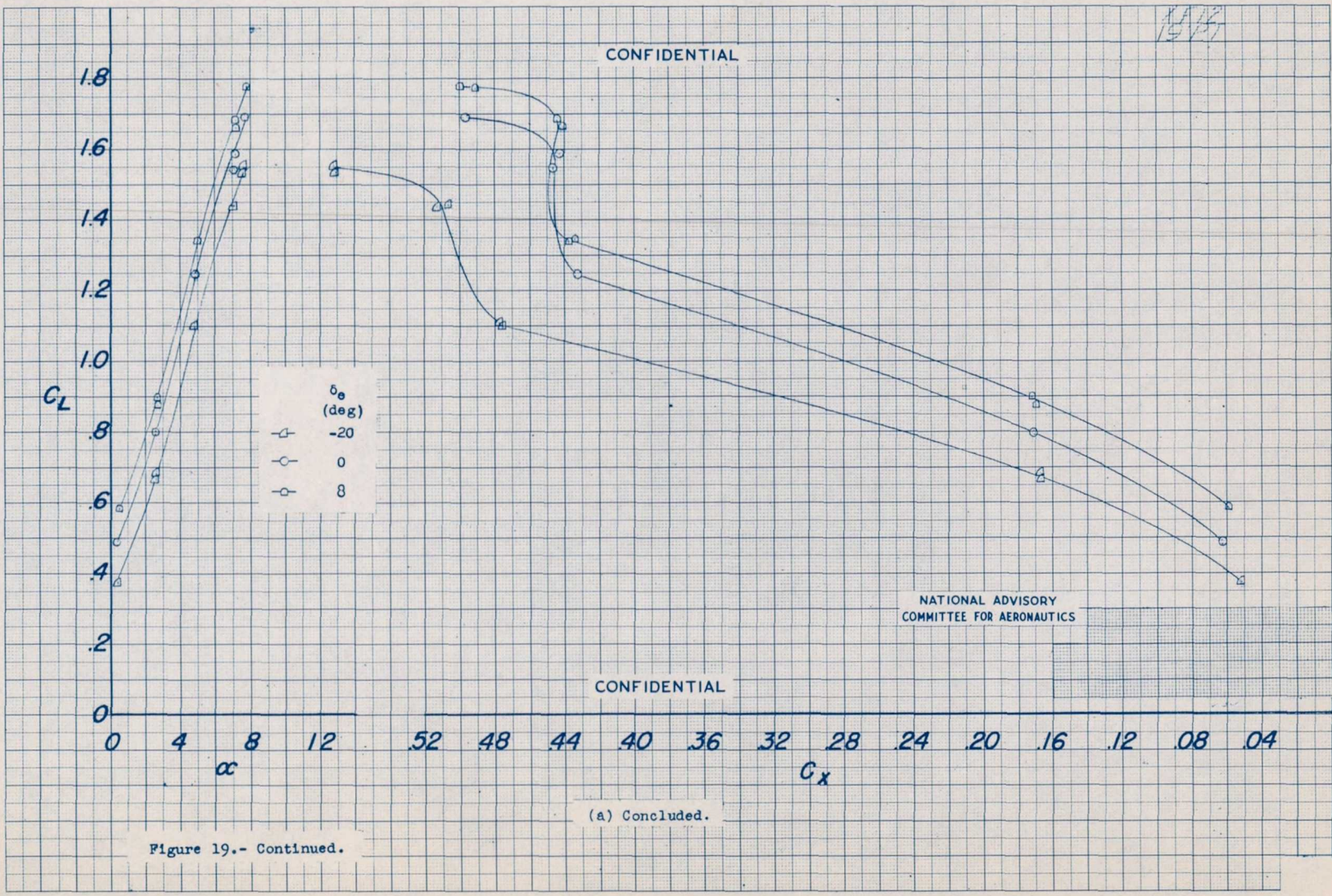


Figure 19.- Continued.

(a) Concluded.

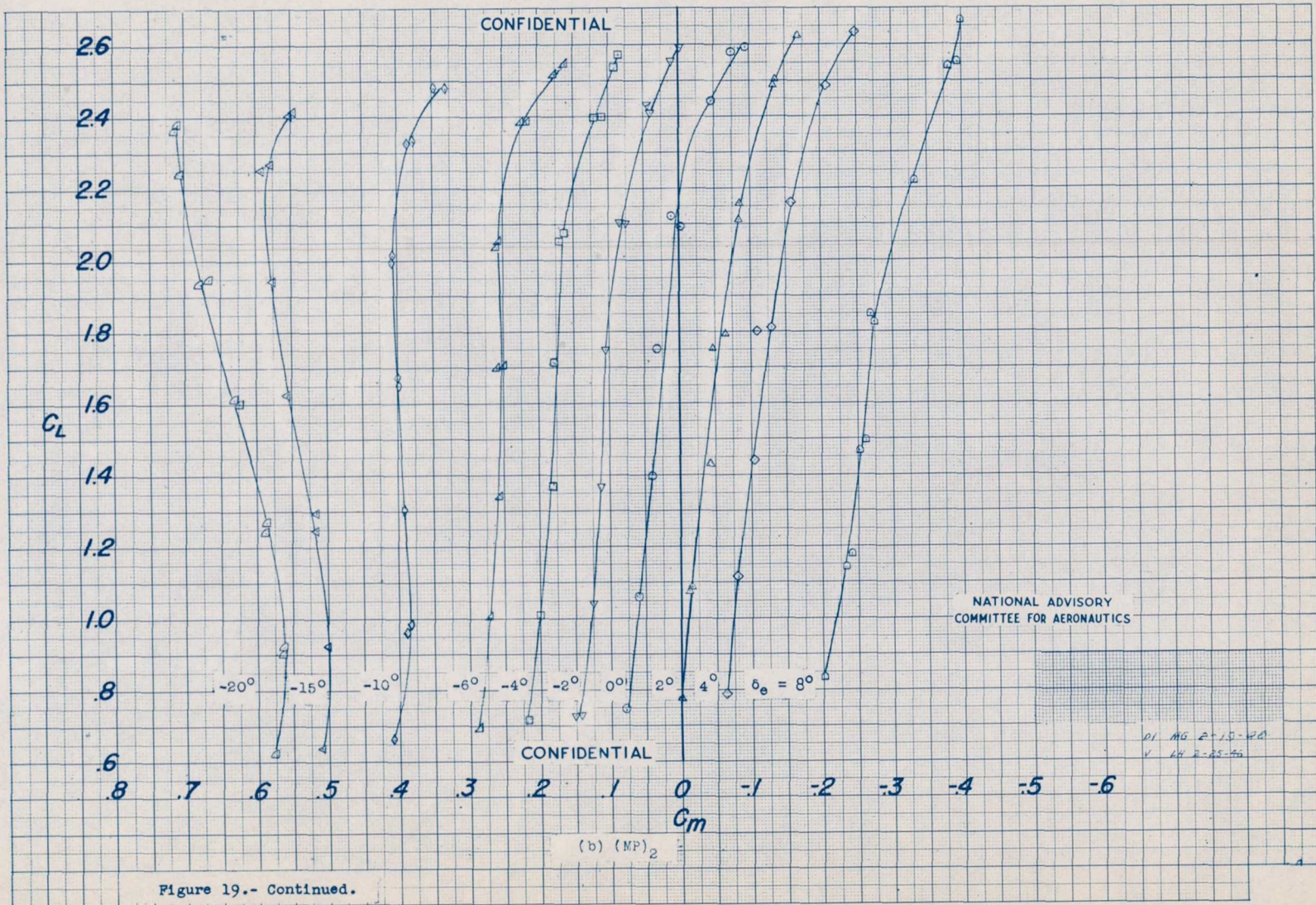


Figure 19.- Continued.

1955

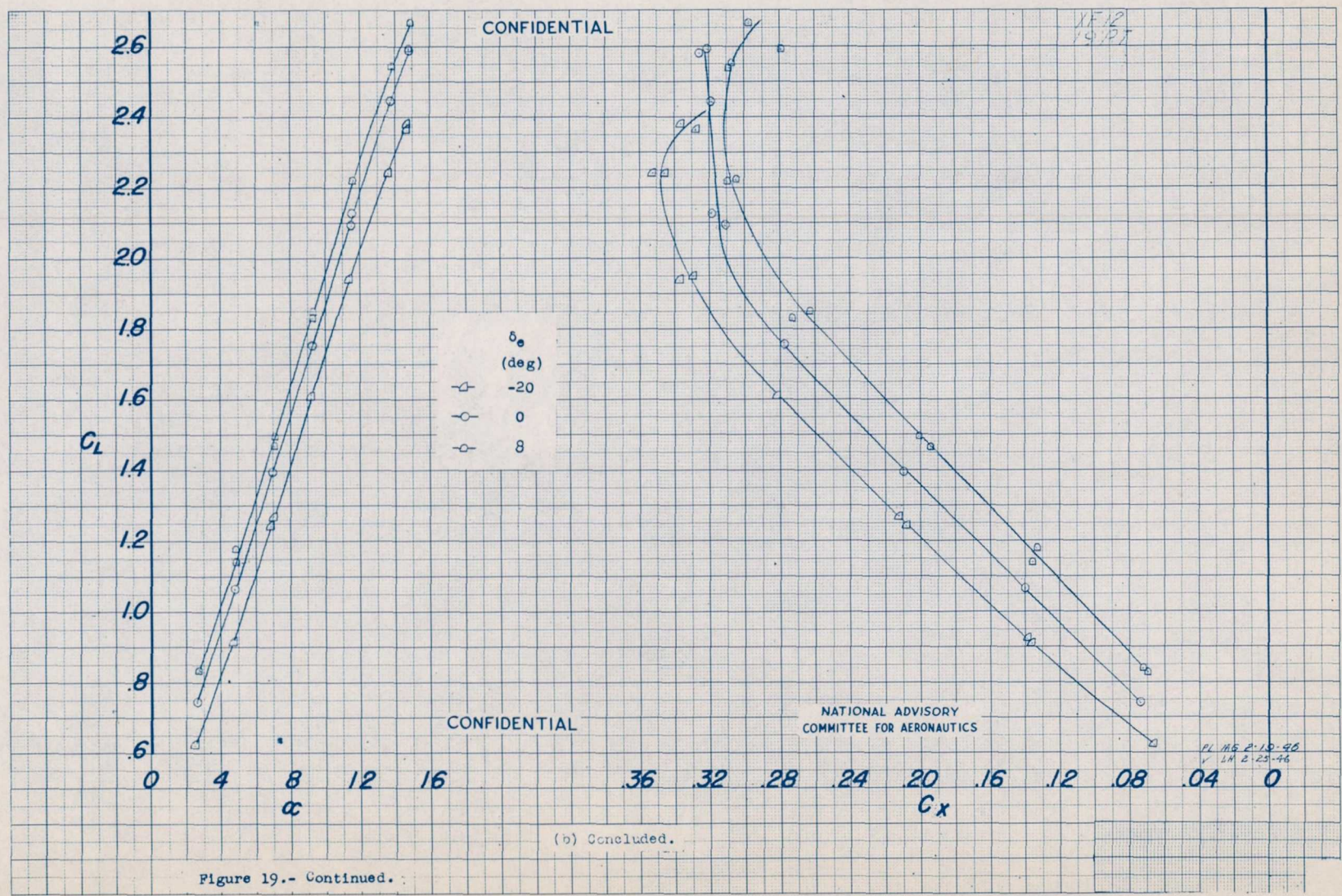


Figure 19.- Continued.

(b) Concluded.

1951

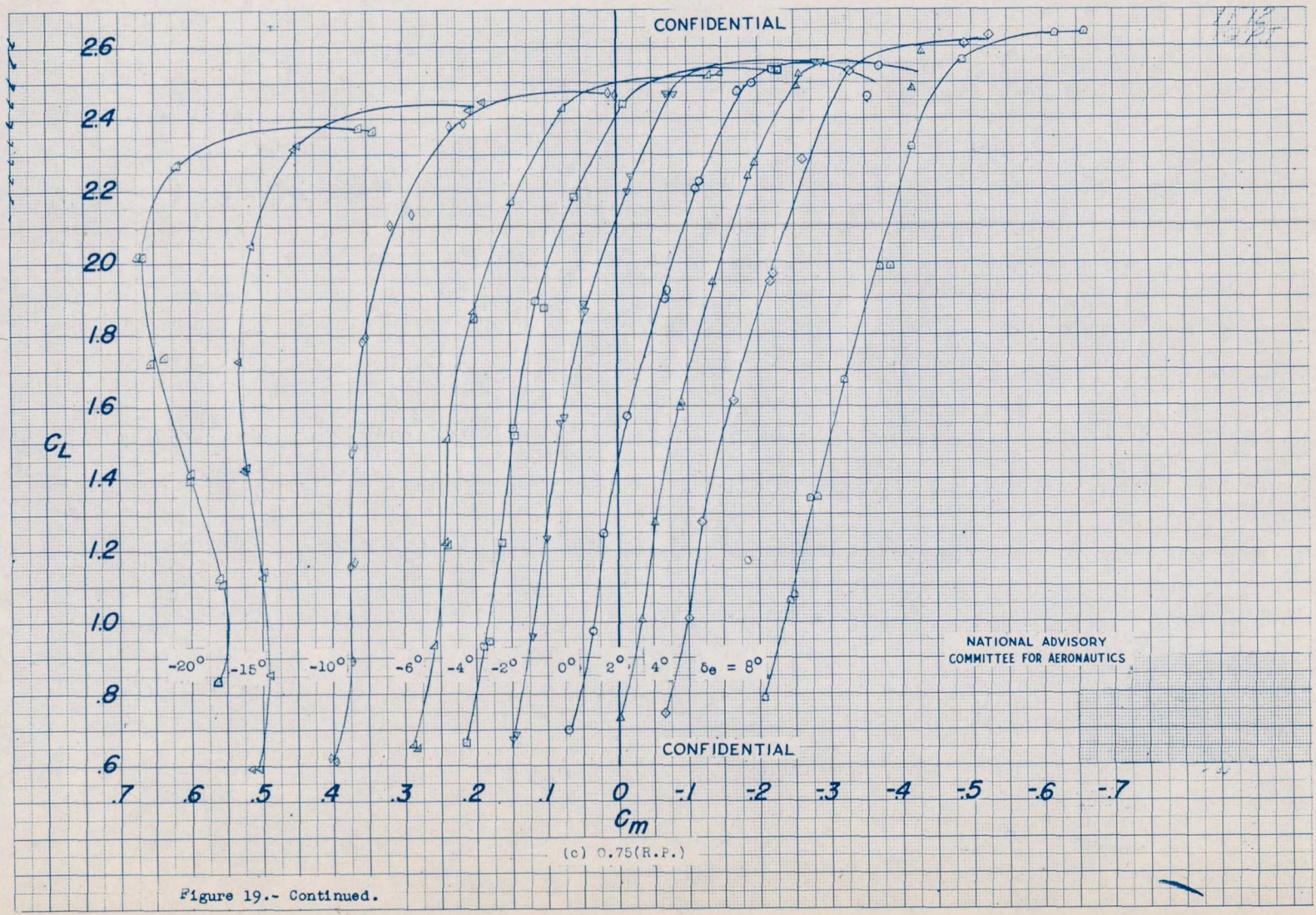


Figure 19.- Continued.

(c) O.75(R.P.)

19019

NACA RM No. L6L12

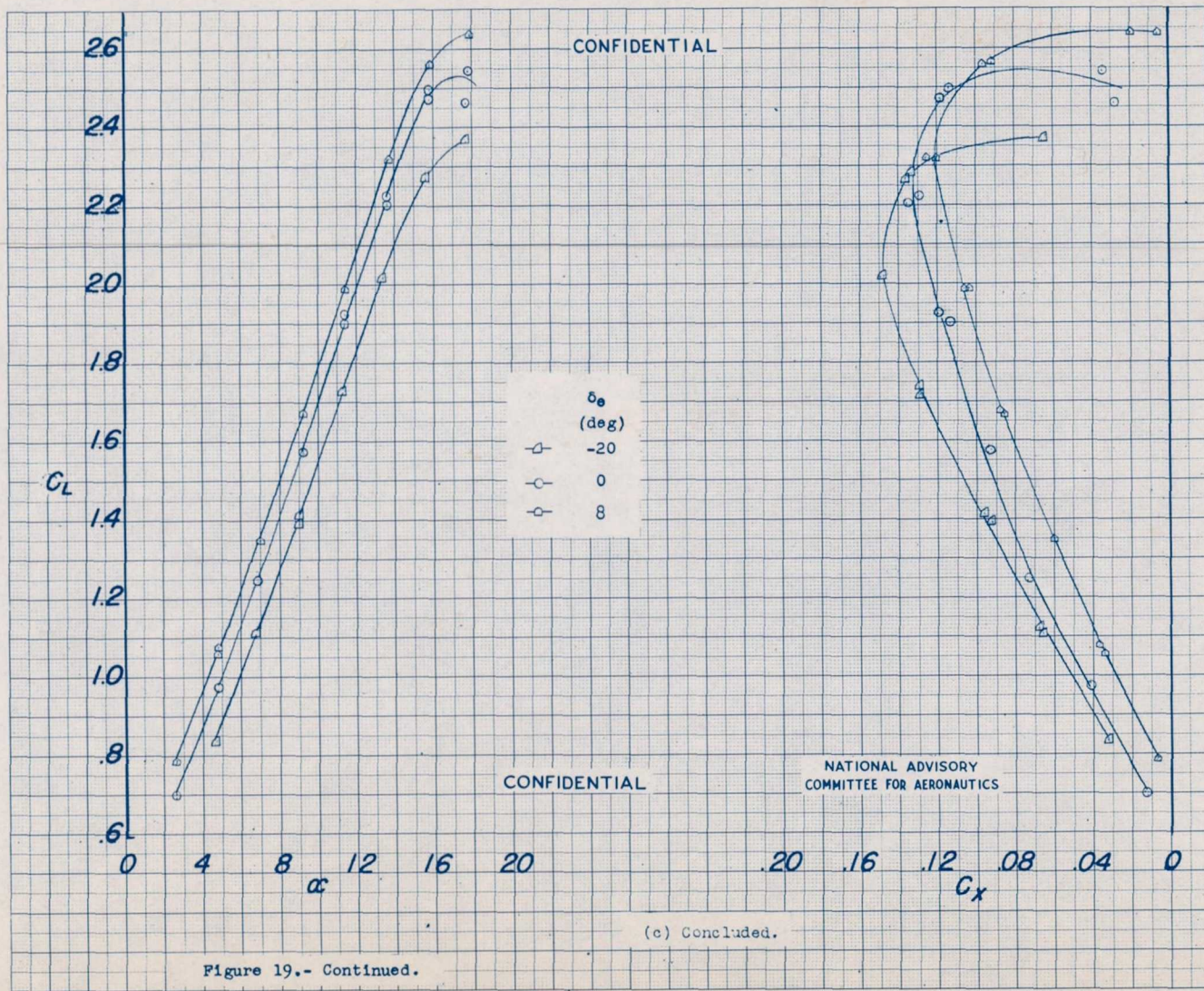


Figure 19.- Continued.

Fig. 19c conc.

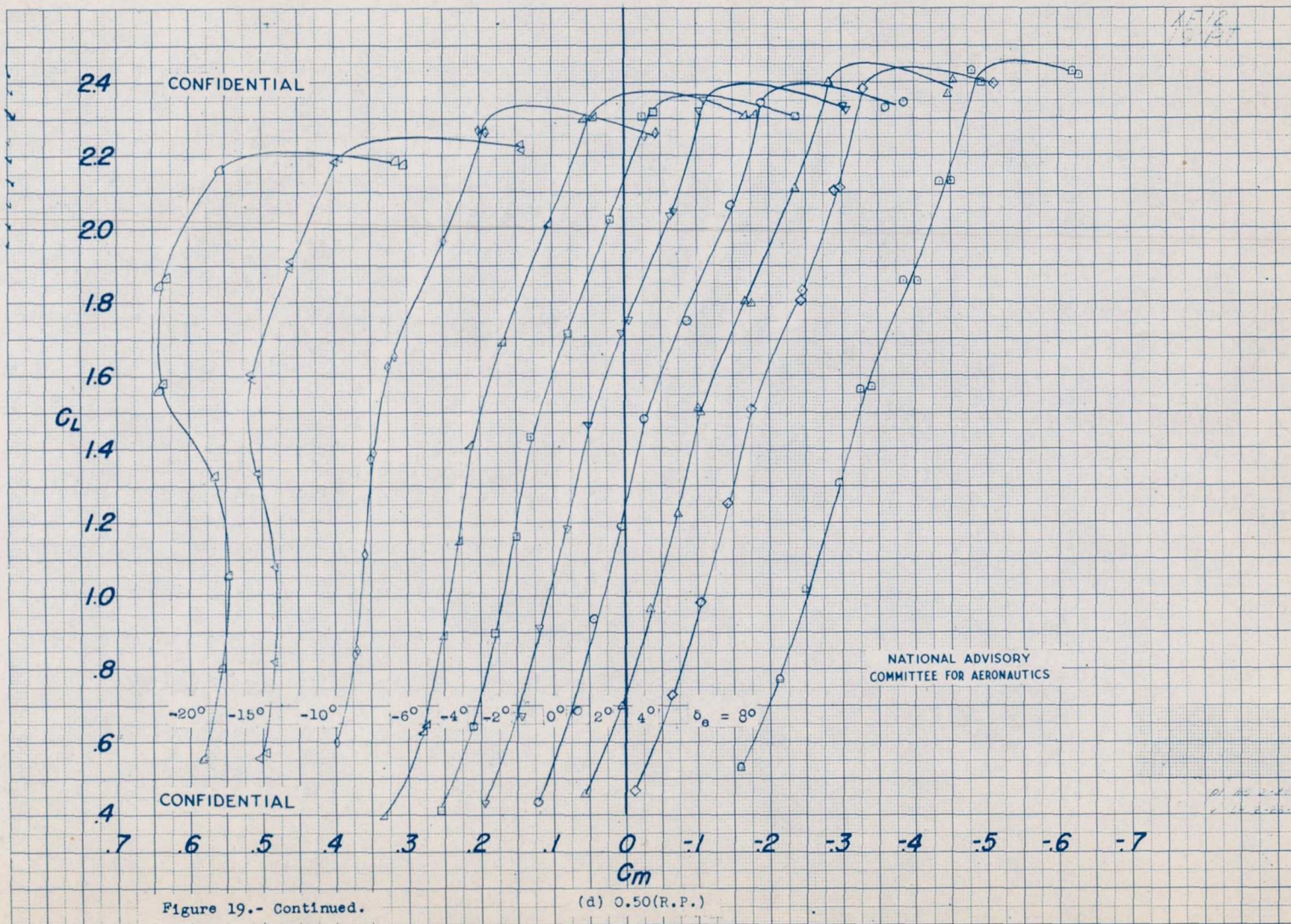
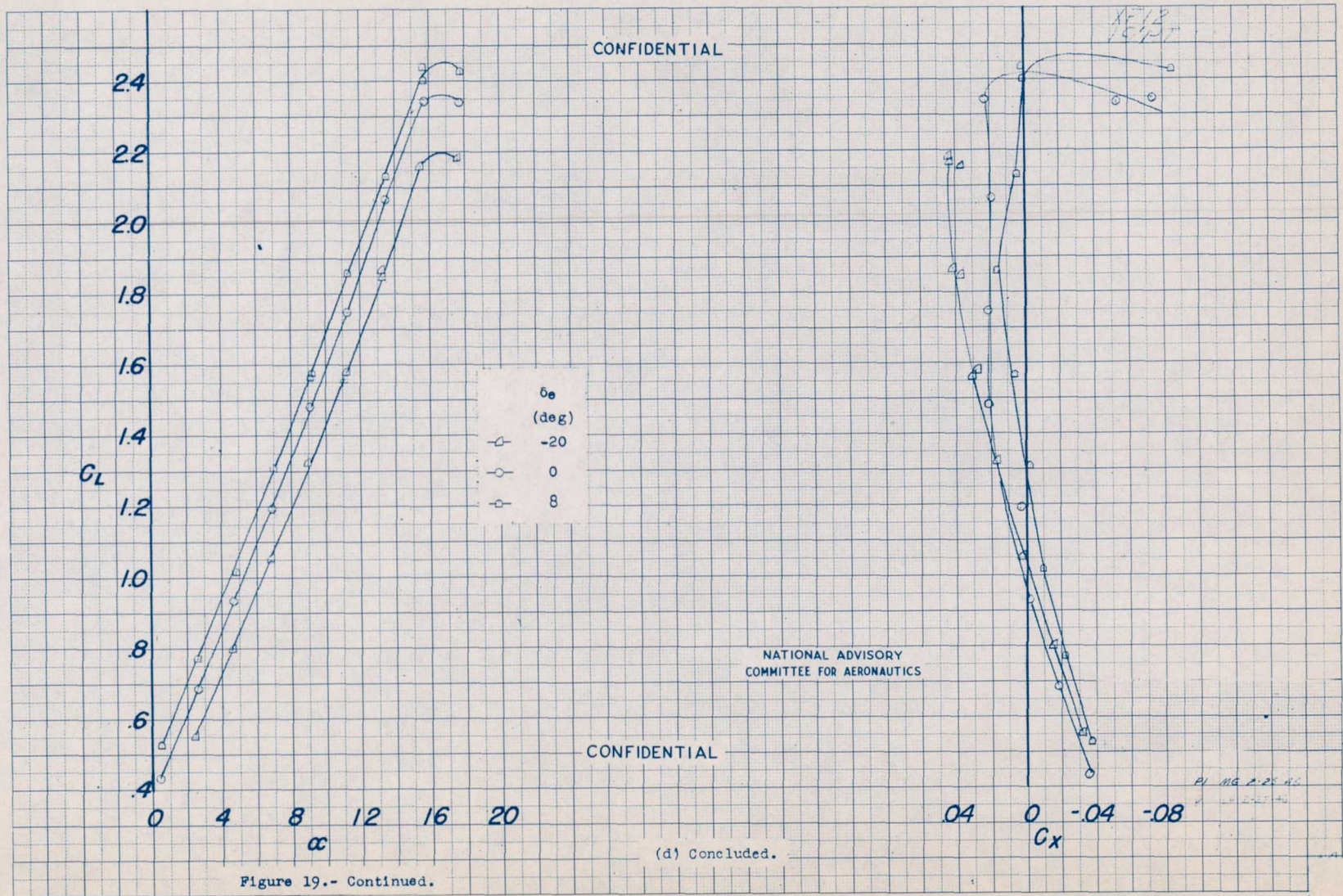


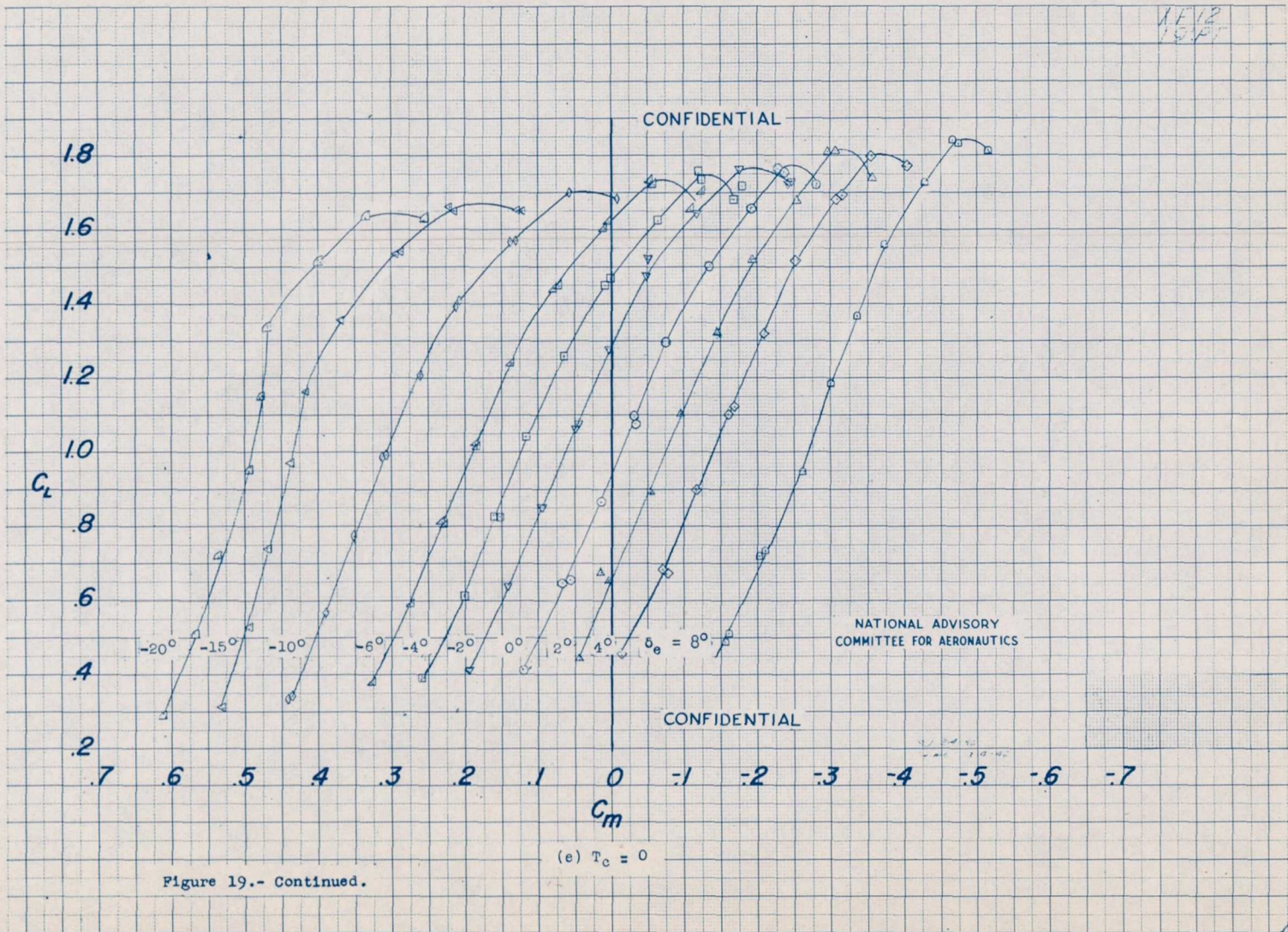
Figure 19.- Continued.

(d) 0.50(R.P.)

10810



1951



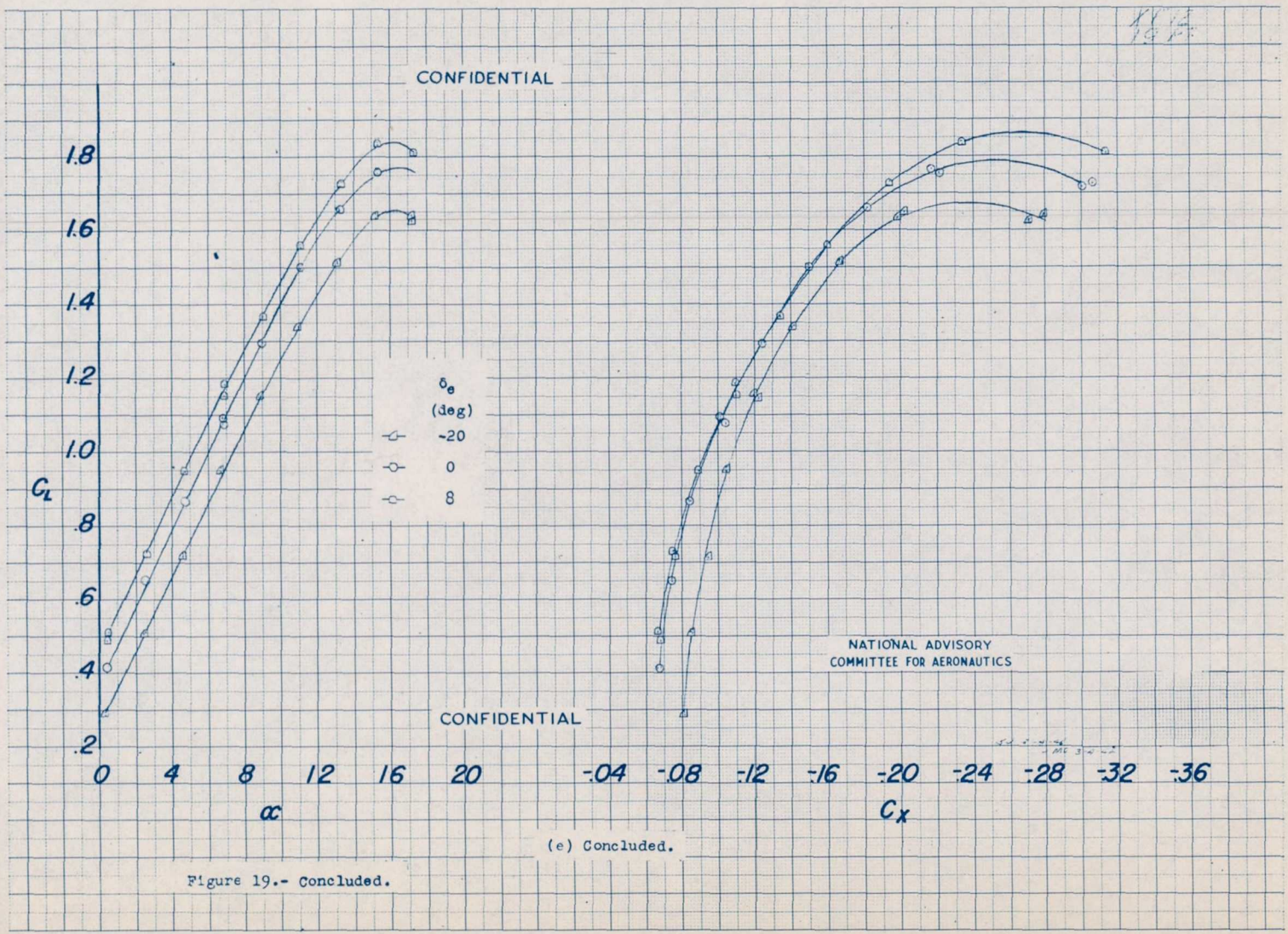


Figure 19.- Concluded.

(e) Concluded.

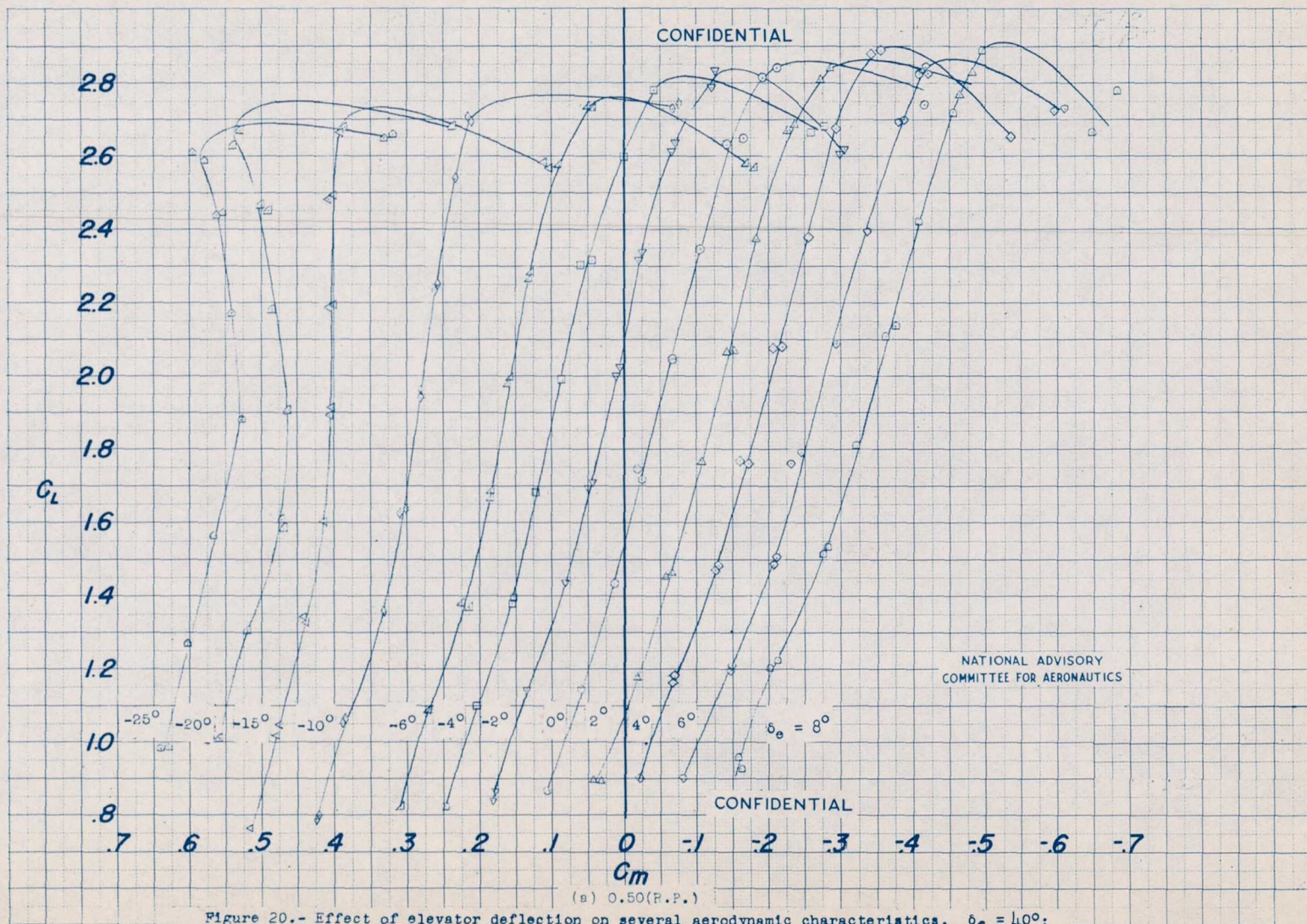
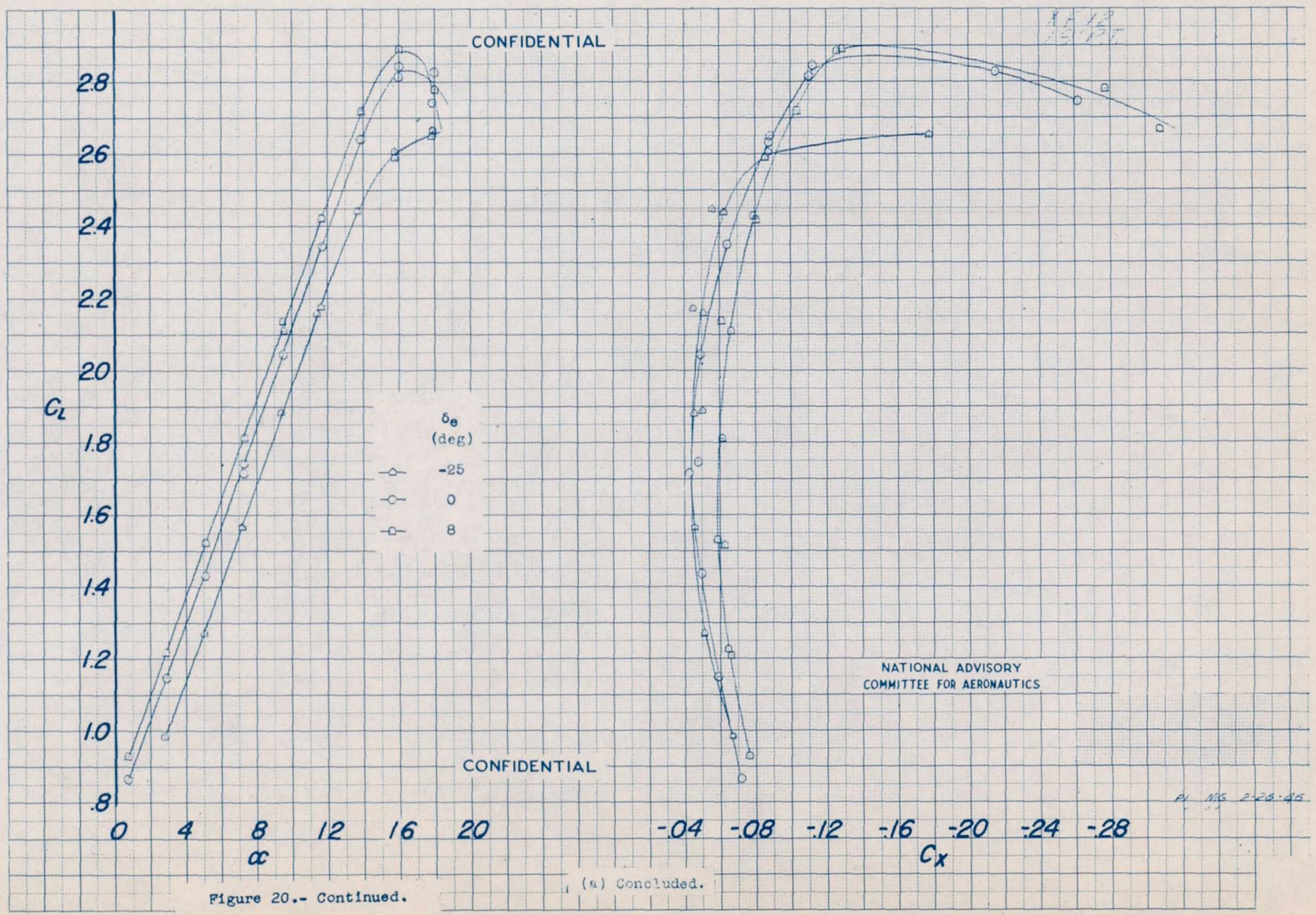


Figure 20.- Effect of elevator deflection on several aerodynamic characteristics. $\delta_r = 40^\circ$;
 $i_t = -2^\circ$; $R \approx 2,330,000$; $M \approx 0.09$.

1985



1980

NACA RM No. L6L12

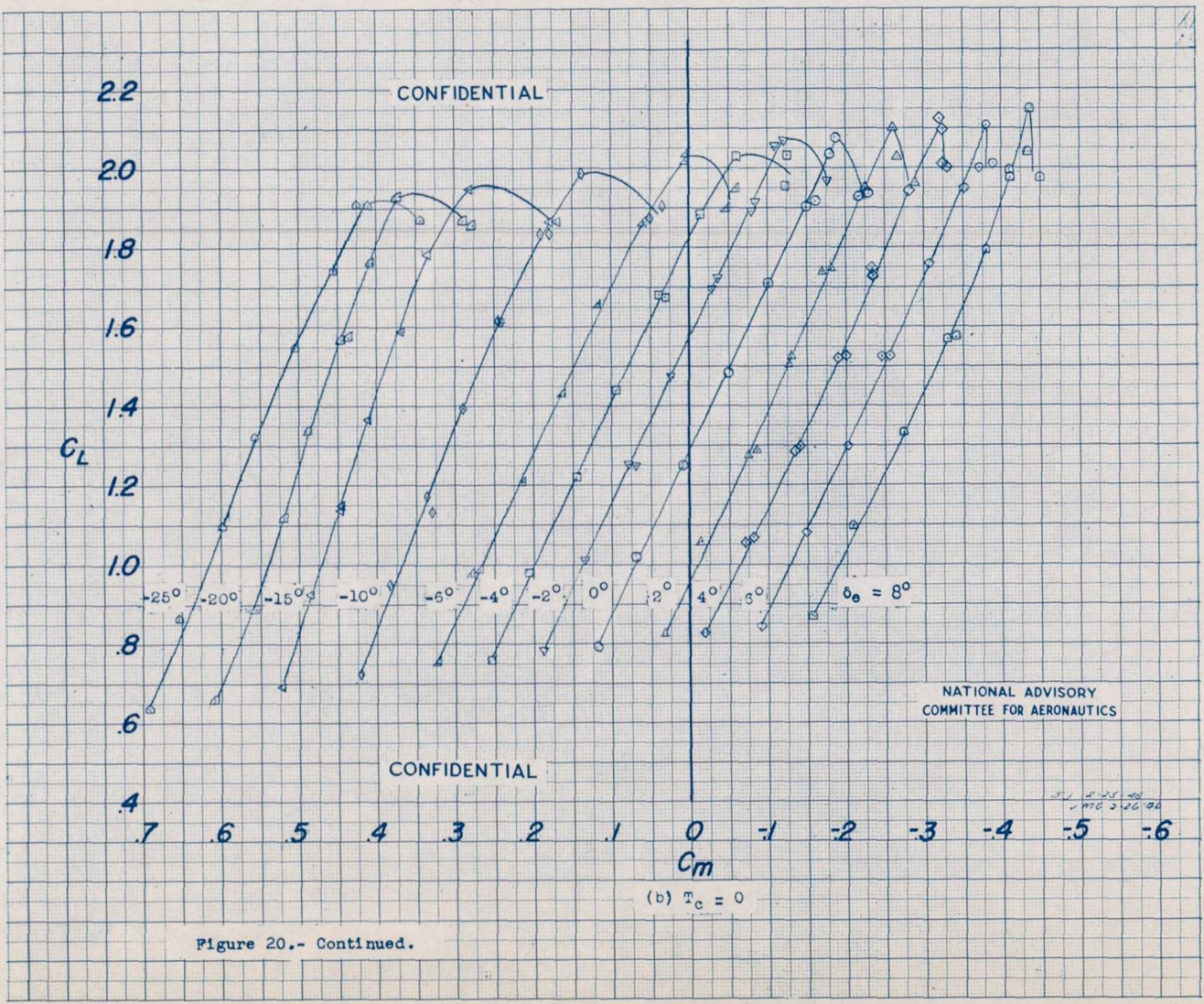


Fig. 20b

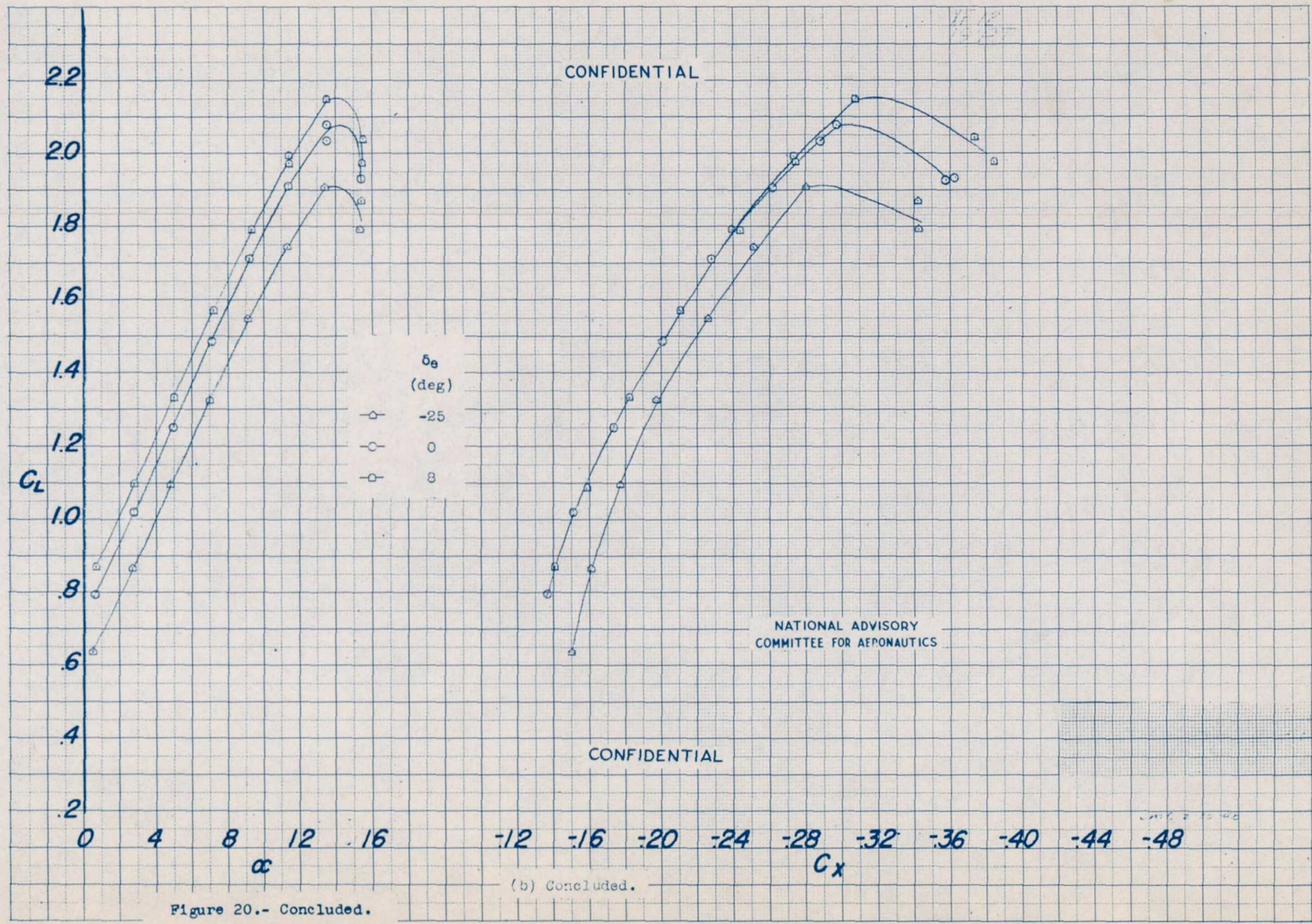
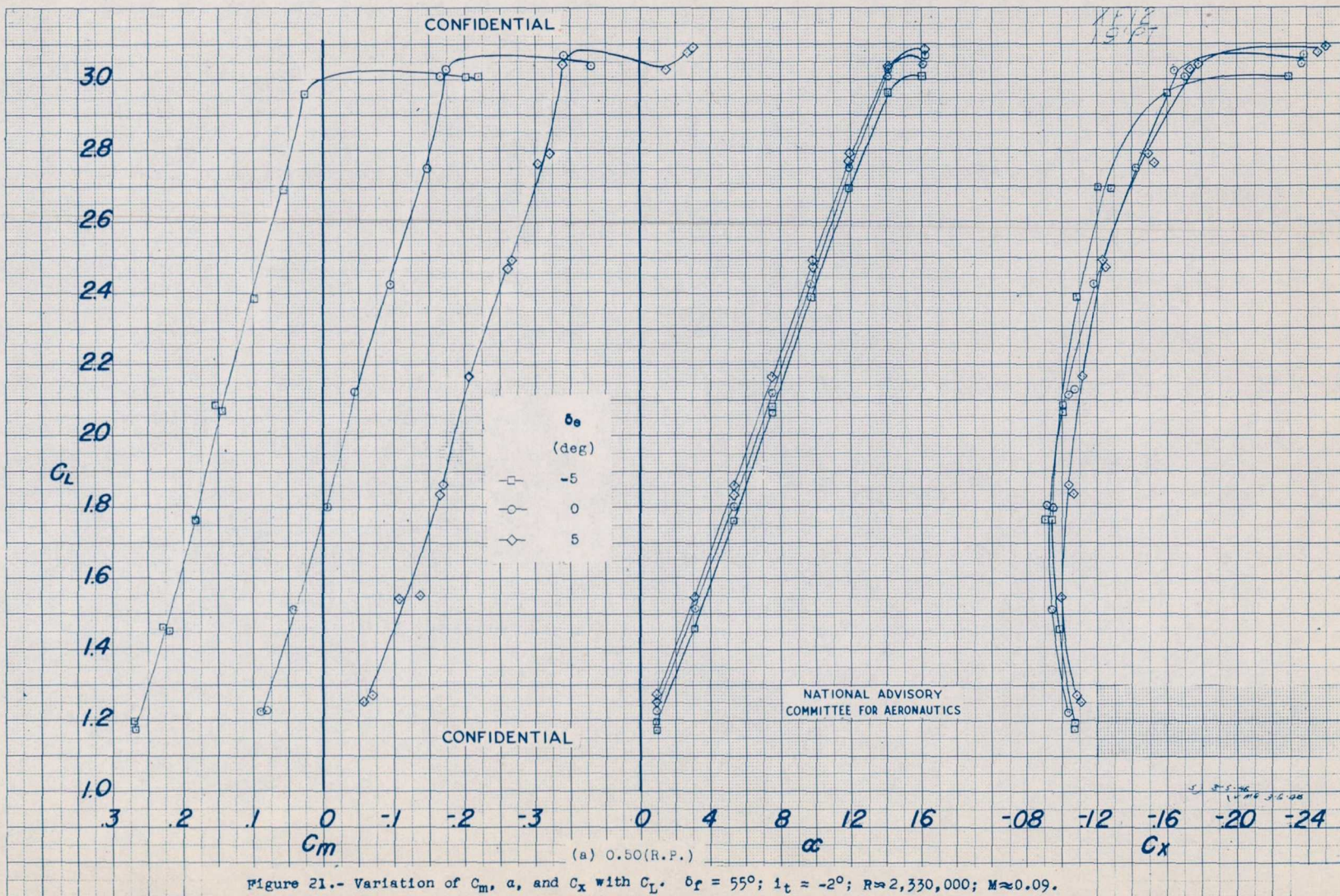


Figure 20.- Concluded.



1985

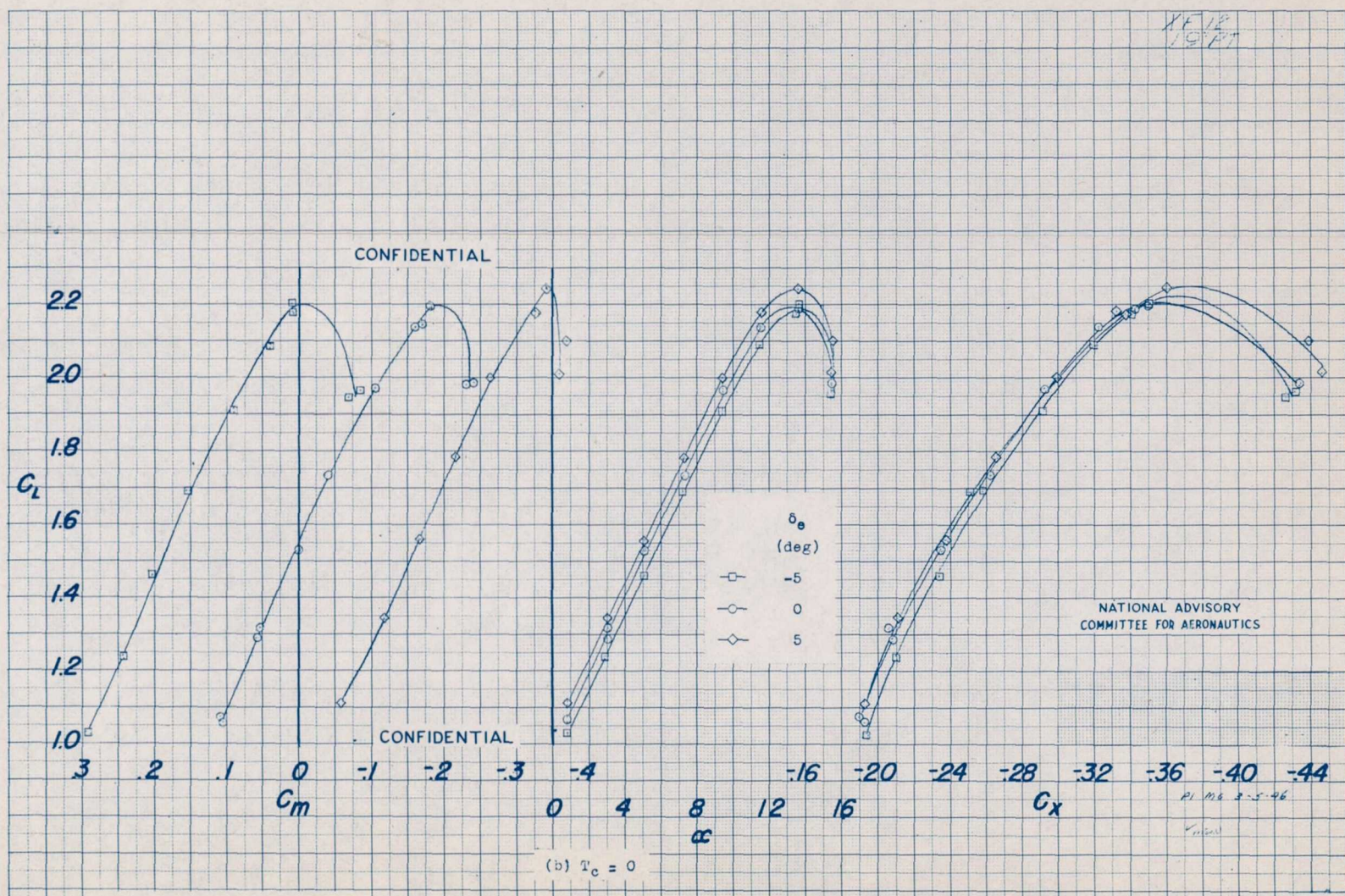


Figure 21.- Continued.

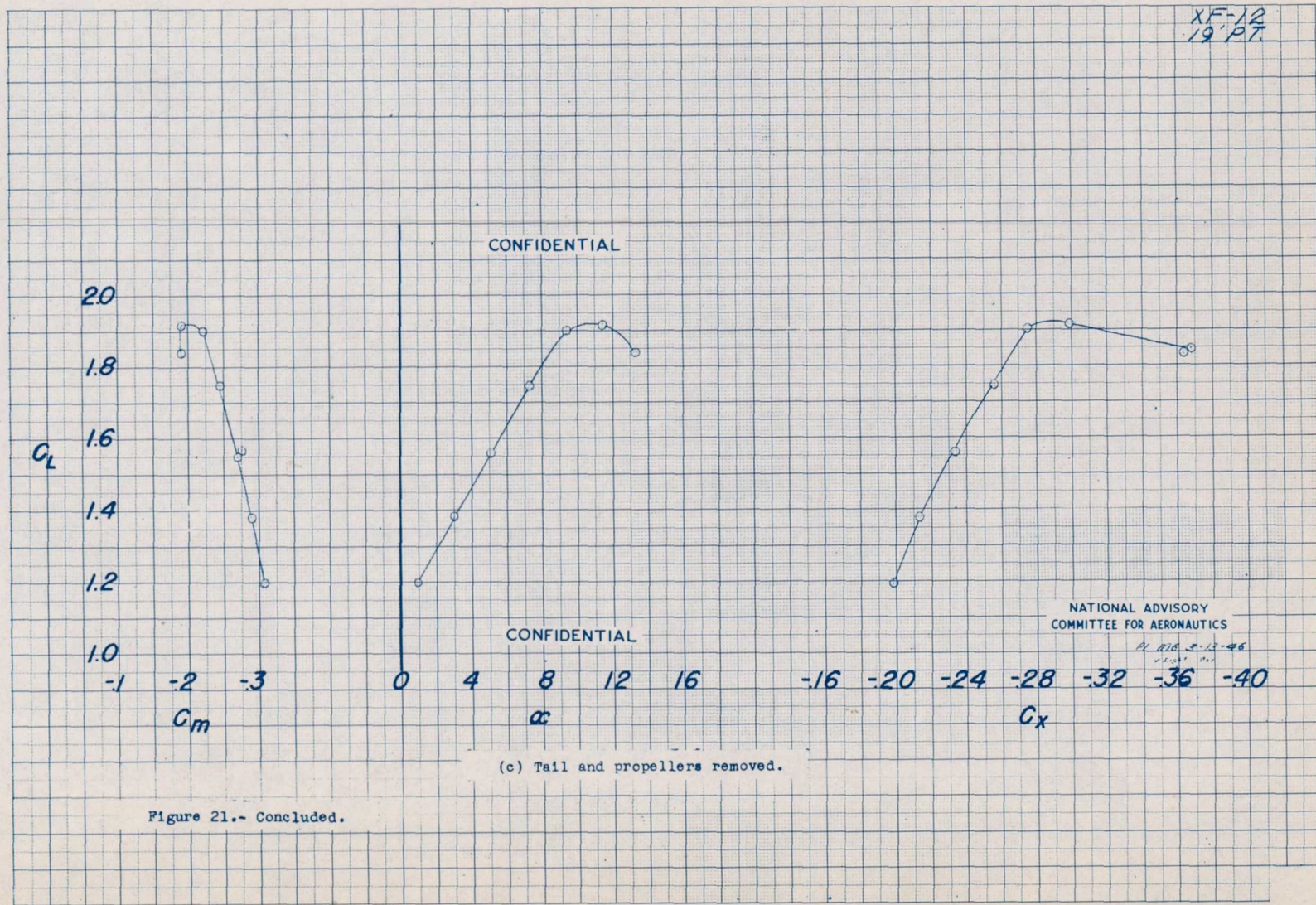


Figure 21.- Concluded.

1960

NACA RM No. L6L12

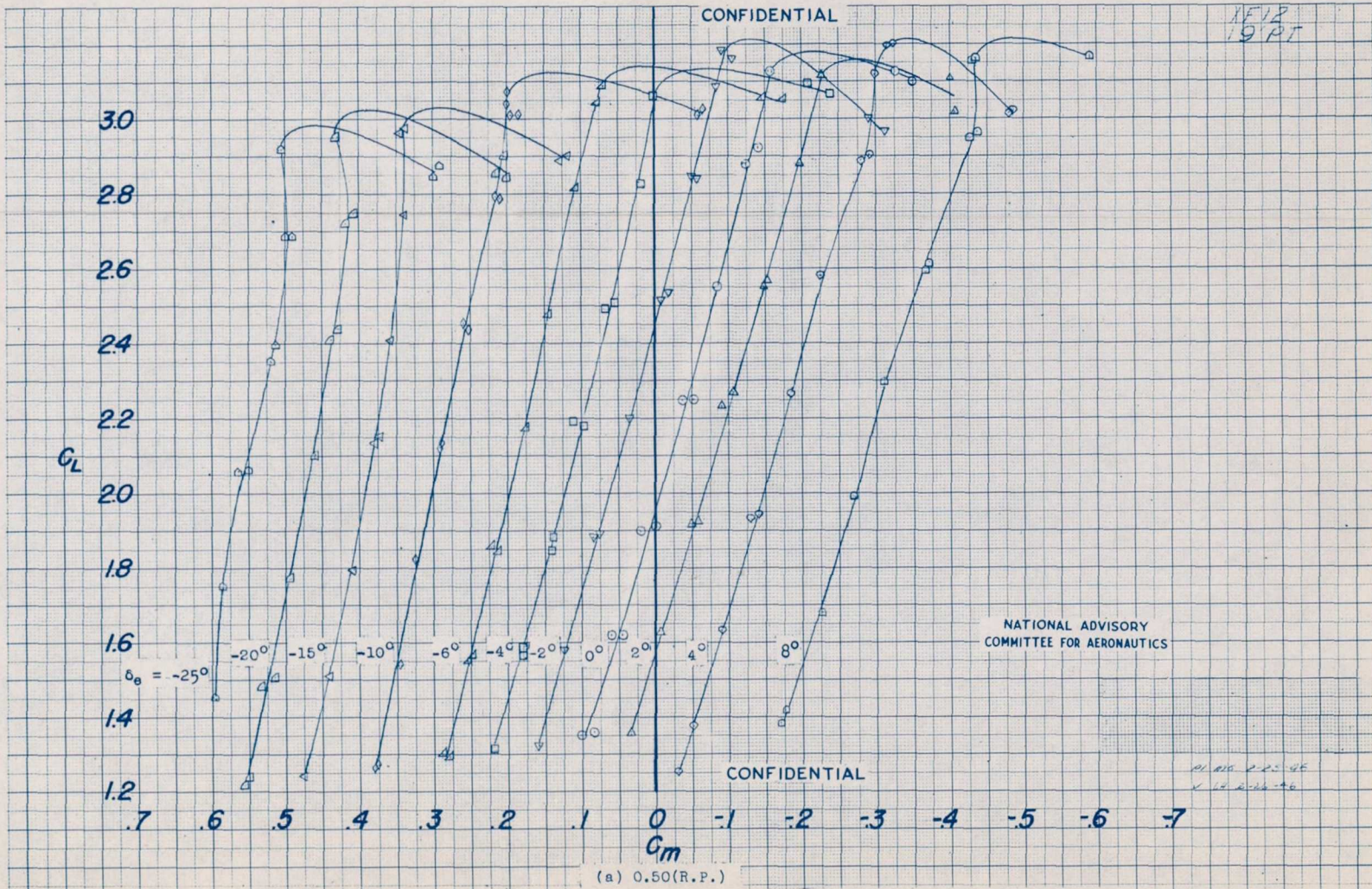


Figure 22.- Effect of elevator deflection on several aerodynamic characteristics. $\delta_f = 65^\circ$; $l_t = -2^\circ$; $R \approx 2,330,000$; $M \approx 0.09$.

Fig. 22a

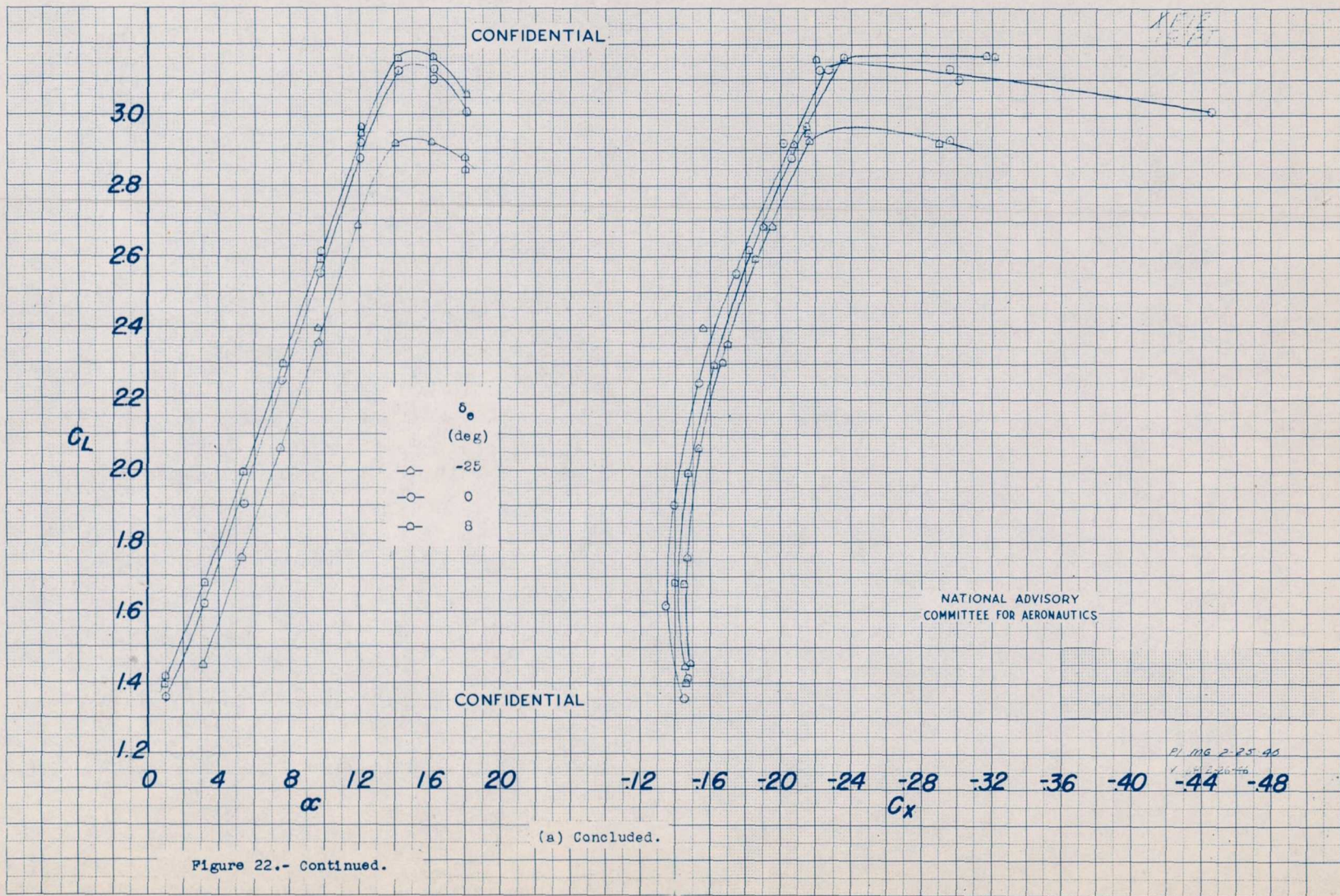


Figure 22.- Continued.

(a) Concluded.

198800

NACA RM No. L6L12

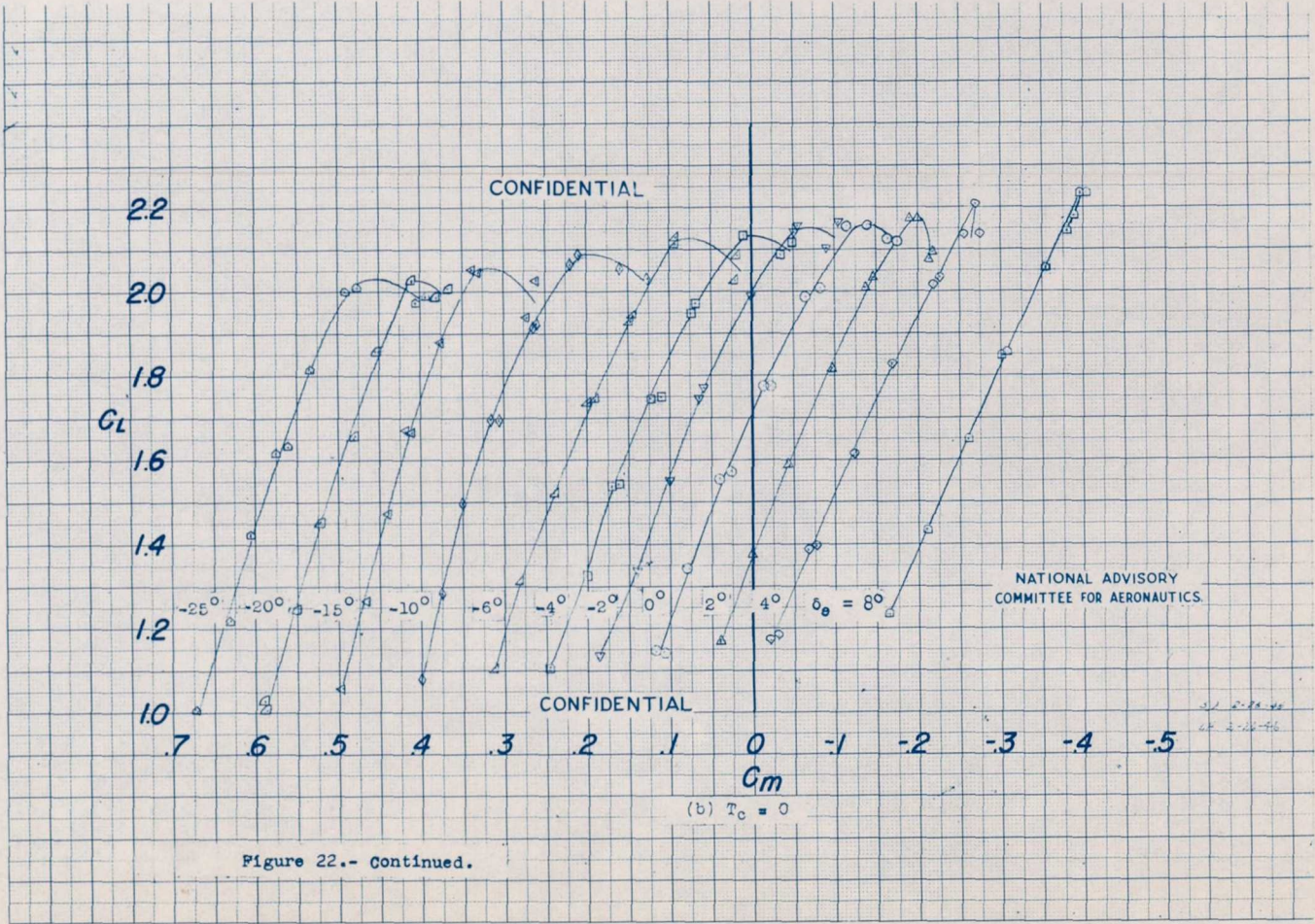


Figure 22.- Continued.

Fig. 22b

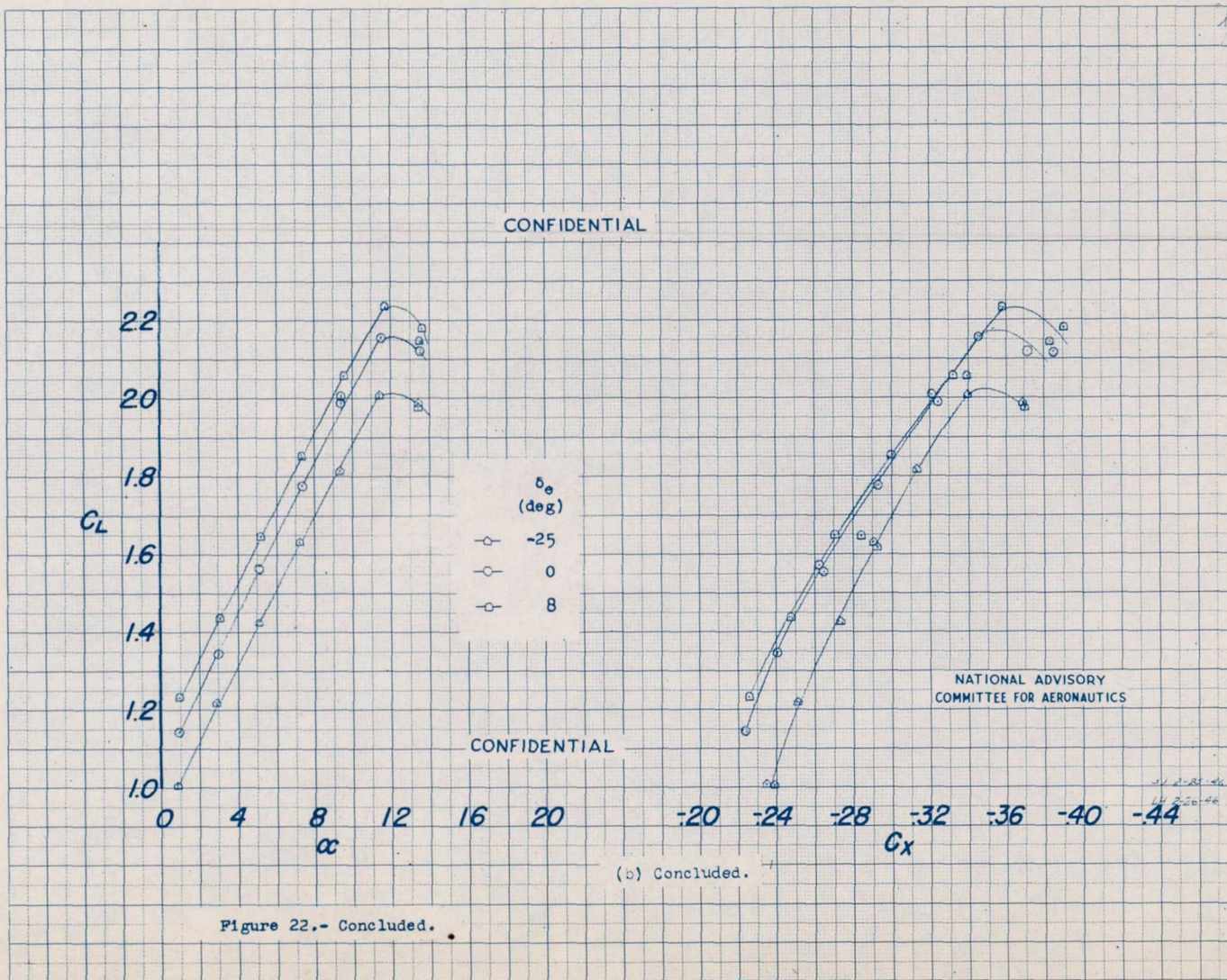
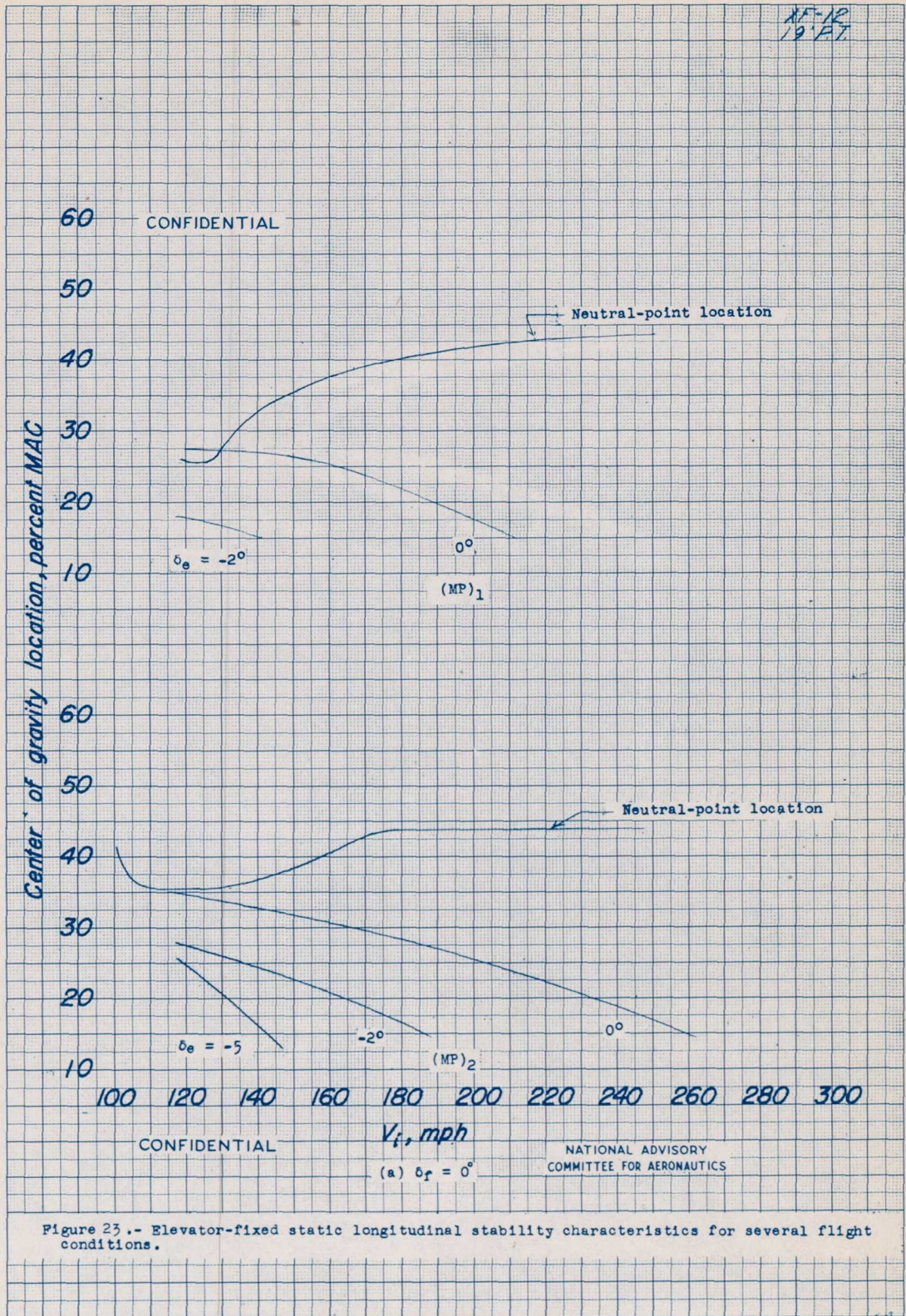


Fig. 22b conc.



X.F. 12
19 PT.

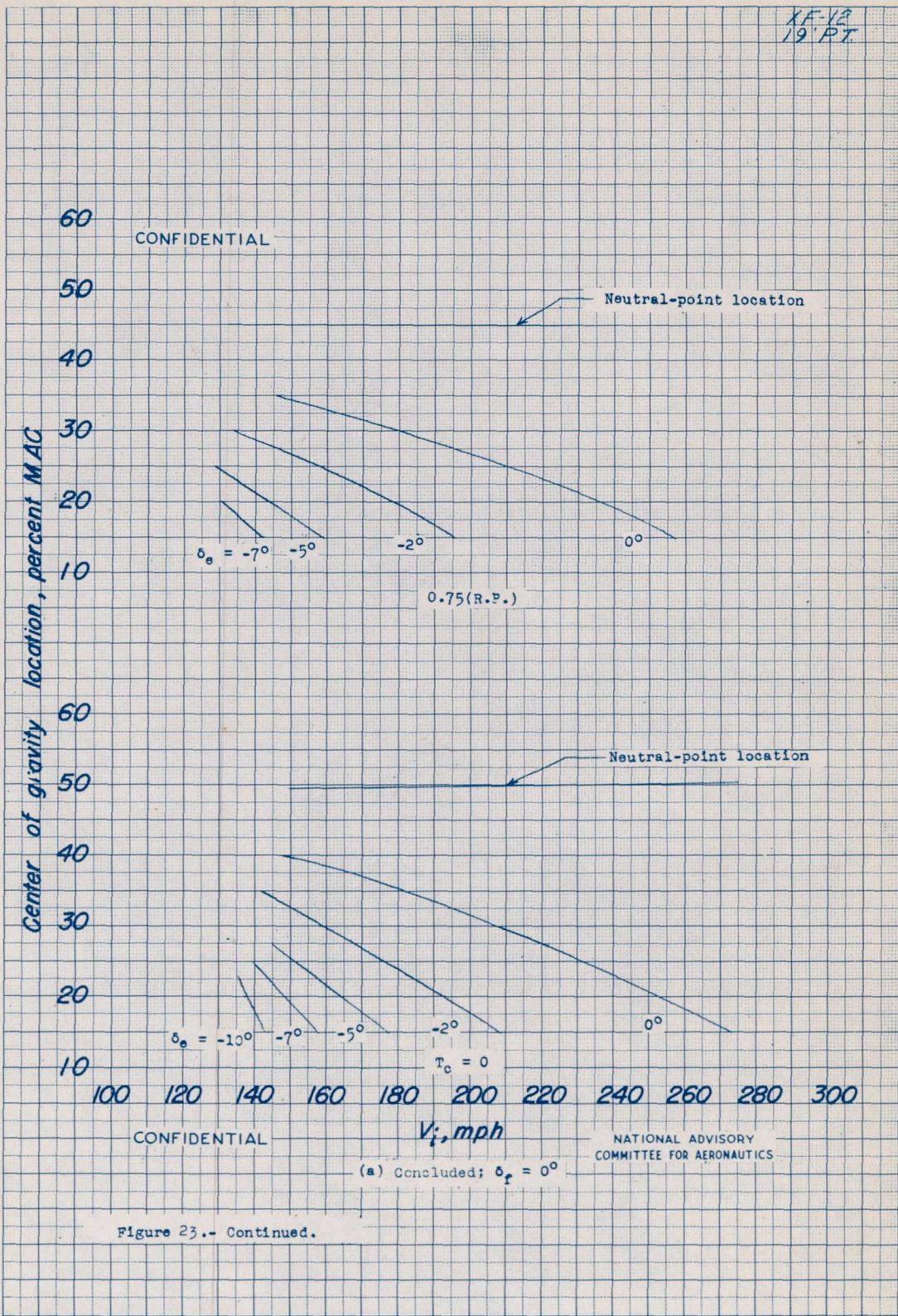


Figure 23.- Continued.

(a) Concluded; $\delta_f = 0^\circ$

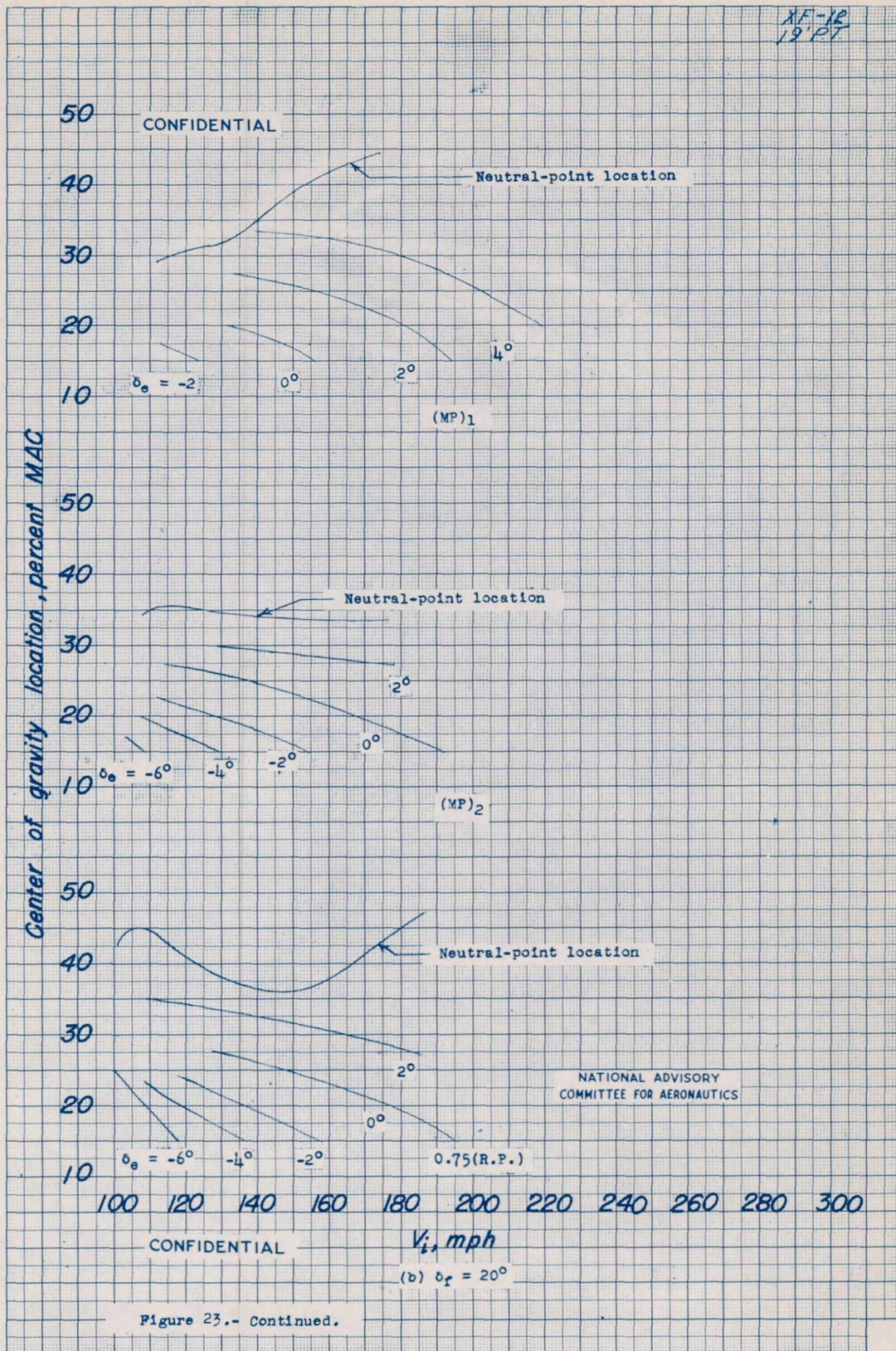


Figure 23.- Continued.

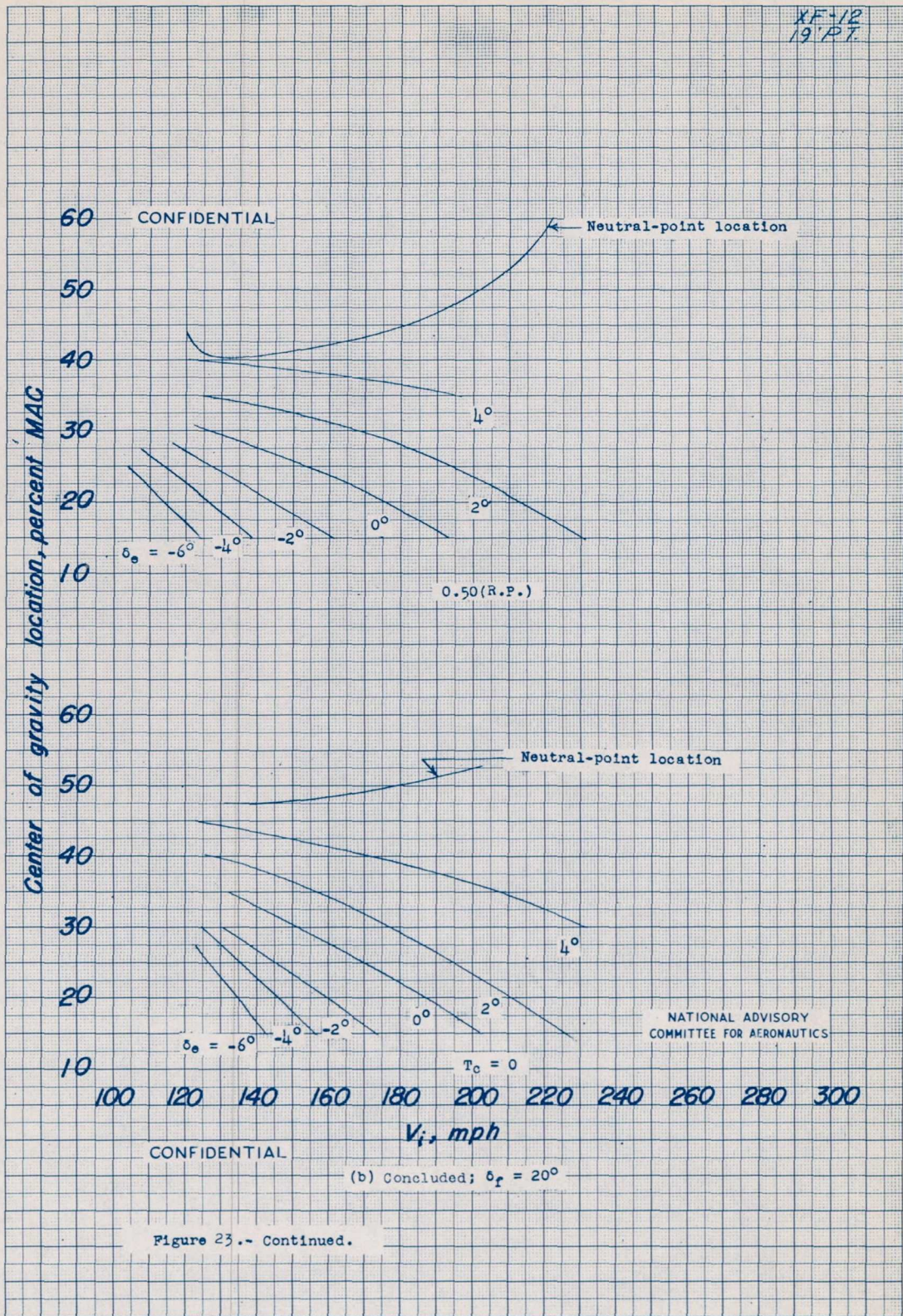
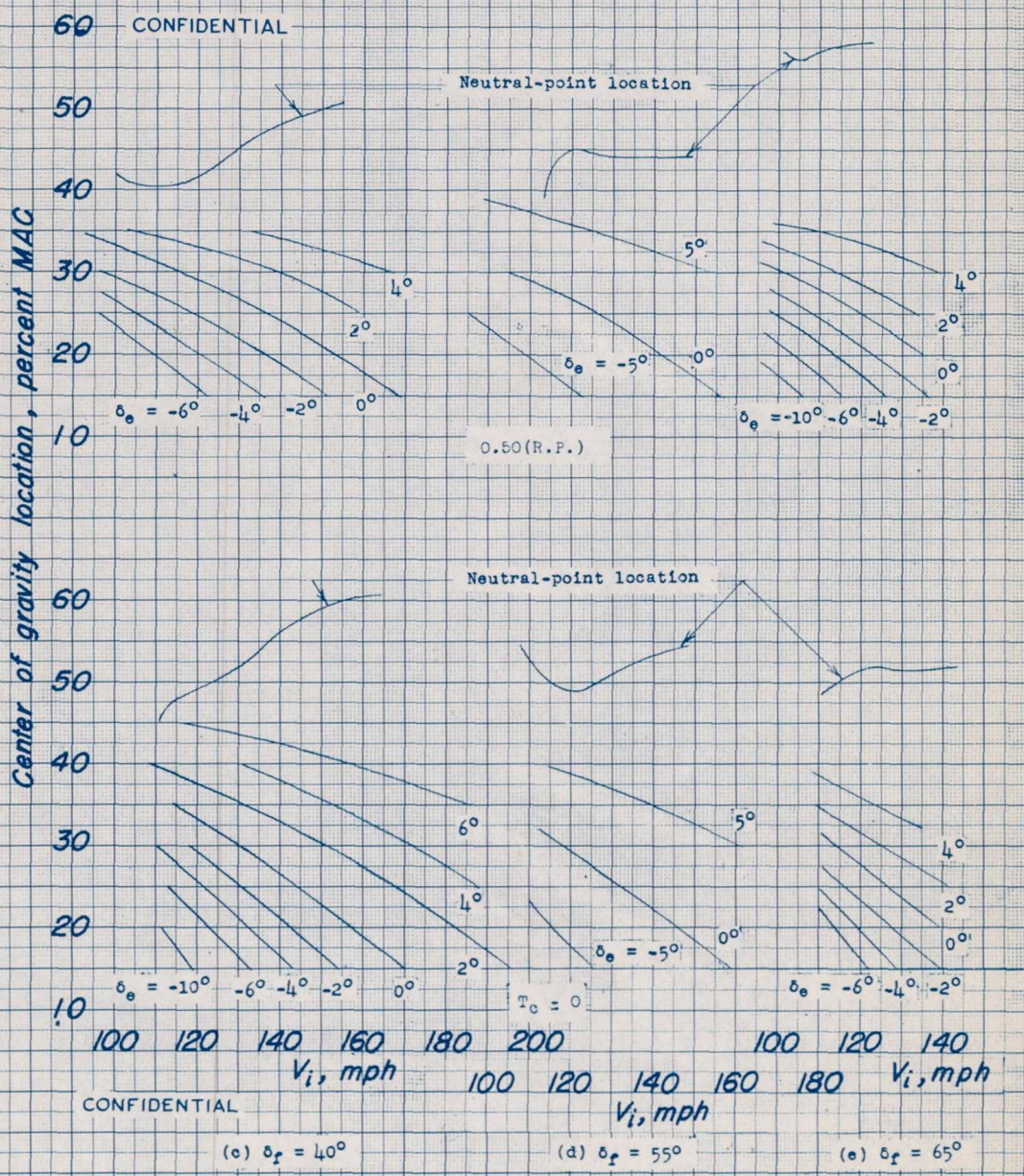


Figure 23.- Continued.

XF-12
19 PT



CONFIDENTIAL

NATIONAL ADVISORY
COMMITTEE FOR AERONAUTICS

Figure 23.- Concluded.

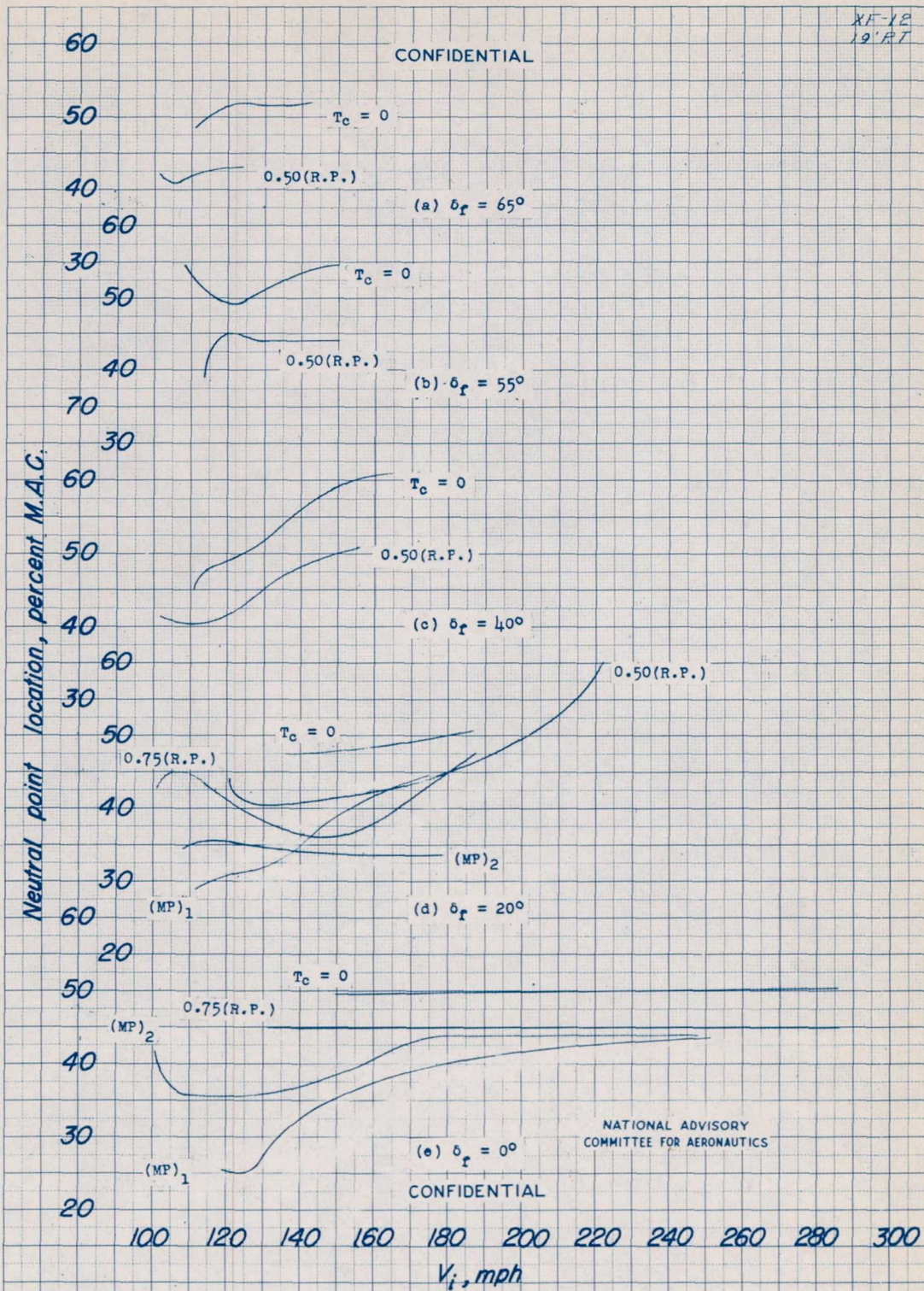


Figure 24.- Variation of neutral point location with V_1 for several flight conditions.

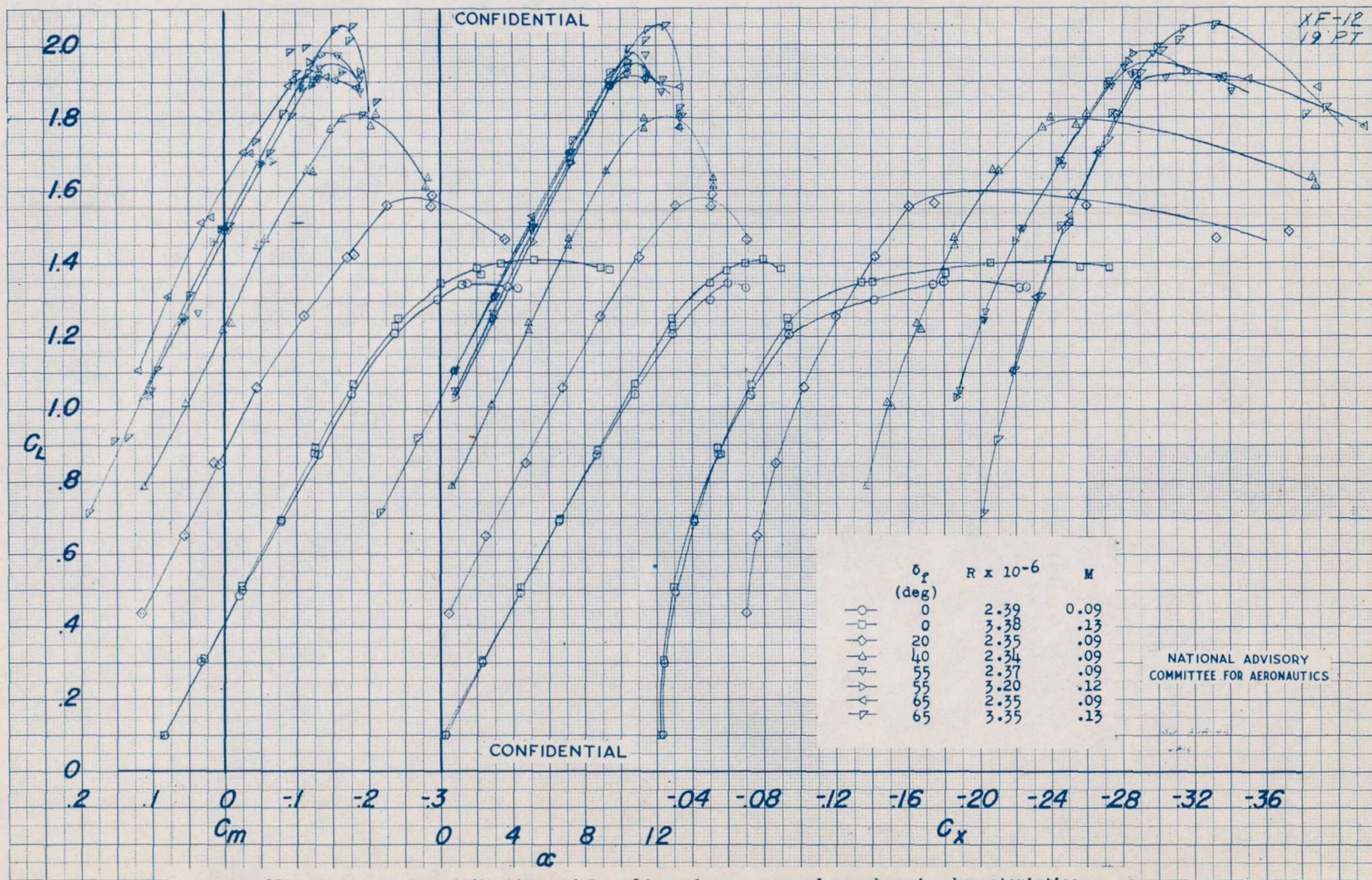
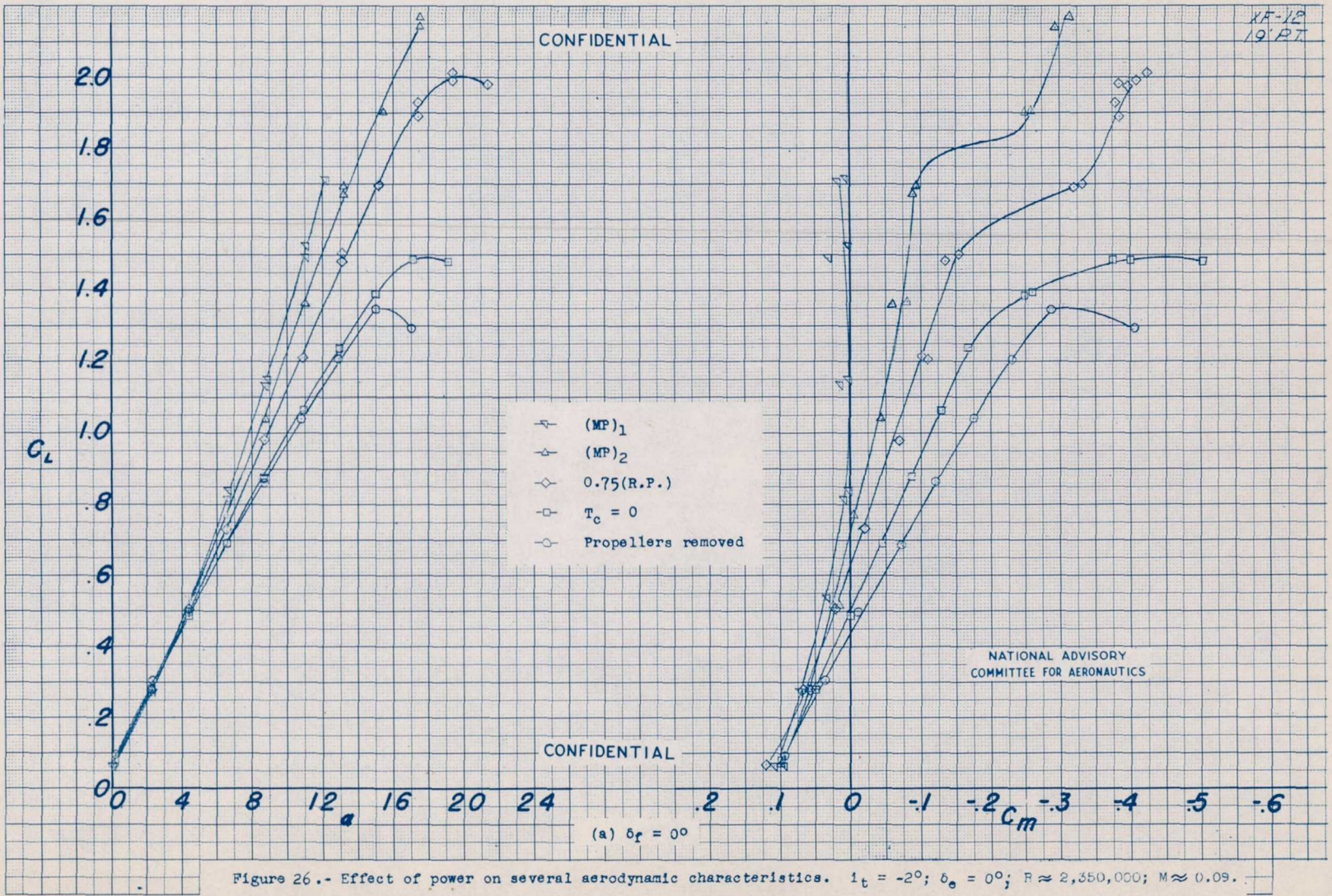


Figure 25.- Effect of flap deflection and Reynolds number on several aerodynamic characteristics. Propellers removed; $i_t = -2^\circ$; $\delta_e = 0^\circ$.

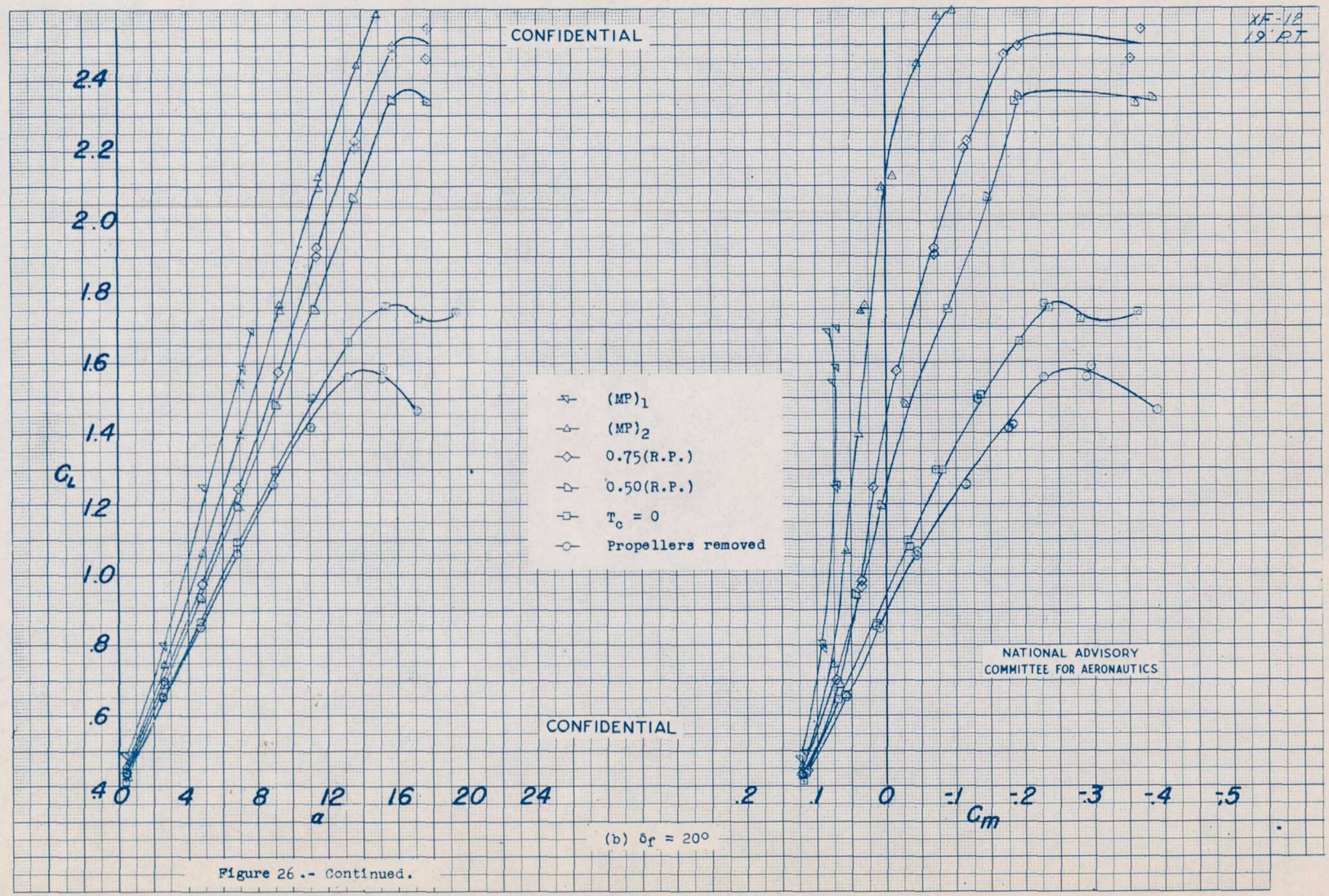
19000



198808

NACA RM No. L6L12

XF-12
19 PT



2.4
2.2
2.0
1.8
1.6
1.4
1.2
1.0
.8
.6
4.0
4
8
12
16
20
24

- ✦ (MP)₁
- △ (MP)₂
- ◇ 0.75(R.P.)
- ◻ 0.50(R.P.)
- T_c = 0
- Propellers removed

.2
1
0
-1
-2
-3
-4
-5

Figure 26.- Continued.

Figure 26b

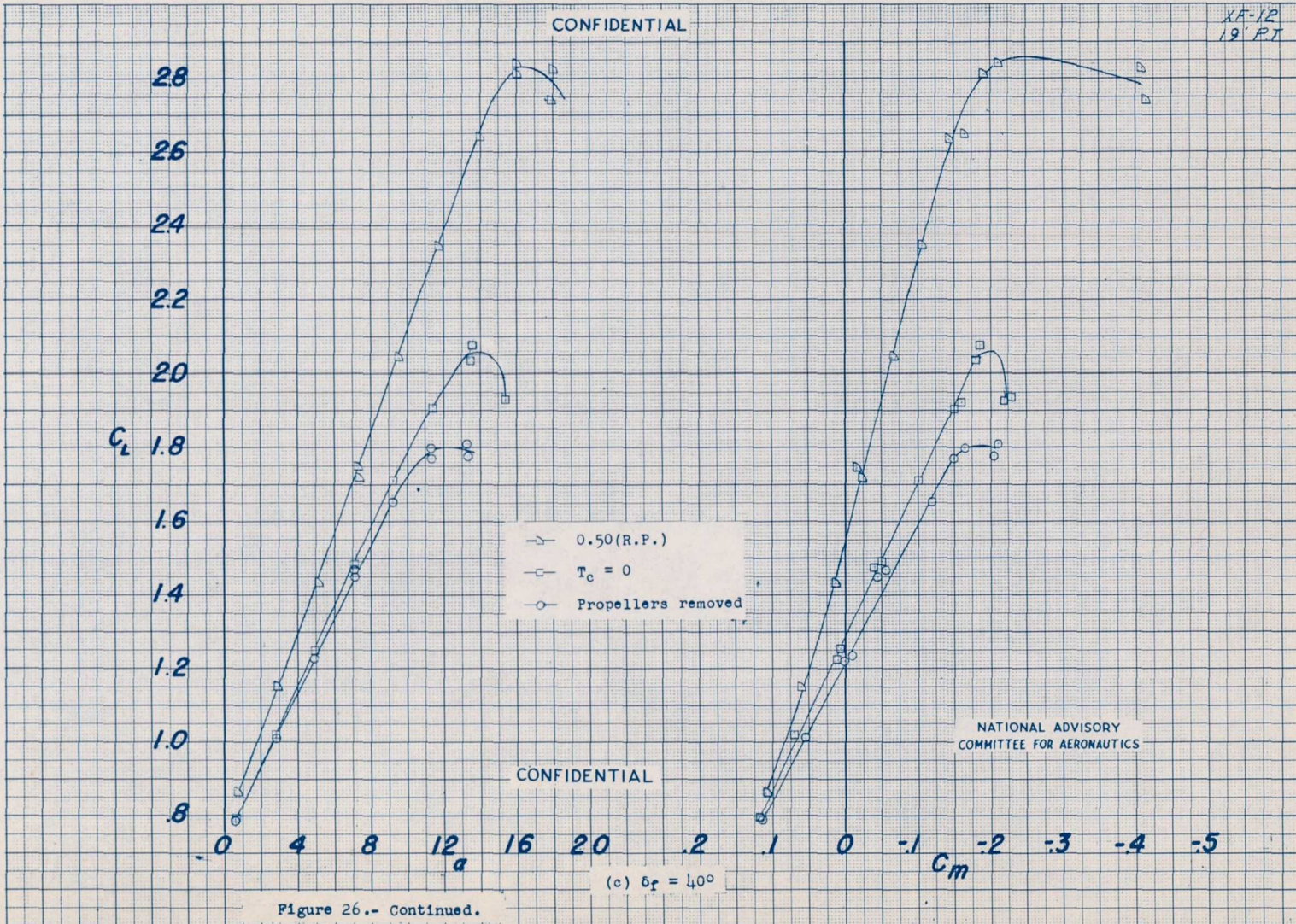


Figure 26.- Continued.

19858

NACA RM No. L6L12

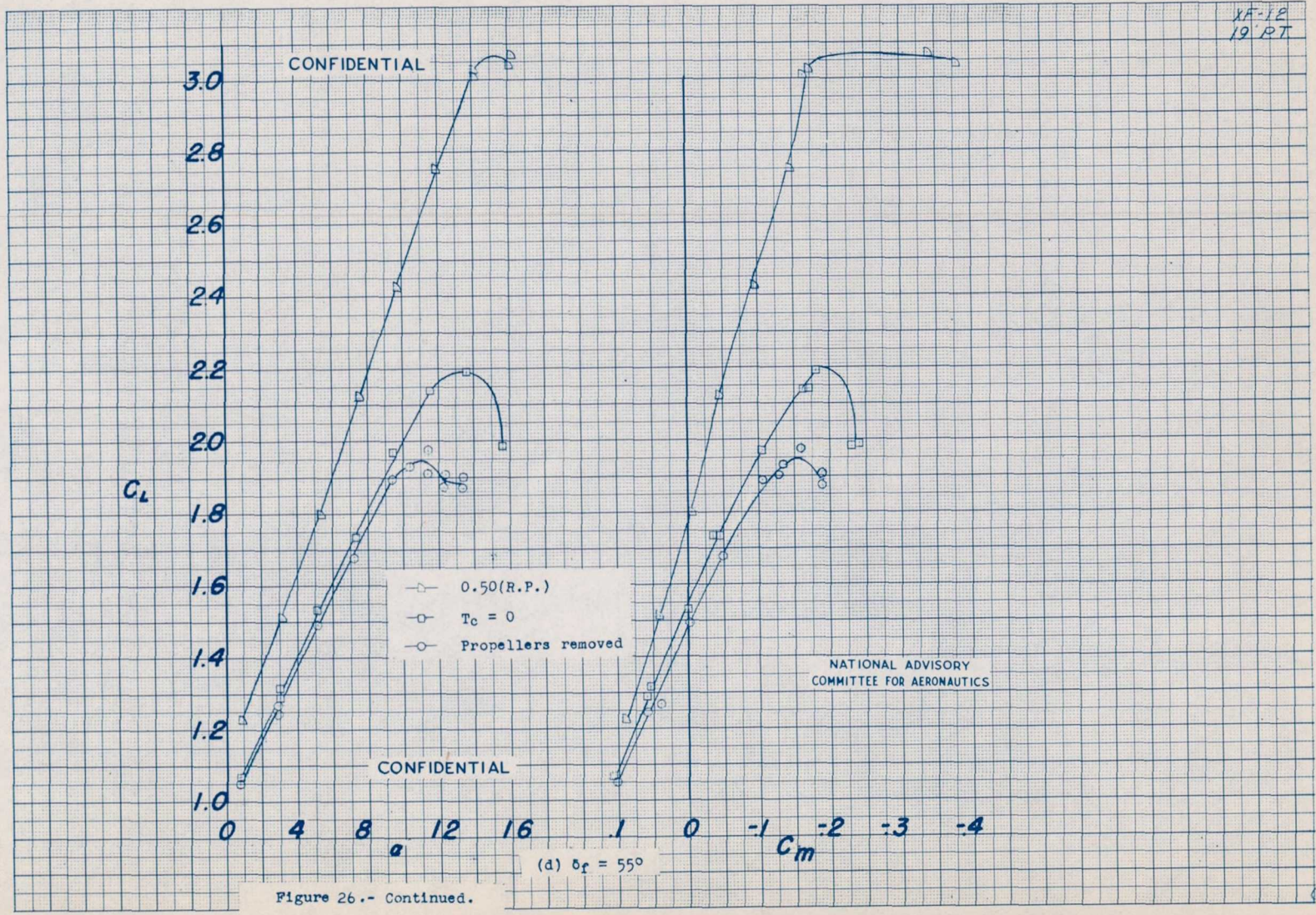


Figure 26.- Continued.

Fig. 26d

1950

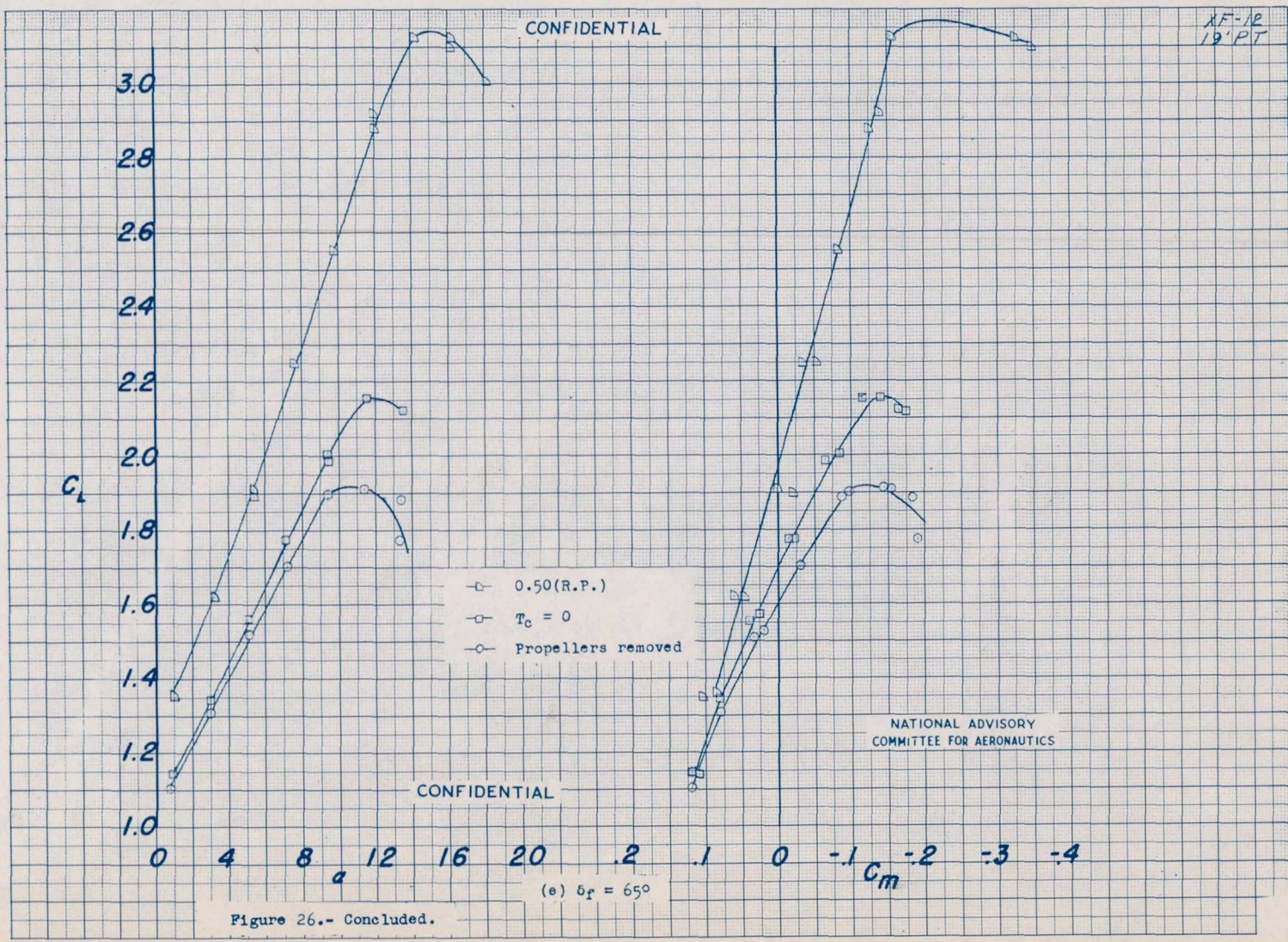


Figure 26.- Concluded.

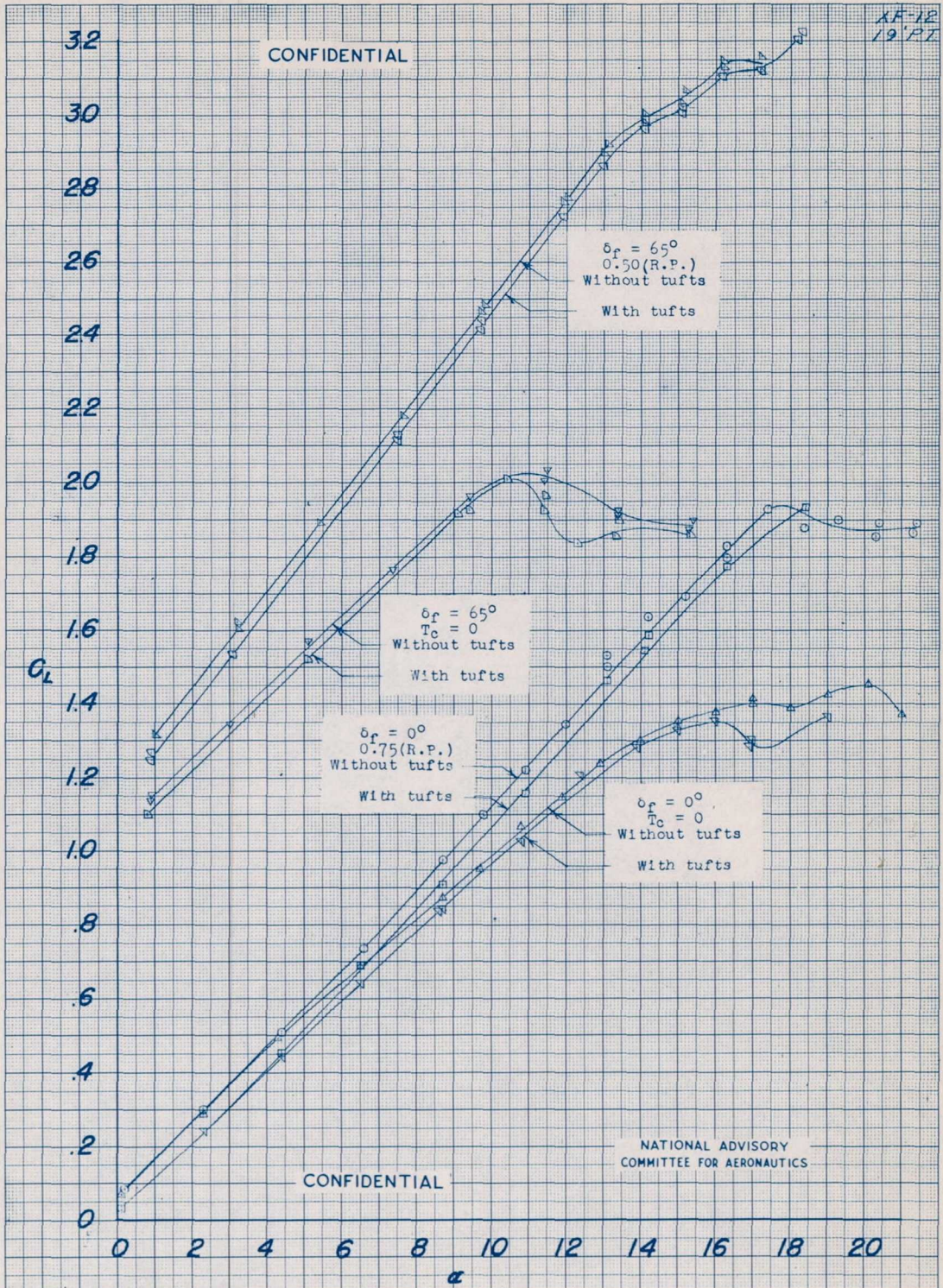
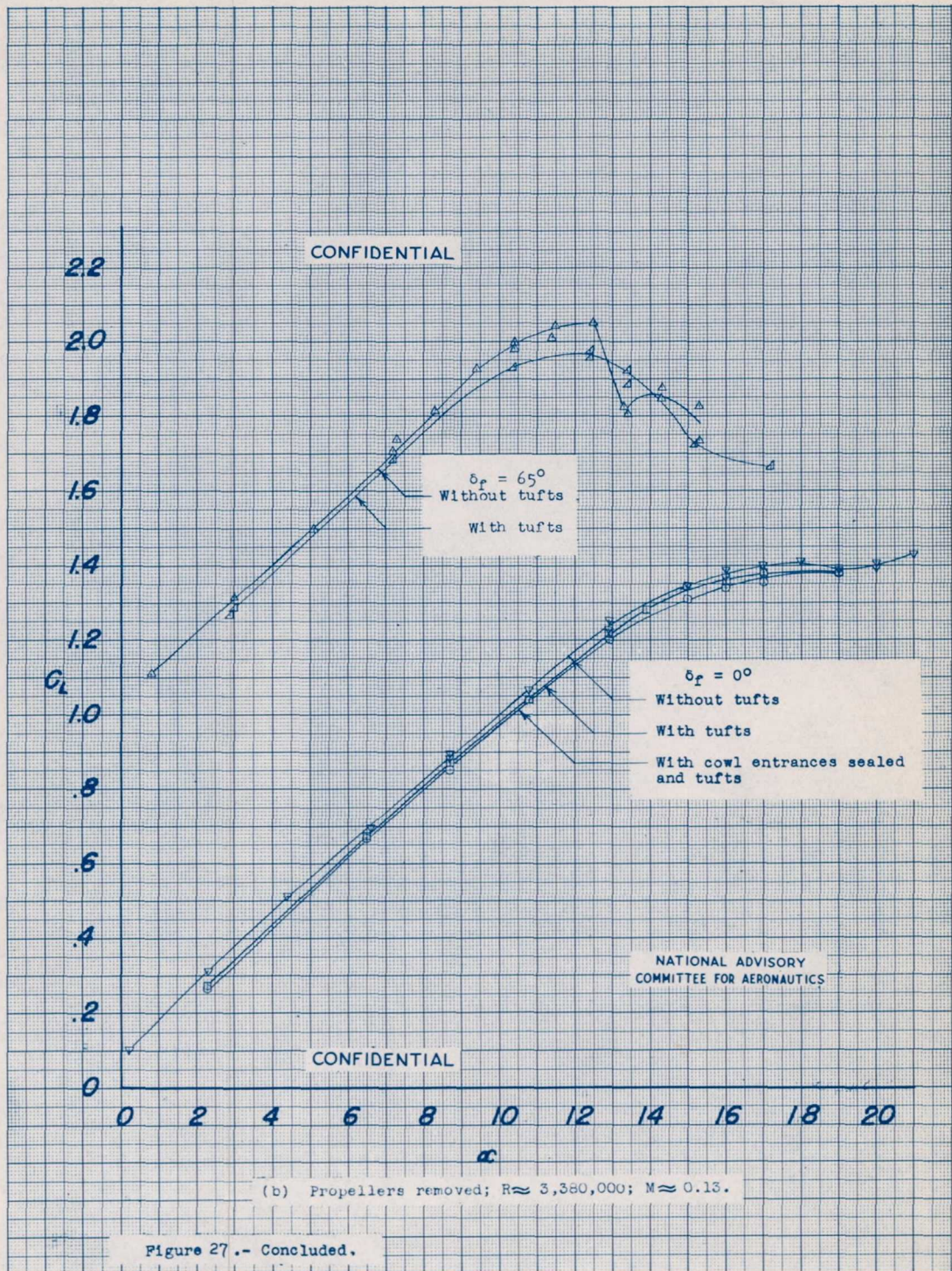
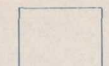
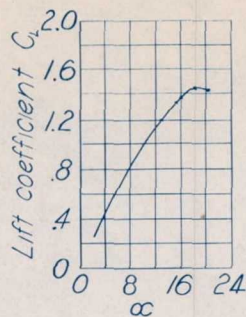


Figure 27.- Effect of tufts on lift coefficient for several flight conditions.
 $i_t = -2^\circ$; $\delta_e = 0^\circ$.



CONFIDENTIAL



Unstalled



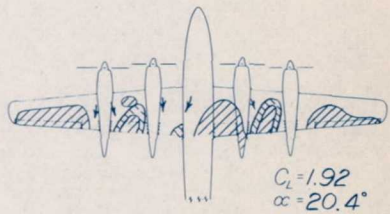
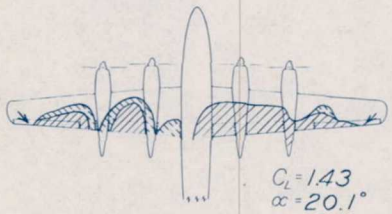
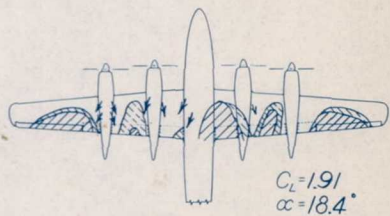
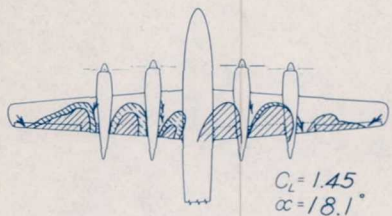
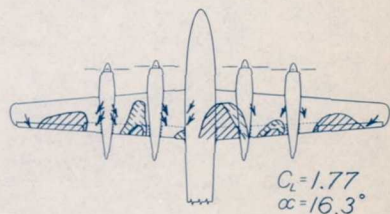
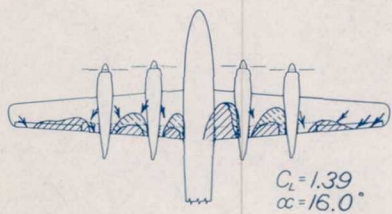
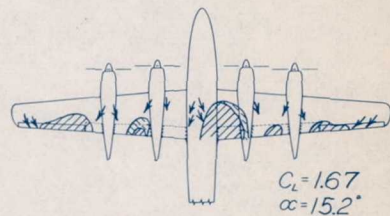
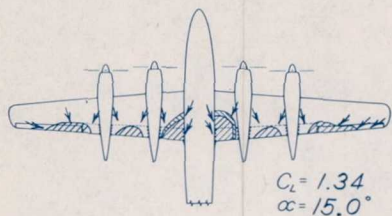
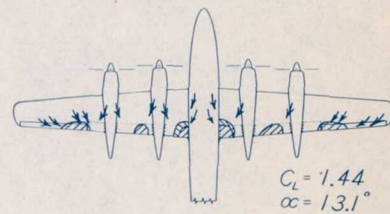
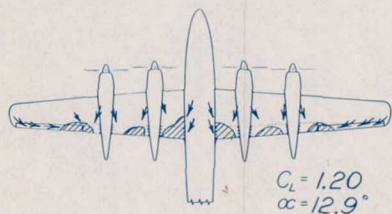
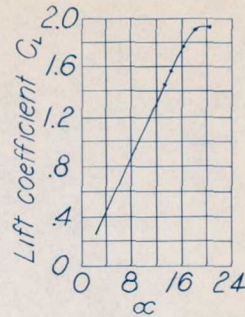
Intermittently stalled



Completely stalled



Flow in the direction of arrows



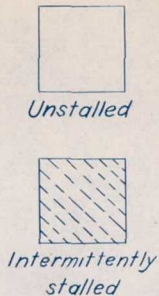
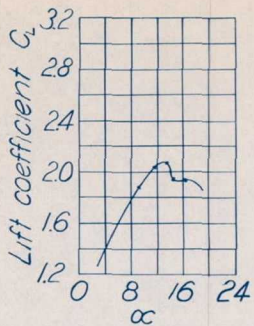
$T_c = 0$

NATIONAL ADVISORY COMMITTEE FOR AERONAUTICS

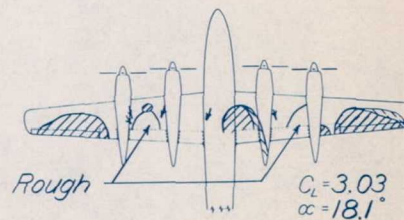
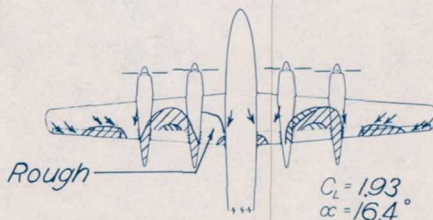
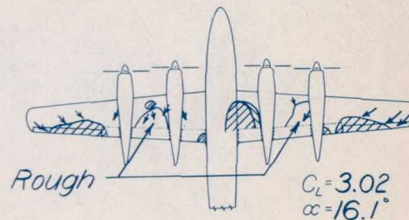
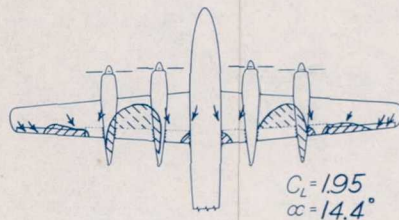
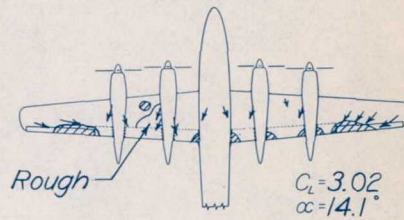
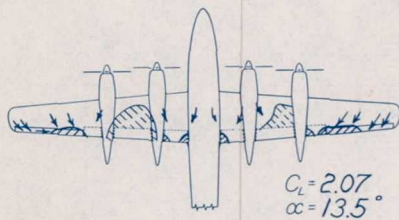
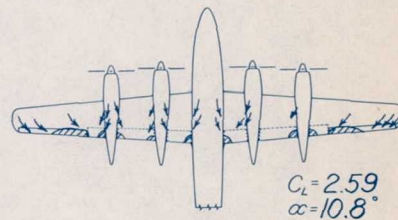
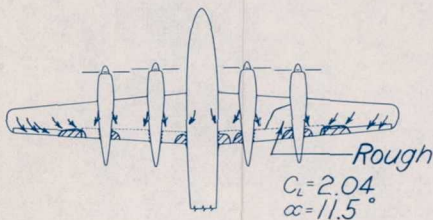
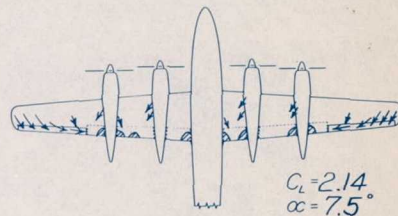
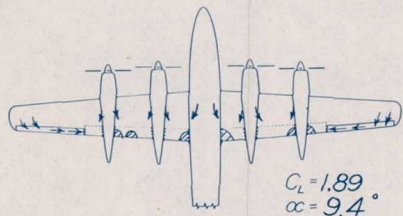
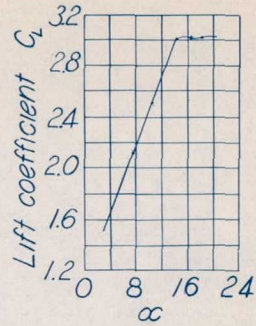
0.75(R.P.)

CONFIDENTIAL

Figure 28.- Stall diagrams of the $\frac{1}{8.33}$ -scale model of the Republic XF-12 airplane; $\delta_r = 0^\circ$; $\delta_l = 2^\circ$; $\delta_e = 0^\circ$; $R \approx 2,430,000$; $M = 0.09$.



CONFIDENTIAL



$T_c = 0$

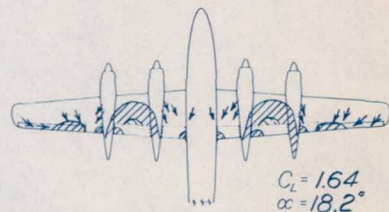
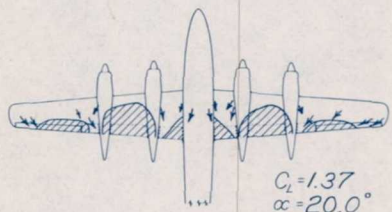
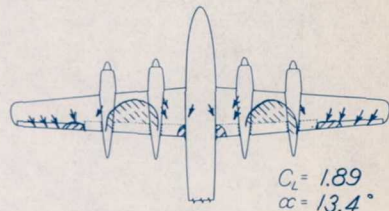
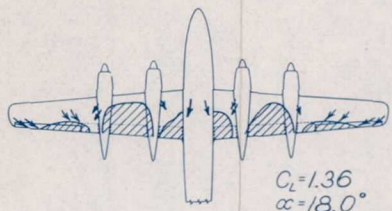
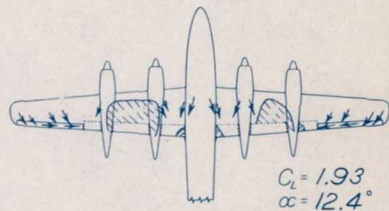
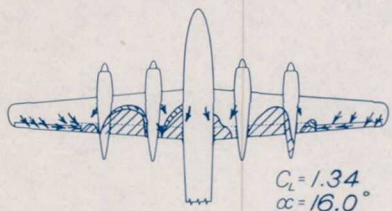
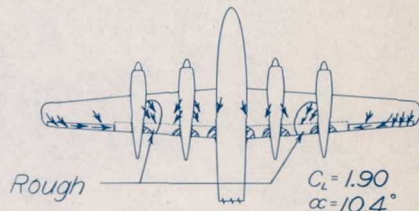
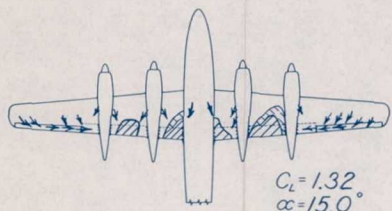
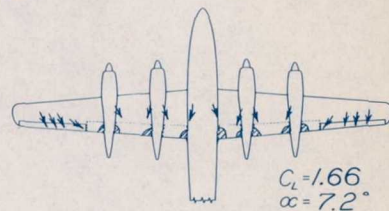
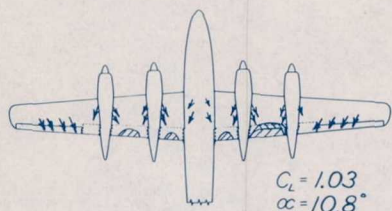
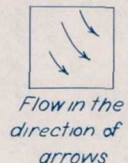
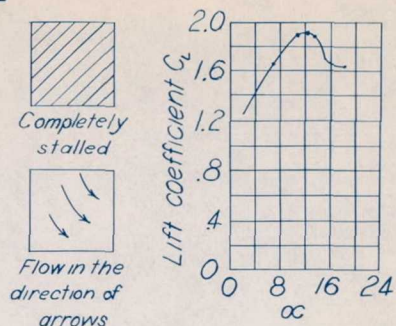
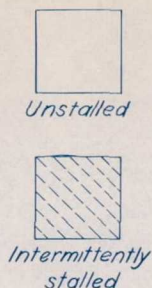
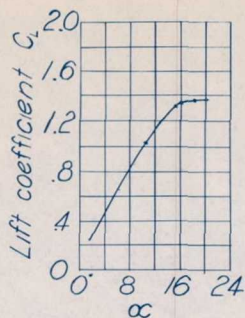
0.50(R.P.)

CONFIDENTIAL

NATIONAL ADVISORY COMMITTEE FOR AERONAUTICS

Figure 29.- Stall diagrams of the $\frac{1}{8.33}$ -scale model of the Republic XF-12 airplane; $\delta_f = 65^\circ$; $\delta_e = 2^\circ$; $\delta_e = 0^\circ$; $R \approx 2,350,000$; $M = 0.09$.

CONFIDENTIAL



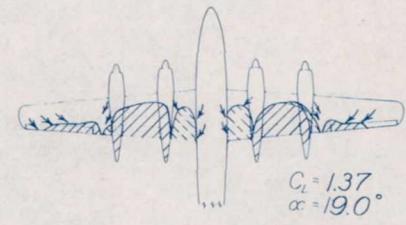
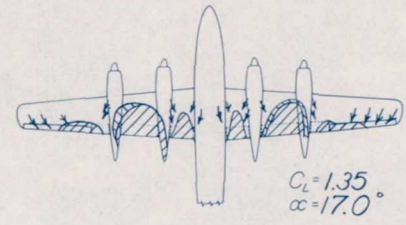
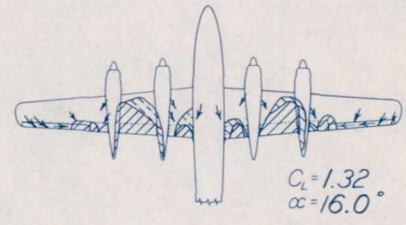
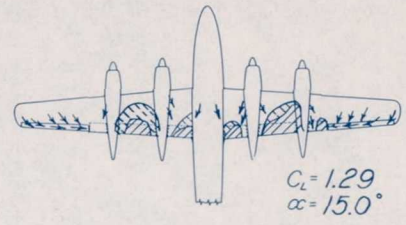
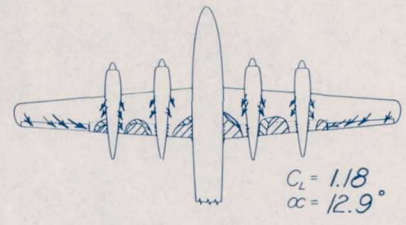
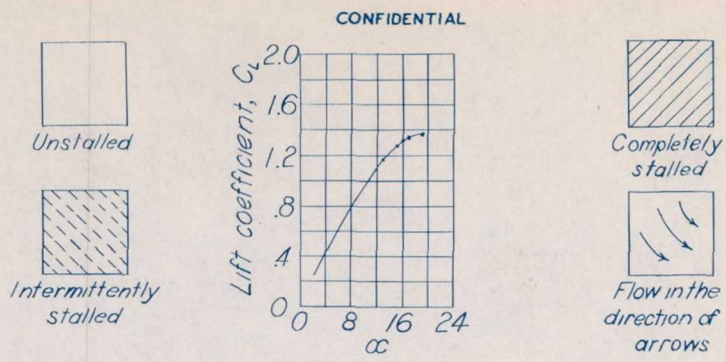
$\delta_f = 0^\circ$

CONFIDENTIAL

NATIONAL ADVISORY COMMITTEE FOR AERONAUTICS

$\delta_f = 65^\circ$

Figure 30.-Stall diagrams of the $\frac{1}{8.33}$ -scale model of the Republic XF-12 airplane; propellers removed; $i_p = 2^\circ$; $\delta_e = 0$; $R \approx 3,410,000$; $M = 0.13$.



NATIONAL ADVISORY
COMMITTEE FOR AERONAUTICS

CONFIDENTIAL

Figure 31. - Stall diagrams of the $\frac{1}{833}$ -scale model of the Republic XF-12 airplane; nacelle cowl-inlets sealed; propellers removed; $\delta_f = 0^\circ$; $\delta_e = 0^\circ$; $R \approx 3,400,000$; $M = 0.13$.

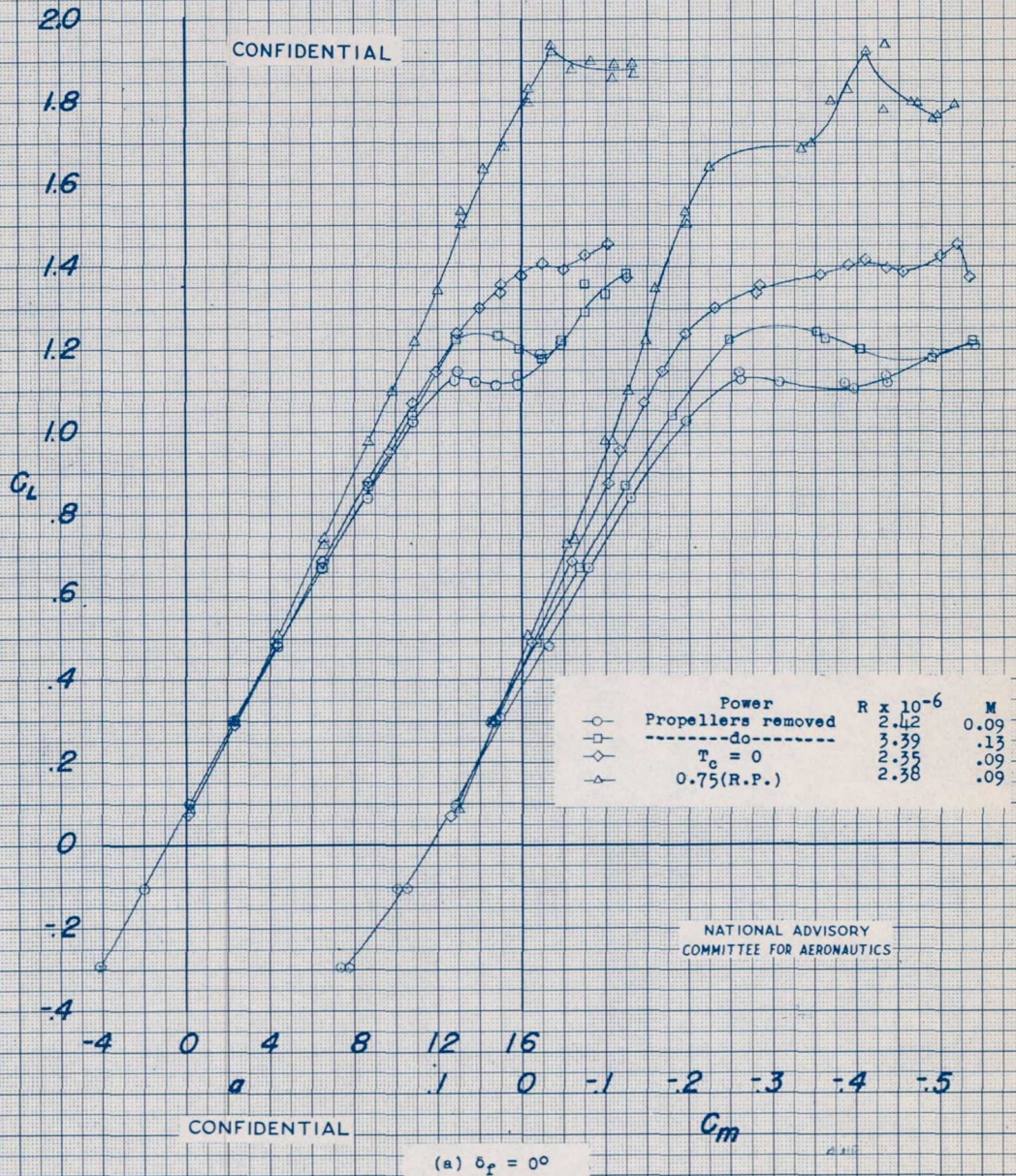
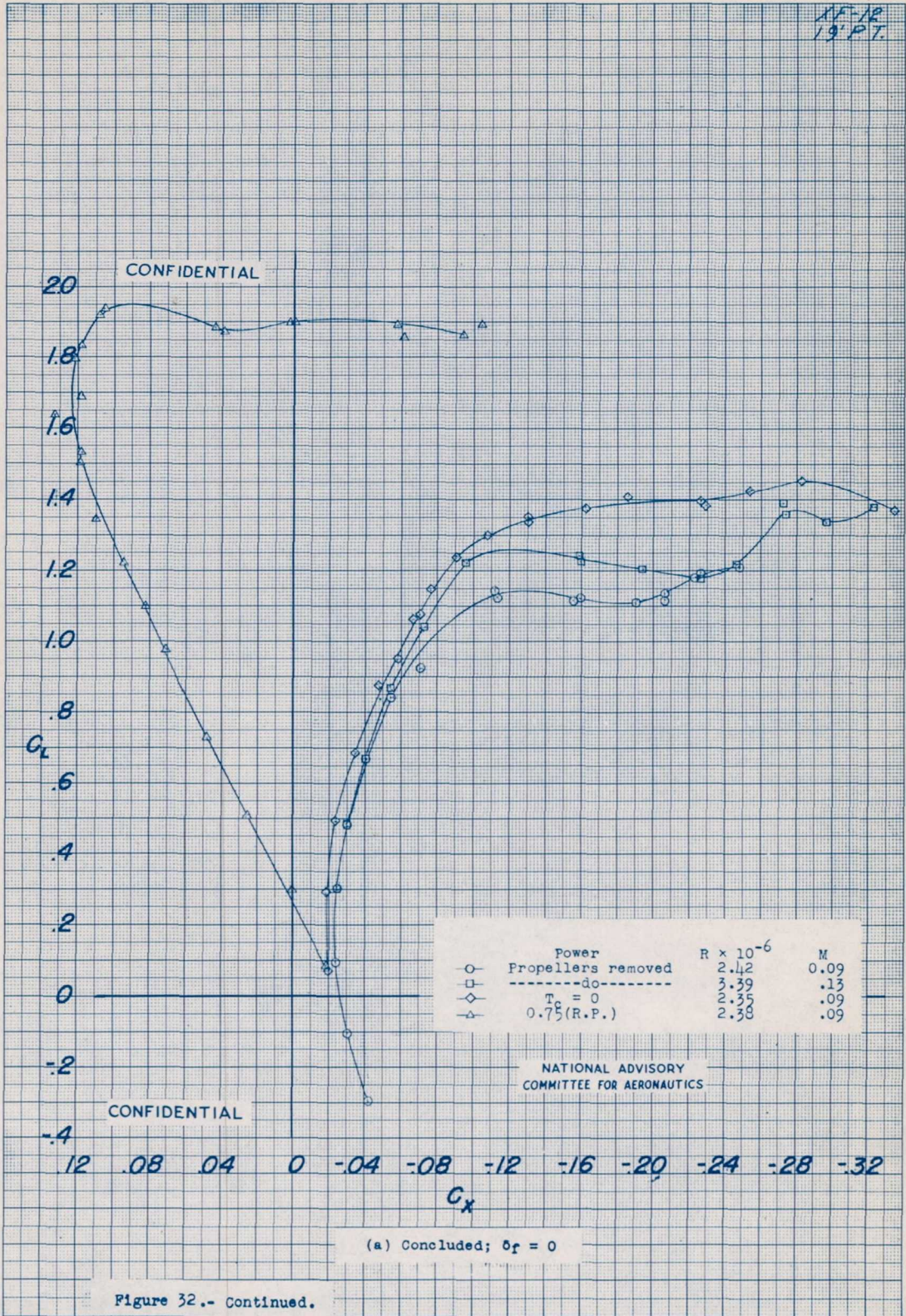


Figure 32.- Effect of power on several aerodynamic characteristics. Original wing duct inlet;

$i_t = -2^\circ$; $\delta_e = 0^\circ$.

17-18
19 P.T.



XF-12
19 PT

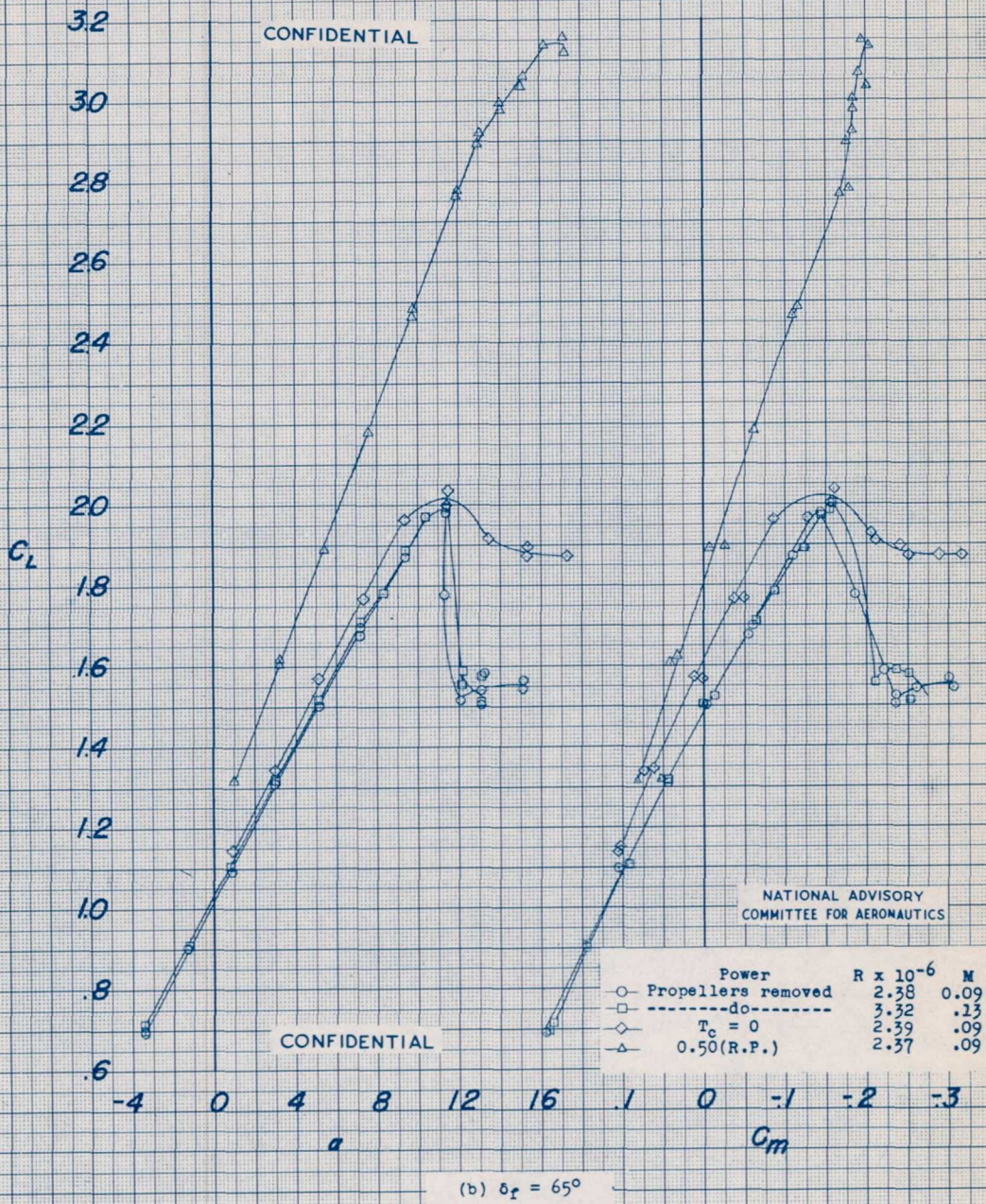


Figure 32.- Continued.

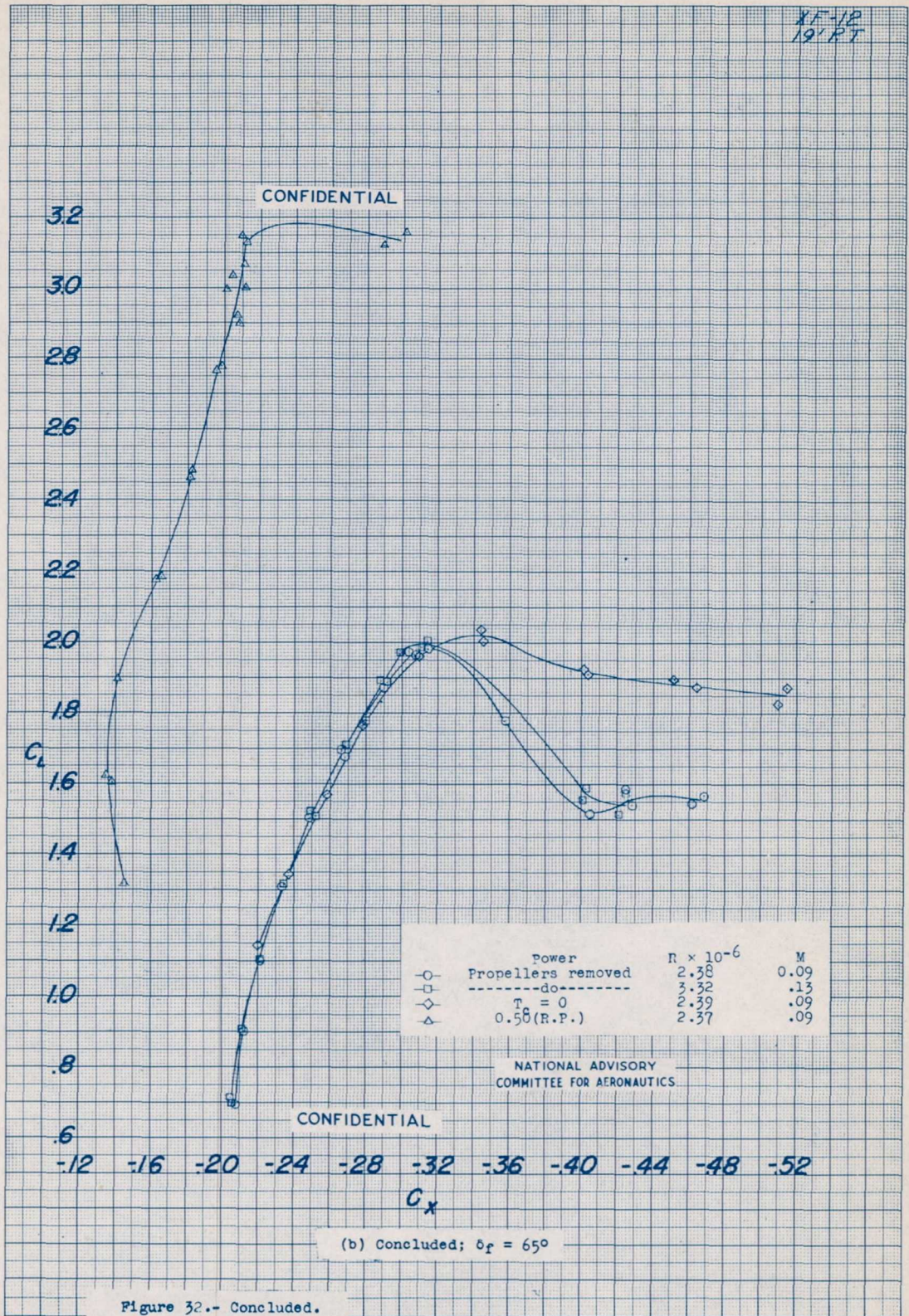


Figure 32.- Concluded.

CONFIDENTIAL

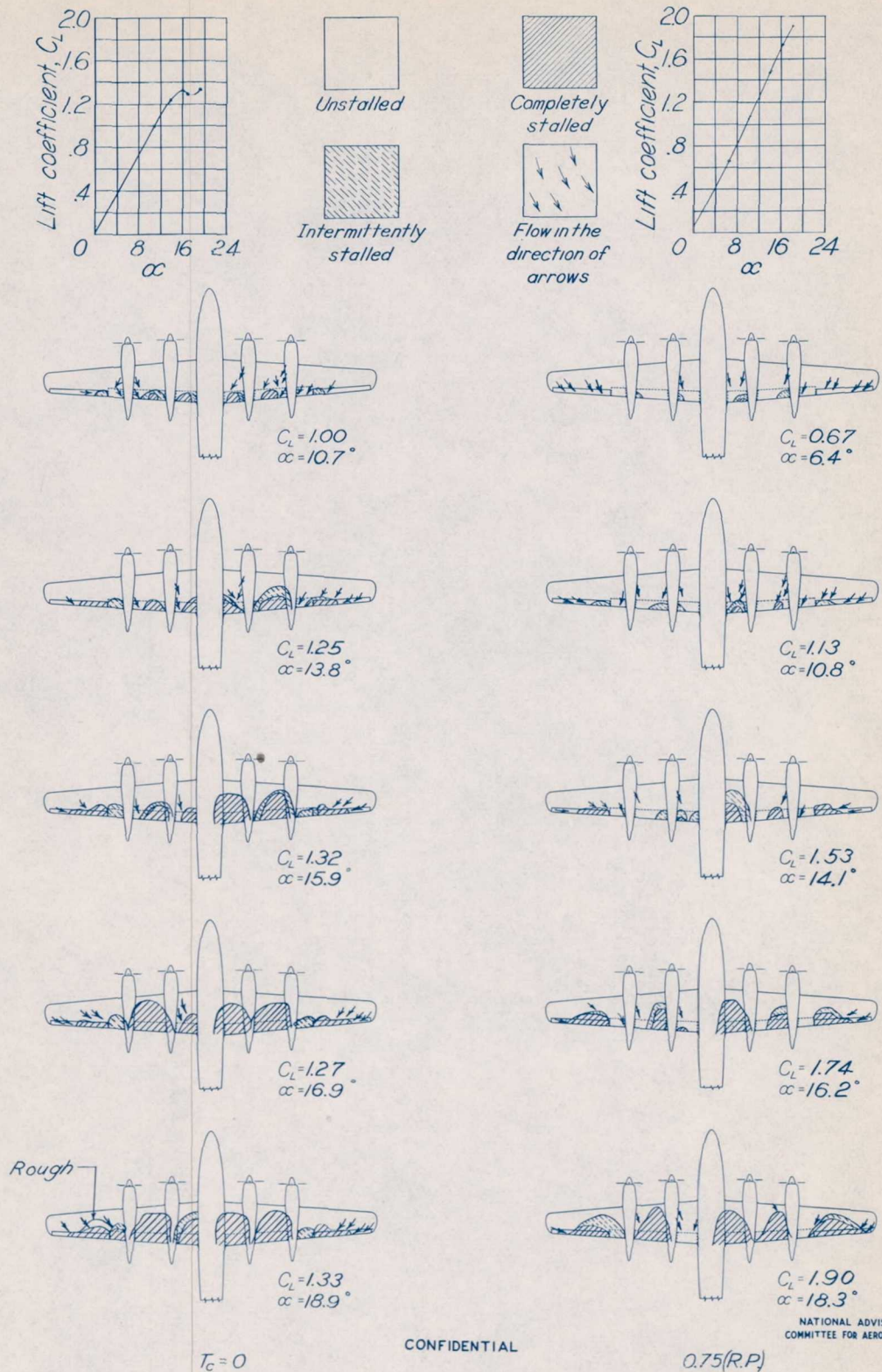
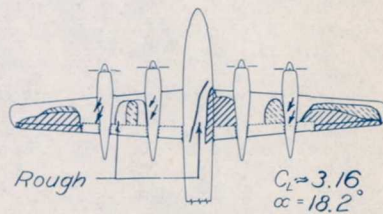
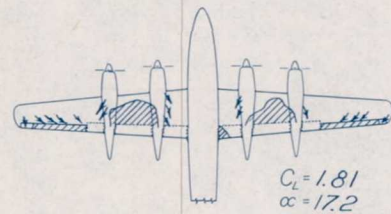
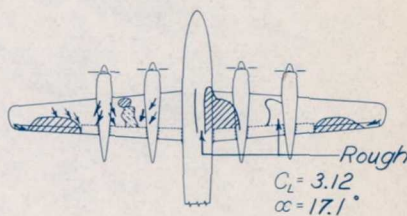
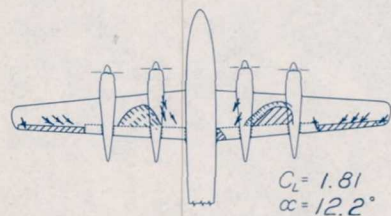
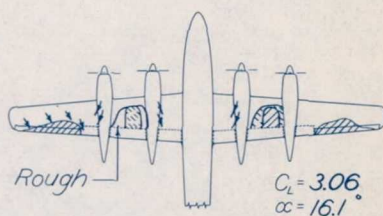
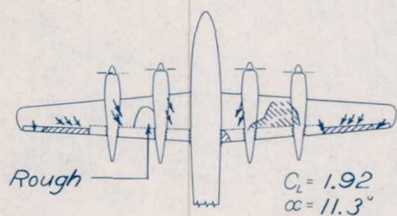
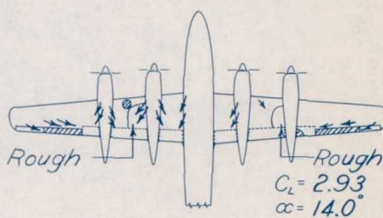
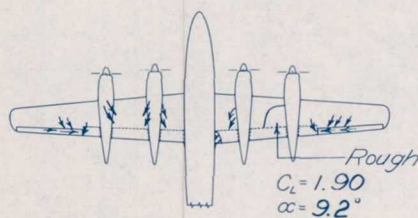
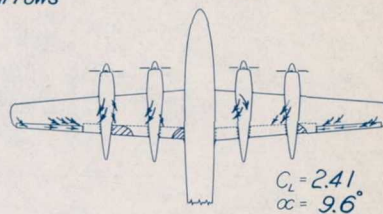
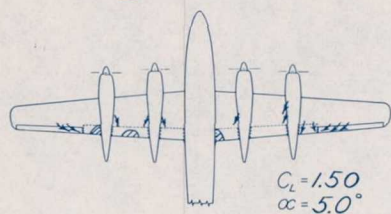
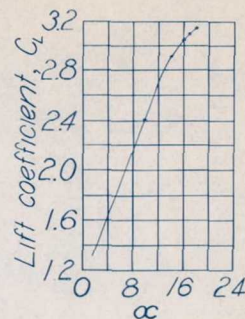
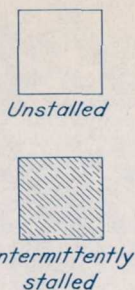
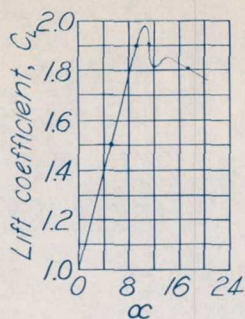


Figure 33.-Stall diagrams of the 1/8.33-scale model of the XF-12 airplane. Original Republic wing duct inlet; $\delta_f = 0^\circ$; $i_f = -2$; $\delta_e = 0$; $R \approx 2,380,000$; $M \approx 0.09$.

CONFIDENTIAL



$T_c = 0$

CONFIDENTIAL

0.50(R.P.)

NATIONAL ADVISORY
COMMITTEE FOR AERONAUTICS

Figure 34.-Stall diagrams of the 1/8.33-scale model of the XF-12 airplane. Original Republic wing duct inlet; $\delta_f = 65^\circ$; $i_f = -2^\circ$; $\delta_e = 0^\circ$; $R \approx 2,380,000$; $M \approx 0.09$.

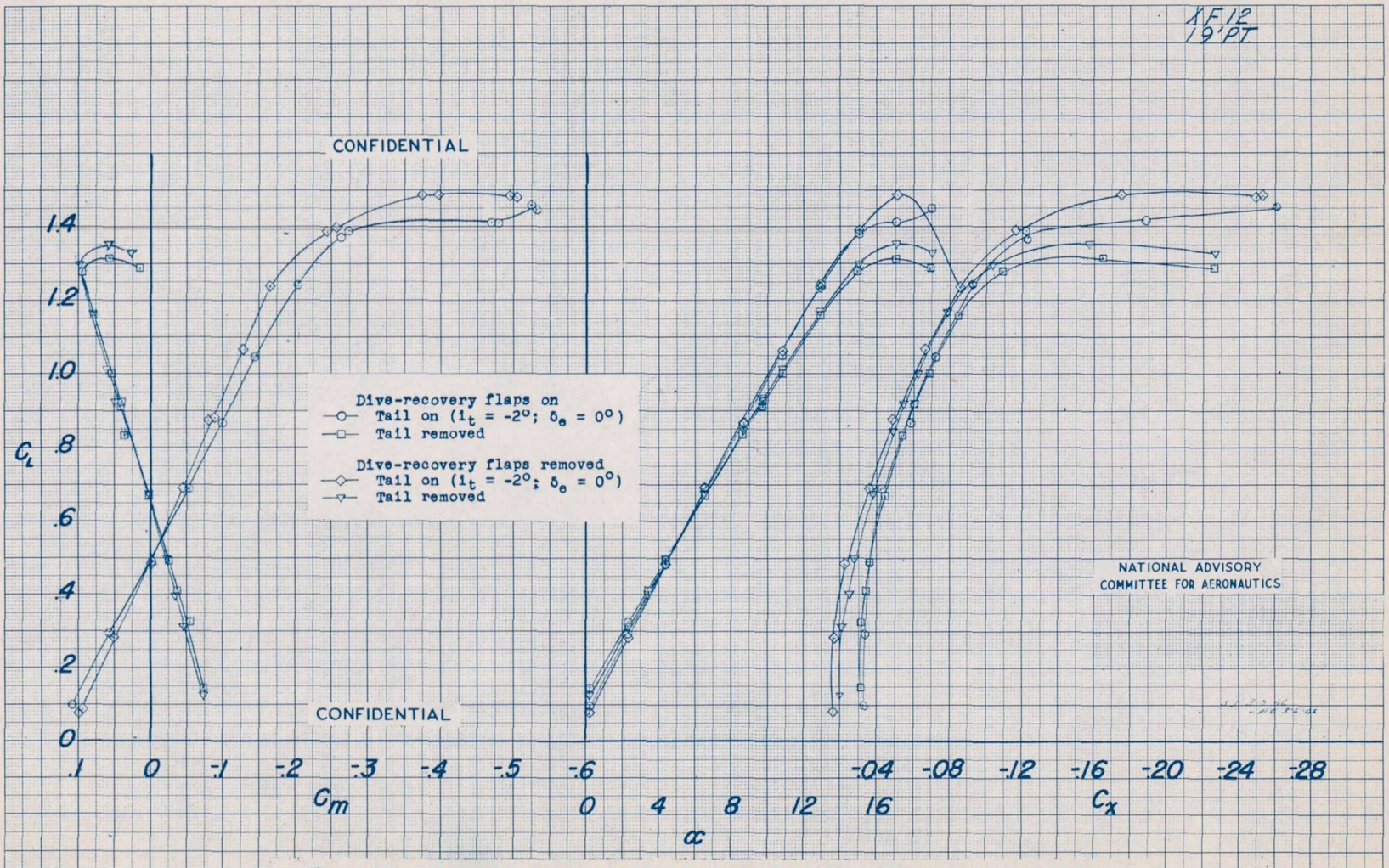


Figure 35.- Effect of dive-recovery flaps on several aerodynamic characteristics. $T_c = 0$; $\delta_f = 0$; $R \approx 2,300,000$; $M \approx 0.09$.

1908 30

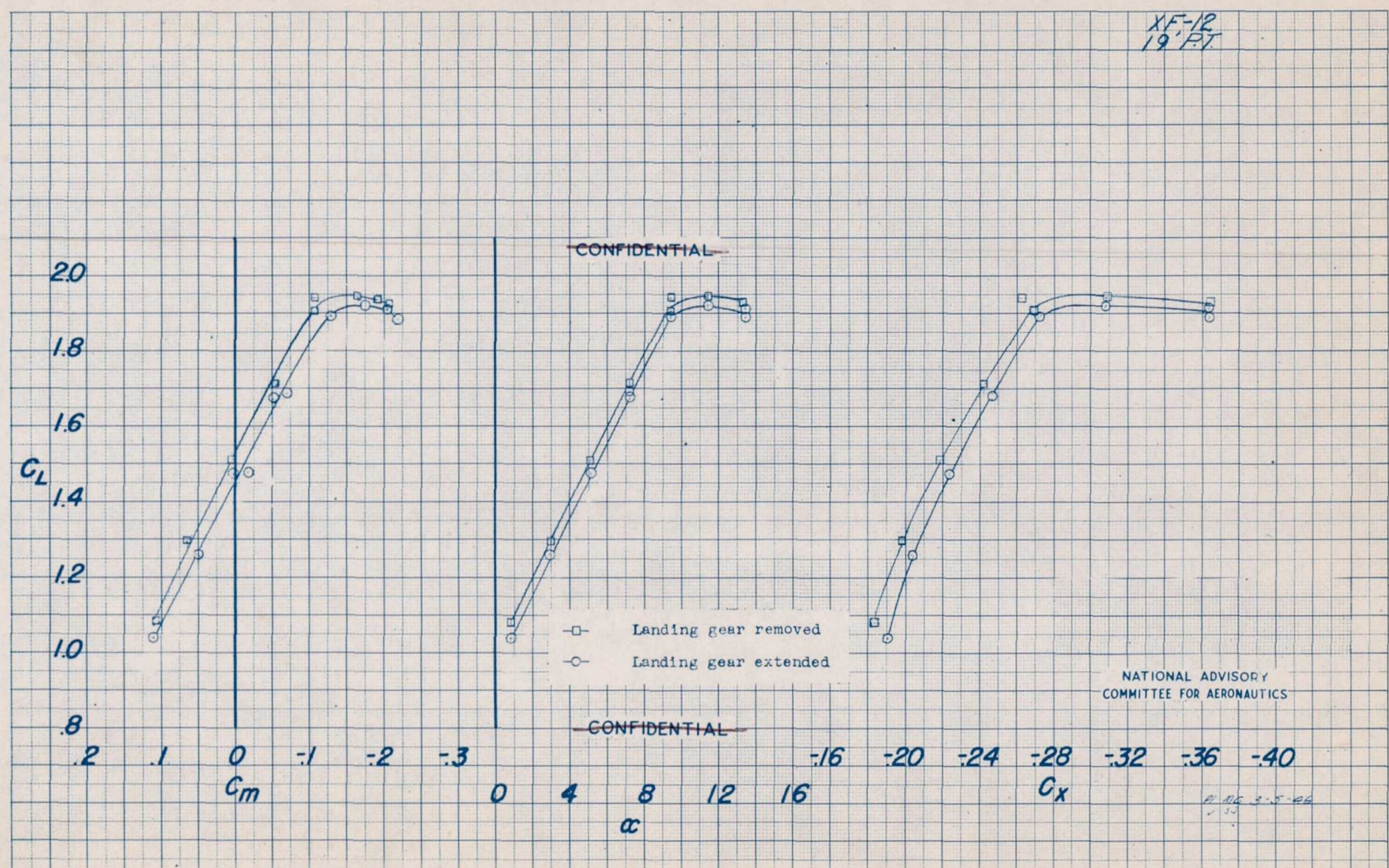


Figure 36.- Effect of landing gear on several aerodynamic characteristics. Propellers removed; $\delta_r = 55^\circ$; $\delta_e = 0^\circ$; $i_t = -2^\circ$; $R \approx 3,180,000$; $M \approx 0.09$.